MECHANISM (S) OF THE PATHOGENESIS OF VENEZUELAN EQUINE ENCEPHALITIS VIRUS INFECTION

Thesis

Submitted in the partial fulfillment of the requirements for the degree of

DOCTOR OF PHILOSOPHY

by

Anuj Sharma

Under the supervision of

Prof. R.K. Maheshwari, PhD

Birla Institute of Technology and Sciences
Pilani (Rajasthan) India
2007

Completed at Uniformed Services University of the Health Sciences, Bethesda, Maryland, USA under INDO-USUHS Collaboration

BIRLA INSTITUTE OF TECHNOLOGY AND SCIENCE
PILANI (RAJASTHAN)

CERTIFICATE

This is to certify that the thesis entitled **Mechanism(s) of the Pathogenesis of Venezuelan Equine Encephalitis Virus Infection** and submitted by **Anuj Sharma** ID No **2001PH29099** for award of Ph. D. Degree of the Institute embodies original work done by him under my supervision.

Signature in full of the Supervisor: _____

Name in capital block letters: **RK MAHESHWARI, PhD**

Designation: **Prof., Dept. of Pathology, USUHS, Bethesda, MD, USA**

Date:

DEDICATION

This thesis is dedicated to Dr. Vishwa Nath Sharma and Mrs. Ashok Sharma, my parents, who gave me strength to move forward and do something better. To my family that gives me strength and purpose in life.

To mice, working with these little animals has infused in me a deep sense of gratitude towards them; their contribution to science and human kind is immense and cannot be measured in any terms.

"For science must breathe the oxygen of freedom."

-John Charles Polanyi

Acknowledgement

The writing of this dissertation has been one of the most significant steps ahead in my academic career. The experience of graduate education encompasses many people, friends, teachers and colleagues.

This thesis would not have been possible without the kind support, the trenchant critiques, the probing questions, and the remarkable patience of my thesis advisor Prof. Radha Maheshwari. He is actively involved in the work of all his students, and clearly always has their best interest in mind. The freedom and encouragement he gave me to learn and try novel experiments helped me a lot in designing and carrying out this dissertation. His guidance, patience and support were critical, helpful and encouraging through out the course of my study. Thank you *guruji*! On the personal side, he did not hesitate to invite graduate students to be part of his extended family. Thank you for all those *diwali* festivities that were shared with us by you and your family.

I was fortunate enough to interact with Dr. Anoop Singh at the early phase of my PhD. His mentoring towards experimental design and troubleshooting helped me profoundly not only throughout this entire study but will be for the rest of my research life.

The USUHS-BITS collaboration program has helped numerous students achieve their doctoral degree and it would not have been possible but for the magnanimous thoughtfulness and constant support of Dr. Robert Friedman, chair, Department of Pathology. I am proud to have gained my doctoral degree as part of this collaborative effort, integrating best of both worlds.

I am very grateful to Drs. Raj Puri and Bhaskar Bhattacharya at Center for Biologics Evaluation and Research, Food and Drug Administration, Bethesda, Maryland for their help and guidance in conducting microarray studies and Drs. Robert Blumenthal and Yossi Raviv at Centre for Cancer Research, National Cancer Research Institute, Frederick, MD for their invaluable help and suggestions in the vaccine study for VEEV.

Thank you for accepting to be my advisory committee and guiding me through my thesis, Drs. SK Verma, AK Das and Utpal Roy, of BITS- Biosciences division. Both academic and personal interactions with all of you through the course of my masters as well as doctoral degree programs have been wonderful.

My parents, Dr. VN Sharma, and Mrs. A Sharma, need special mention for all the love, support and sacrifices they made over the years. My mom whom I have talked countless times while commuting to work, has listened me out even though many a time she didn't have any clue about what I am talking. Her quick recipes over phone were very helpful. My father has been a mentor all my life. He is a good friend and a teacher with strength and determination I always try to possess. It is to them I owe my dissertation most. Sai, my loving wife, her love, and support have been invaluable. Though we are away from each other she has been patient while I vented out my frustration. Her, positive attitude, hope and compromises have given me strength to complete my PhD. My family, Naveen Bhaiya, Anu Bhabhi, Meeta di, Deepa di, and all other memebers, you guys have been great, thanks for all your support and blessings.

Both at USUHS and BITS-Pilani, I was surrounded by great friends, who constantly provided intellectual stimulation as well as, were just fun to hang out with, which is of utmost importance for graduate education. Rajesh and I go way back. I am

glad we shared the memories of grad school and the life's deciding moments together. Rajesh NV, your spontaneous jokes made working a blast thank you for teaching me animal handling. Dimple, thank you for being extremely helpful through out and a trouble shooter in my experiments. Far from home all of us have enjoyed the sumptuous delight of your cooking. Pawan, your rasmalis were a treat. Bharat, thank you for helping me in siRNA work, and I have always enjoyed our discussions while sharing our lunch. Jim, thank you for your help in BSL3. Manmohan, I have always enjoyed discussions with you, thanks for being such a great company. Thanks to Manish, Paridhi, and all other friends with whom I had good times in and out of lab.

Elaine, Marta, Stacy and Dawn of Pathology Department need special mention for their help with official paperwork and for being such wonderfully kind and obliging people.

I am grateful to the Laboratory of Animal Medicine and Bio Instrumentation Center of USUHS for their help in animal experiments and analytical facilities respectively through out this work. Special thanks must go to LTC James Sheets, Director LAM for his advice and guidance in writing animal protocols and LTC Daniel Hamilton, Deputy Director EHOS for his constant support in keeping BSL3 laboratory up and running.

Birla Institute of Technology and Science, Pilani and Uniformed Services University of the Health Sciences, Bethesda have provided me with an excellent opportunity and environment to pursue PhD degree here at USUHS, Thank you! I am obliged to Research and Consultancy Division, BITS, Pilani for the smooth progress of my research work off campus.

Last but definitely not the least, all the mice that made up for the part of the *in-vivo* studies. I am grateful to their contribution that allowed me to complete this work successfully. Rest in peace guys!

Table of Contents

List of figures

List of Tables

List of Abbreviations

AIDS	Acquired immunodeficiency syndrome
ALHYDROGEL (or Alum)	Aluminum hydroxide gel adjuvant
BBB	Blood brain barrier
BSA	Bovine serum albumin
BSL-3	Biosafety level 3
Ccl	Chemokine (C-C motif) ligand
CFA	Complete freund's adjuvant
CNS	Central nervous system
CPE	Cytopathic effect
CV	Crystal violet
Cxcl	Chemokine (C-X-C motif) ligand
Cxcr	Chemokine (C-C motif) receptor
DMSO	Dimethyl sulfoxide
DPBS	Dulbecco's phosphate buffered saline
EAE	Experimental autoimmune encephalitis
ELISA	Enzyme-linked immunosorbent assay
EM	Electron microscopy
EMCV	Encephalomyocarditis virus
FAK	Focal adhesion kinase
FBS	Fetal bovine serum
FDA	Food and drug administration, USA
GAPDH	Glyceraldehyde-3-phosphate dehydrogenase
GOFFA	Gene ontology for functional analysis
HIV	Human immunodeficiency virus
HLP	Hind limb paralysis
HSV	Herpes Simplex virus
ICAM1	Intercellular adhesion molecule-1
ICAM1-/-	ICAM1 knock out

ICAM +/+	ICAM1 wild type
IFN	Interferon
IL	Interleukin
INA	1-5 iodonapthyl azide
iNOS	Induced nitric oxide synthetase
IRF	Interferon regulatory factor
KO	Knock out
LFA	Lymphocyte functional associated antigen
MEM	Minimum essential medium
MOI	Multiplicity of infection
MS	Multiple sclerosis
MTT	3-[4, 5- dimethylthiazol-2-yl]-2, 5-diphenyl tetrazolium bromide
Nfkb	Nuclear factor kappa beta
NSP	Non-structural protein
PBS	Phosphate buffered saline
PCR	Polymerase chain reaction
PFU	Plaque forming unit
Pfv	Post first vaccination
Rpm	Rotation per minute
RT	Reverse transcription
SCID	Severe combined immune deficiency
SFV	Semliki forest virus
TCID50	50% tissue culture infective dose
TLR	Toll like receptor
TNF	Tumor necrosis factor
VCAM1	Vascular cell adhesion molecule1
VEEV	Venezuelan equine encephalitis virus
WNV	West nile virus
WT	Wild type

Introduction

Venezuelan equine encephalitis virus (VEEV) causes a highly virulent central nervous system (CNS) disease in horses and humans and is transmitted to humans by mosquitoes. It causes frequent outbreaks at the span of every 5-10 years and has been identified as emerging infectious disease. VEEV also belongs to a small group of viruses that have been developed as a biological warfare agent and is of both military and civilian concern.

History

VEEV was first isolated in 1938 from the brain of the infected equines in Yaracuy state, Venezuela and identified in 1939 by Kubes and Rios [Kubes and Rios 1939, reviewed in Weaver et al 2004]. This strain was later identified as antigenic subtype IAB. First known epidemic of VEEV occurred in 1935 in the central valley of Columbia and in 1936 it spread into the Guajira Peninsula of northern Columbia and Venezuela. Major VEEV outbreaks occurred from 1938 to 1973 at an interval of 5-10 years in Venezuela, Peru, Colombia and Ecuador [Sanmartin and Osorno 1954, Sanmartin et al 1971, 1973, Johnson and Martin 1974]. In early 1960s (1962-1964), the human disease was documented including encephalitis and death in children associated with the equine outbreaks of VEEV (identified as VEEV subtype IC) in Venezuela [reviewed in Weaver 2004, Johnson and Martin 1974, Briceno Rossi 1967]. Between 1950 and 1970 several clinically silent enzootic virus cycles in Culex mosquito and wild rodents were documented in South, Central and North America [Galdino 1972, reviewed in Johnson and Martin 1974]. One of the largest outbreaks of VEEV occurred in 1960s where over 200,000 human infections and 100,000 equine mortality was documented in Central

Colombia [reviewed in weaver 2004]. In 1969 a major outbreak of VEEV started in Ecuador, which within a year spread to Guatemala, El Salvador and southern Mexico and by 1971 reached Texas region of North America. Vigorous immunization of equine population and anti-mosquito spray contained further spread of this outbreak. VEEV subtype IB was identified as causative agent of this outbreak [Zehmer et al 1974, Calisher and Maness 1974]. Then no outbreak of VEEV was documented from 1973 to 1992. This is speculated to be due to death of large equine population, reduced mosquito population and development of a long lasting immunity as a result of 1969 VEEV outbreak and the following vigorous vaccination of equine population. In 1992, a small outbreak of VEEV subtype IC was documented (24 equine and four human cases) in Trujillo and Zulia state of western Venezuela [reviewed in Weaver 1994, Rico-Hesse et al 1995]. In 1993 and 1996 VEEV outbreaks of only equine population was reported in the Chiapas and Oaxaca state of Mexico respectively with 129 equine cases and 63 deaths in Chiapas and 32 equine cases and 12 deaths in Oaxaca. Virus isolated from these two outbreaks was VEEV subtype IE [Oberste et al 1998]. In 1995 largest outbreak of VEEV occurred in Venezuela and Colombia. People of all ages were infected with an estimated 75000 to 100,000 human cases. More than 20 human fatalities were reported from all age groups and autopsy of brain from several still born fetuses revealed infection with VEEV. The actual death number remains unknown but human mortality rate was ~0.5%. The VEEV strain isolated from this outbreak was identified as VEEV subtype IC [Weaver 1996]. Emergency control measures such as vaccination of equines and their movement restriction along with aerial spray of insecticides prevented further spread of this outbreak

into more populated area of Colombia. Since 1995 no outbreak of VEEV has been reported but as experienced in the last 5 decades, it might just be waiting to happen.

Taxonomy

VEEV is a member of group arboviruses. It belongs to the group A arboviruses along with eastern equine encephalitis virus (EEEV) and western equine encephalitis virus (WEEV). Group B arboviruses constitute of dengue, St Louis encephalitis and yellow fever viruses. Group A arboviruses are genus *Alphavirus* within the family *Togaviridae.* Togaviridae are enveloped single stranded RNA viruses. These are further classified into six antigenic complexes. VEEV, EEEV and WEEV are three of those six complexes. VEE complex have six subtypes based on hemagglutination inhibition and neutralization test called subtype I-VI (Table 1). These subtypes are further divided into IA, IB, ID, IE, IF, II, IIIA, IIIB, IIIC, IIID, IV, V and VI. Subtypes can be classified as epizootic (that causes epidemics) and enzootic strains (that does not cause epidemics). Epizootic strains are IAB and IC and enzootic are ID, IE, IF, II, IIIA, IIIB, IIIC, IIID, IV, V and VI [Griffin 1999, Smith et al 1997. Weaver et al 1992, 2004].

Table 1: ***VEE Antigenic Complexes.***

Subtype	Species	Variety	Transmission pattern	Equine virulence	Location	Vector
I	VEE virus	AB	Epizootic	Yes	Central, South, and North America	Mammalophilic mosquitoes
	VEE virus	C	Epizootic	Yes	South America	Mammalophilic mosquitoes
	VEE virus	D	Epizootic	No	Central and South America	C. (Mel.) *aikenii s.sl* (*ocossa, panocossa*); *vomerifer*, *pedroi*, *adamesi*
	VEE virus	E	Enzootic	Variable	Central America and Mexico	C. (Mel.) *taeniopus*
	Mosso das Pedras virus	F	Enzootic	Unknown	Brazil	Unknown
II	Everglades virus		Enzootic	No	Southern Florida	C. (Mel.) *cedecei*
III	Mucambo virus	A	Enzootic	No	South America	C. (Mel.) *portesi*
	Tonate virus	B (Also Bijou Bridge virus)	Enzootic	Unknown	South and North America	Unknown, Oeciacus vicarius (cliff swallow bug)
	Mucambo virus	C (strain 71D1252)	Enzootic	Unknown	Western Peru	Unknown
	Mucambo virus	D (strain V407660)	Enzootic	Unknown	Western Peru	Unknown
IV	Pixuna virus		Enzootic	Unknown	Brazil	Unknown
V	Cabassou virus		Enzootic	Unknown	French Guiana	Unknown
VI	Rio Negro virus		Enzootic	Unknown	Northern Argentina	C. (Mel.) *delpontei*

Adapted from "*Weaver et al. Venezuelan equine encephalitis Annu Rev Entomol 2004; Vol 49: p141-174*"

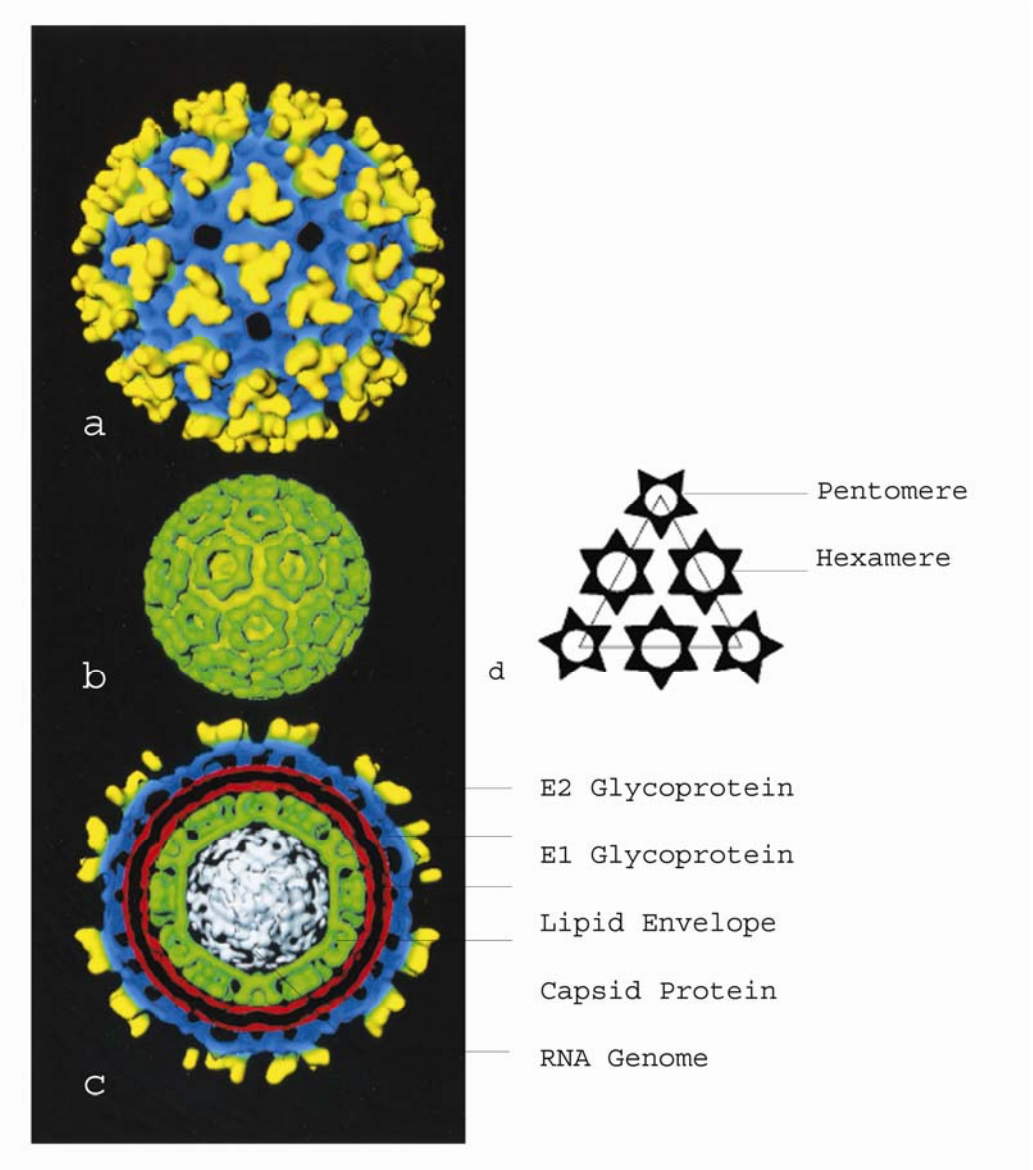

Figure 1: ***Structure of VEE***. (a) Three dimensional structure of the VEEV virion. Outer spike trimers are indicated in yellow and blue indicates the envelope. (b) Three dimensional structure of VEE virus nucleocapsid. (c) Cross-sectional view of VEE virus perpendicular to the threefold axis: trimers (yellow); envelope skirt (blue); virus membrane (red); nucleocapsid (green); and RNA genome (white). (d) Schematic representation of pentameric and hexameric capsomere organization within the nucleocapsid of VEE virus. (*Adopted from Paredes A, Alwell-Warda K, Weaver SC, Chiu W, Watowich SJ. Venezuelan equine encephalomyelitis virus structure and its divergence from old world alphaviruses. TJ Virol. 2001 Oct;75(19):9532-7*)

Structure

Alphaviruses are single stranded RNA viruses. VEEV virions are 60-65nm in diameter. Single strand RNA genome is enclosed in icosahedral capsid. This nucleocapsid is enclosed in a host plasma membrane derived lipid bilayer envelope. Two virus encoded glycoprotein, E1 and E2 are incorporated in the envelope. E1 and E2 glycoprotein heterodimers make spike like trimer on the surface of the virus. 240 copies of each glycoprotein interact with 240 copies of capsid protein. (Figure 1 a and c) [Griffin 1999].

Genome

Genome of VEEV consists of one 49S, 11.444 kb, single stranded, message sense RNA [Kinney et al 1989, Oberste et al 1996] (Figure 1b) 5` capped and 3` polyadenylated. 5` capped genome encodes for non-structural polyproteins nsp1-4. The terminal 26S of the genome encodes for structural proteins C, E3, E2, 6K and E1 (Figure 1b) [Griffin 1999, Weaver et al 1992, 2004]. The message sense RNA genome of VEEV is infectious under suitable conditions [Griffin 1999, Smith et al 1997, Guzman et al 2005] and cDNA copies of the genomic RNA can be used to transcribe infectious RNA [Kolykhalov et al. 1992, Pratt et al 2003].

Capsid

RNA genome is enclosed in a capsid made of 240 copies of a single protein [reviewed in Strauss and Strauss 1994, Weaver et al 2004, Smith et al 1997]. Capsid is made of multiple copies of single polypeptide, C protein [Schlesinger 1988]. The capsid protein is 275 amino acid long [Griffin 1999]. The N-terminal region binds to genomic RNA [Strauss et al 1968, Paredes et al 2001] and C-terminal is presumed to bind to cytoplasmic tail of E2 glycoprotein. The nucleocapsid has T=4 asymmetry [Choi et al

1991, Paredes et al 2003] indicating one-to-one interaction of each capsid protein with envelope glycoprotein (Figure 1b) [reviewed in Strauss and Strauss 1994]. The isolated nucleocapsid is ~ 420Å in diameter and when enclosed in envelope it is ~ 384-392 Å in diameters [Paredes et al 2001, 2003]. Capsid proteins are arranged in pentons and quasihexons (Figure 1d) [Paredes et al 2003]. Recently capsid protein has been shown to be responsible for shutting down host cellular transcription by VEEV and EEEV [Gramashova et al 2006].

Envelope

Envelope is derived from host cell membrane and has two virus encoded glycoprotein, E1 and E2 integrated in the membrane [Griffin 1999, reviewed in Strauss and Strauss 1994]. Envelope is composed of 80 protein trimers [three heterodimers of E1 and E2 glycoprotein] with each trimer forming a part of overlapping series of pentons and hexons capsomer arranged on a T=4 icosahedra lattice [Paredes et al 2001, Strauss and Strauss 1994]. Envelope trimers have a counter clock wise hand and rise ~ 50 Å above envelope protein surface and have an outer diameter of ~ 139 Å. The distance between the two tips of the trimer is ~ 107 Å. [Paredes et al 2001]. The trimers are maintained by E1-E1 interaction [reviewed in Strauss and Strauss 1994]. E2 protein is 423 amino acid long and E1 is 442 amino acid long having three and two N-linked glycosylation site respectively [Griffin 1999]. E2 glycoprotein is formed from the precursor called PE2 or p62 that is cleaved into E2 and E3 [reviewed in Strauss and Strauss 1994, White and Fenner 1994, Griffin 1999]. E3 is 59 amino acid long and probably serves as a signal sequence for E2 and is shed into supernatant fluid after cleavage [Griffin 1999, Strauss and Strauss 1994]. Another protein 6K is 55amino acid

long and probably serves as a signal peptide for E1 and may also be incorporated into the virion [Strauss and Strauss 1994, Griffin 1999]. By analogy with semliki forest virus (SFV) E2 has a cytoplasmic domain of about 30 amino acid residue [Simmons et al, 1980] and E1 has a short cytoplasmic domain of only one or two amino acid residue [Griffin 1999].

Replication of VEEV

The first step of cellular infection of VEEV is electrostatic adsorption to the cell membrane. Penetration is complete in 30 min at 35^0C and viral RNA and viral RNA polymerase can be detected by 2hr post infection. There is a latent period of 3-4 hr followed by increasing virus in supernatant from 8-14 hour, persistent VEEV virion production may occur upto 80hr post infection [reviewed in Johnson and Martin 1974, Strauss and Strauss 1986]. VEEV has a broad host range, it infects cells from lower to higher vertebrates [Shope 1985, Scherer et al 1976] and many insects mainly mosquitoes and ticks [Ludwig et al 1996, Cupp et al 1979, Linthicum et al 1991, Turrel et al 1992, Scherer et al 1976, Saudia et al 1975]. VEEV causes persistent lifelong infection in arthropods and a short acute infection in vertebrate host. Similarly in cell culture VEEV causes a persistent infection of mosquito cells. VEEV does not shut down the mosquito cell macromolecule synthesis and low levels of viral products are produced. In vertebrate cells, it shuts down the host cell protein synthesis and high level of virus products are synthesized [Esparza and Sanchez 1975, reviewed in Strauss and Strauss 1994]. *In-vitro* VEEV can utilize laminin binding protein as a receptor for entry into the cell via receptor mediated endocytosis [reviewed in Weaver 2004, Ludwig et al 1996]. Since laminin binding domains are highly conserved, it may explain the broad range of VEEV hosts. By

analogy in sindbis virus amino acid changes in the E2 protein alter viral entry and affects early steps in viral replication [Griffin 1998]. Mutations in E2 protein especially at the glycosylation site have been considered to be important in VEEV virulence determination and enzootic phenotype evolution [Kinney et al 1998, Brault et al 2005, Anishchenko et al 2006].

Binding of the virion to the host cell membrane provides the necessary physical association of virion to host cells and thus facilitates the entry of the virus into cell. After endocytosis a hydrophobic domain of the E1 glycoprotein undergoes conformational change and initiates the fusion of the virus envelope with the endosomal membrane at low pH [Weaver 2004, Lanzrein et al 1994, Griffin 1998]. The low pH of the endosomes initiates disruption of the E1-E2 heterodimers and the E1 fusion loop domain is inserted into the target membrane. It is a low pH and cholesterol dependent interaction. A mono-trimer of E1 glycoprotein is formed which then undergoes conformational changes, make a ring of 5-6 mono-trimers and bring about the fusion of virus envelope and endosomal membrane [reviewed in Kielian 2006]. The genome is then released into the cytoplasm and the entire replication occurs in the cytoplasm though, functional nucleus is required for infection in mosquito cells and to some extent in the vertebrate cells. Following release into the cytoplasm 5` capped two third viral genome is translated into large polyproteins, P123 and P1234 [reviewed in Strauss and Strauss 1994, Kinney et al 1989], which has a protease activity and cleaves itself into four early non structural proteins namely, nsp1, nsp2, nsp3 and nsp4. Nsp1 (535 amino acid in VEEV) is involved in the methylation and capping of the viral RNA, initiation of viral minus strand RNA synthesis and modulation of proteinase activity of nsp2 (Figure 2). Mutation in nsp1 affects the

neurovirulence of Sindbis virus [Heise et al 2000]. Nsp2 (794 amino acid in VEEV) has both viral protease and helicase activity. C-terminal of VEEV nsp2 has proteolytic activity and processes VEEV polyprotein complex to generate individual nonstructural proteins [Russo et al 2006, Russo and Watowich 2006]. Nsp2 also binds to ribosomal protein S6 and may contribute to the differential translation of host and viral message [Montgomery et al 2006]. In Sindbis and SFV, nsp2 is also suggested to make a switch from early to late phases of virus infection [Sawicki et al 2006]. Nsp3 (557 amino acid in VEEV) converts RNA replicase to plus strand replicase and Nsp4 (607 amino acid in VEEV) is viral RNA polymerase. These early proteins are required for the virus replication as their inhibition results in inhibition of virus replication [Schlesinger and Kaariainen 1980]. These nonstructural proteins then convert plus strand viral RNA to minus strand viral RNA. This minus strand RNA is then transcribed into full length genomic RNA and a small 26S sub genomic RNA corresponding to the 3`one third genomic RNA. The 26S sub genomic RNA is then translated into a polyprotein. This polypeptide contains from N-terminus to C-terminus, nucleocapsid, E3, E2 (E3 and E2 combined are called PE2), 6K and E1 protein. Nucleocapsid protein, called protein C, is a serine protease and cleaves itself from the polypeptide [reviewed in Strauss and Strauss 1994]. Once the nucleocapsid is released, the N-terminus region of polypeptide (PE26KE1) is inserted into endoplasmic reticulum (ER). PE2, 6K and E1 are sequentially cleaved by signalase inside ER lumen. E3 and 6K act as signaling sequences for the translocation of PE2 and E1 into the ER lumen. In ER PE2 and E1 forms heterodimers and are glycosylated in the ER lumen and transport through Golgi apparatus. During transport through the transgolgi network PE2 is cleaved to form E2 and E3 by cellular

proteinases, furin. The E2-E1 heterodimers are eventually transported to the cell surface [reviewed in Strauss and Strauss 1994 , Strauss and Strauss 1986]. Inside the cytoplasm highly charged N-terminus of the capsid protein (240 copies) binds to a single viral genomic RNA and closes upon itself to form an icosahedral T=4 symmetry. During budding of virus capsid contracts and there is a 1:1 interaction of 240 capsid proteins with the cytoplasmic tail of E2 glycoprotein in E2-E1 heterodimer [reviewed in Strauss and Strauss 1994, Garoff et al 2004]. The tyrosine residue in the E2 cytoplasmic tail is important for the hydrophobic interaction with the capsid protein and initiation of budding [reviewed in Garoff et al 2004]. A new model of horizontal interactions between the surface glycoproteins has been proposed to induce budding along with the nucleocapsid or glycoprotein derived budding model [Garoff et al 2004].

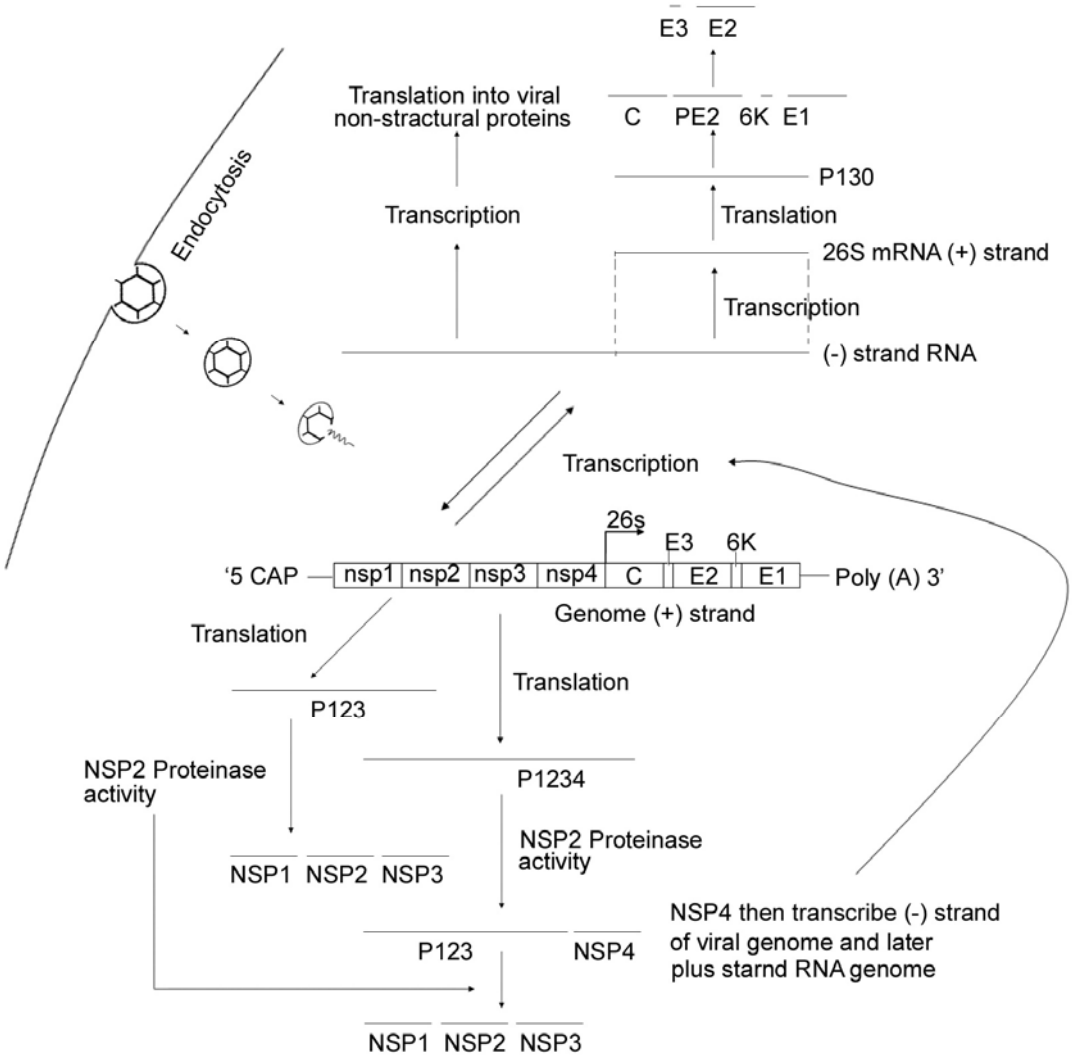

Figure 2: ***Replication of VEEV virus.*** After attaching to the host cell VEEV enters into the cell by endocytosis. In endolysosome VEEV envelope fuses with the endosomal membrane and the VEEV genome is released into the cytoplasm. In cytoplasm positive sense mRNA is translated into the early non structural proteins i.e. Nsp1 to 4. Nsp4 is a viral polymerase that then transcribes positive sense genome to negative sense RNA. From this negative sense RNA is then transcribed small positive sense 26s mRNA that is then translated into structural proteins i.e. C, E1, E2, E3 and 6K. Full length negative sense RNA is also transcribed into full length positive sense genomic RNA. *Information extracted from previous reports* (*Weaver et al 2004, Strauss and Strauss 1994, Kinney et al 1989*).

Pathogenesis of VEEV

Alphaviruses in nature are transmitted by mosquito vector in nature. VEEV causes a biphasic infection in equines and humans. Initial multiplication occurs in dendritic cells, monocyte macrophages, fibroblast and skeletal muscle, causes viremia and disseminates to other lymphatic organs [Jackson et al 1991, Henderson et al 1971, Bowen 1976, Grieder et al 1995]. Lymphatic phase is followed by the CNS phase [Charles et al 1995]. Entry of VEEV into brain is poorly understood but olfactory neuroepithelium is suggested to be primary route of entry by axonal transport through olfactory neurons. VEEV enters into brain through trigeminal nerve and brain endothelium later in the infection [Charles et al 1995, Ryzhikov et al 1995, Steele et al 2006]. In CNS, neurons and glias are the primary target of infection [Schoneboom 1999]. VEEV infection results in cell death, reactive gliosis and intense inflammatory response in brain characterized by perivascular cuffing and interstitial mononuclear infiltration [Jackson et al 1991, Grieder et al 1995, Schoneboom et al 2000, Ludwig et al 2001]. Neurodegeneration observed in VEEV infected brain is accounted to both VEEV infection of neurons and inflammation [Schoneboom 2000, Grieder et al 1995, Ludwig et al 2001, Jackson et al 1991].

Role of immune responses in VEEV encephalitis

Immune response against VEEV is complex. Virulent VEEV infects skin dendritic cells (DC) at the site of inoculation (mosquito bite or experimental injection), which migrate to draining lymph node following activation. Avirulent strain that is unable to spread beyond the draining lymph node fails to infect skin DC [MacDonald and Johnston 2000]. Anti-VEEV activity of Interferon alpha/ beta and interferon regulatory factor 1 and 2 in early protection from VEEV has been well established [Grieder et al

1999, White et al 2001]. VEEV spread to brain is accelerated in IFN α/β receptor knock out (IFNAR1$^{-/-}$) mice [Schoneboom et al 2000] and these mice have a very short survival time as compared to their wild type counterpart [White et al 2001]. Importance of inflammation in clearance of VEEV from brain and periphery is implicated in studies with IRF2 knock out (IRF2$^{-/-}$) mice where IRF2$^{-/-}$ mice have reduced inflammation, severe neurodegeneration and higher virus titer as compared to control C57BL/6 mice [Grieder and Nguyen 1999]. These mice also did not have any inducible nitric oxide synthase (iNOS) induction in brain and were not protected by attenuated strain of VEEV [Schoneboom et al 2000]. Further IFN-γ is up regulated upon virulent VEEV infection following the avirulent VEEV strain and may be involved in the protection conferred by avirulent attenuated VEEV strains towards virulent VEEV. Treatment with anti-IFN-alpha/beta antibody prior to VEE infection worsened virulent VEE disease [Grieder et al 1997]. The IFNAR1 $^{-/-}$ mice that lack the IFN α/β signaling exhibited amplified inflammation in spleen and brains [Schoneboom et al 2000]. Comparative study of the immunopathogenesis of VEEV in immunocompetent and immunocompromised SCID mice shows the importance of intact host immune system in clearing of virus from the peripheral tissues and serum. In the same experiment though, the mean survival time of SCID mice was longer than the wild type mice indicating the immunologic component of inflammatory damage in brain [Charles et al 2001]. Inflammatory response to VEEV in brain is not restricted to area positive for VEEV antigen and apoptosis of neurons occur in areas of astrogliosis along with areas positive for VEEV antigen [Schoneboom et al 2000]. VEEV infection of CNS results in marked encephalitis, astrogliosis and cerebral edema accompanied with up regulation of proinflammatory genes such as interleukins

(IL), IFN, iNOS and tumor necrosis factor- α (TNF-α) [Schoneboom et al 1999, 2000]. Furthermore, mice lacking iNOS and TNF-α expression have prolonged survival as compared to the controls. Following viral infection, astrocytes and microglia undergo transition involving proliferation, becoming phagocytic and finally cytotoxic, secreting cytokines, growth factors, and free radicals such as nitric oxide [Schoneboom et al 1999, 2000a]. However, a maximal immune response often involves collateral damage to uninfected cells and apoptotic neurons in brain have been shown to be associated with the astrogliosis and regions free of VEEV antigen [Sconeboom et al 2000a,b]. Collectively, these studies suggest that balanced inflammatory response is critical for early protection against VEEV and the extensive inflammation in CNS is responsible for the lethal outcome of VEEV infection in brain.

VEEV along with EEEV and WEEV is potential biological threat agents, because they can be economically grown into high titers in mass cultures, are susceptible to single nucleotide manipulation, relative stable in aerosol therefore, ease to disseminate, have ability to incapacitate and have high rate of infectivity in non-vaccinated populations.

Clinical Symptoms of disease

Equines*:* Equine infection of VEEV may be of three types: i) mild febrile reaction; ii) generalized disease characterized by fever, tachycardia, depression, anorexia and in some cases diarrhea; iii) encephalitis form where generalized disease is followed by CNS infection evident by circling, ataxia, head pressing, continuous chewing and hyper-excitability [Kissling and Chamberlain 1967, reviewed in Johnson and Martin 1974]. The epizootic IABC subtypes of VEEV only causes disease in equines and subtypes ID, IE, IF, II, III, IV, V and VI do not cause disease or cause a low level of

viremia but no encephalitis [Smith 1997 , Johnson and martin 1974, Weaver 2004]. Febrile illness is apparent by day 2 post infection and encephalitis symptoms appear around day 4-5 post infection. Death occurs by day 6-10 post infection [reviewed in Johnson and Martin 1974]. Estimated equine mortality rate in the epizootics is 19%-83% [Weaver 2004]. IABC and Trinidad donkey strain causes severe myeloid depletion of bone marrow, depletion of lymphoid tissue, necrotic and degenerative changes of pancreatic acinar cells. Histopathology of brain ranges from mild neutrophilic infiltration of basal ganglion to diffused inflammation including neuronal degeneration, satellitosis, gliosis, intensive neutrophilic infiltration of grey matter, perivascular cuffing, and necrotizing vasculitis [Reviewed in Johnson and Martin 1976].

Humans: VEEV infection in humans has an incubation period of 2-6 days and is accompanied by leukopenia, neutropenia and elevated glutamic-oxaloacetic transaminase [Smith 1997, Johnson and Martin 1976]. Symptom onset is abrupt and patient present with severe myalgia (thighs and lumbar region), fever, chills and retro orbital or occipital headache. Clinical sign include fever, tachycardia, nausea accompanied by vomiting and diarrhea in some. Inflamed pharynx was also reported in about a quarter of the patients (Johnson and Martin 1976, Smith et al 1997, Weaver 2004). Usually human infection of VEEV is symptomatic but in small number of cases (in natural outbreaks ~ 0.5% in adult and ~4% in children) infection proceeds to CNS. CNS infection is evident by lethargy, somnolence, mild confusion, and photophobia. Acute disease subsides with in day 4-6 and is followed by variable period of asthenia lasting for several weeks. Some cases experience biphasic illness with full blown clinical symptoms appearing 4- 8 days after initial occurrence [Johnson and Martin 1976, Weaver 2004]. Severe neurological disease,

more common in age 15 or less in natural outbreaks includes seizures, ataxia, stupor or coma, paralysis and sometime followed by death. For cases surviving the CNS infection neurological recovery is usually complete [Smith 1997, reviewed in Weaver 2004, reviewed in Johnson and Martin 1976]. Lethal VEEV infection has diffused congestion, edema and hemorrhage in brain, gastrointestinal tract and lungs [reviewed in Weaver 2004]. In children depletion of lymphoid tissue is prominent and is followed by a lethal course over 48 to 72hr [Smith 1997]. Both epizootic and enzootic strains infect humans [Smith 1997, Weaver et al 1996, Johnson and Martin 1976, Weaver 2004]. Cerebral edema, hemorrhage, neutrophilic infiltration and Purkinje cell destruction is reported in VEEV infected human brain [reviewed in Johnson and Martin 1976].

Treatment and Vaccine

There is no specific therapy for the treatment of VEEV infection or *togaviruses* as such. Treating viral encephalitis is difficult because of almost complete absence of effective anti-viral drugs against these infections. Further, common paradigms of viral elimination and tissue restoration subsequent to the inflammatory responses that are successful in many systemic viral infections fall short in the CNS. Here, specific limitations apply, and inflammatory reactions such as edema and targeted cell destruction can be more detrimental than helpful for the patient. Symptomatic treatment is done e.g., antipyretic, anticonvulsant and prevention of airways. Recently, a pool of siRNAs directed against various portion of VEEV genome has shown inhibition of VEEV *in vitro* [O'brien 2006]. Mucosal and circulating antibodies to E2 glycoprotein are protective against VEEV infection [Johnson and Martin 1976, Smith 1997, Weaver et al 1996, Weaver 2004]. There remains an urgent need for an efficient vaccine for immunization

against VEEV due to its ability to spread and infect through aerosol route (Steele et al 1998) and its potential use as a biowarfare agent [Hawley et al 1997]. Current live attenuated TC-83 vaccine [Berg et al 1961], which is under investigational new drug status, has limited use due to non-responders and residual virulence [Walton et al 1973, Pittman et al 1996, Alevizatos et al 1967, Ludwig et al 2001] and may not prevent against the broad range of VEEV strains [Reed et al 2005]. Several other passive and active immunization strategies have been tested [Phillpotts RJ 2006, Rao et al 2006]. Genetically engineered live attenuated strain such as V3526 has been shown to be protective in non human primate models of VEEV infection and is a promising candidate for VEEV vaccine [Fine et al 2006, Rao et al 2004, 2006, Reed et al 2005, Pratt et al 2003, Hart et al 2000]. Chimeric SIN/VEE [Paessler et al 2003, 2006], recombinant baculoviruses, adenoviruses and vaccinia virus expressing VEEV structure glycoprotein have also been tested [Hodgson et al 1999, Phillpotts et al 2005, Bennett et al 1998]. Monoclonal antibodies [Phillpotts RJ 2002, 2006], microencapsulated VEE virus vaccine [Greenway et al 1995, 1998] have also been tested and found to be protective against virulent VEEV challenge. Compounds such as melatonin have also been evaluated for their efficacy in increasing the efficiency of TC-83 vaccine [Negrette et al 2000, 2001]. Residual virulence, incomplete inactivation, short lived immunity, non- responders and or protection against only few stains of VEEV have plagued these efforts.

Animal Model to Study VEEV Pathogenesis

VEEV is endemic in rodents [Jackson et al 1991, Bowen 1976]. Mice, rats, hamsters and guinea pig serves as the experimental model of VEEV infection with mice being the best described. VEEV infection of non human primates such as Macaque is also

well described. Mice and Macaque infection with VEEV mimics the biphasic infection of VEEV in humans and is the model of choice to study VEEV pathogenesis [Jackson et al 1991, Grieder et al 1995, Reed et al 2005]. Several murine strains have been described as models such as BALB/c, C3H/Hen and Swiss CD-1 [Paessler et al 2003, Bigler et al 1974, Reynolds et al 1980, Spertzel 1975]. Both BALB/c and CD-1 mice initiate humoral antibody response following subcutaneous vaccination with TC-83 vaccine and are a commonly used model to study VEEV pathogenesis [Hart et al 1997, Grieder et al 2006, Steele et al 2006].

Potential Bio-Weapon

Although naturally transmitted by aerosol, it was appreciated relatively shortly after alphaviruses were first isolated that they were highly infectious by aerosol. Prior to the introduction of VEEV vaccines, VEEV was the most common laboratory-acquired infection. Both the United States (prior to 1969) and the former Soviet Union included VEEV as part of their offensive biological weapon programs. Alphaviruses can be economically grown into higher titer in mass culture, are susceptible to single nucleotide manipulation and are relatively stable in aerosol [Steele et al 1998]. VEEV is readily cultured *in vitro* and may have been genetically modified by Russian scientists to create a more potent VEEV/Smallpox hybrid biological warfare agent [Peterson R 1998] and is currently identified under potential biological threat agents [Hawley 2001].

Military Relevance and Significance

VEE poses a unique threat to US troops. US troops are susceptible to VEEV infection, because they are not routinely vaccinated. The currently available VEEV vaccine, the attenuated TC-83 strain, fails to induce neutralizing antibodies in

approximately 20% of those immunized. Thus, even with an aggressive vaccination program, a significant percentage of the troops remain vulnerable to VEE infection. Second, troops have a reasonable chance for exposure. VEEV is both an endemic pathogen in Central and South American countries where troops are deployed and it is also a weaponized biological warfare agent. VEEV is readily cultured in cells and is infectious when delivered by aerosol over large areas as shown by extensive modeling of battlefield hazard studies. Dosage footprints have been estimated for various combinations of delivery methods, dissemination efficiencies, topographies, and times of day. Incapacitation of at least 50% of unprotected personnel by VEEV infections is projected over areas greater than 1,000 km^2 in 30% of the scenarios. Without protection, four of the five Army units modeled in these scenarios would fall below 100% mission effectiveness. Finally, morbidity and casualties for the civilian population would be of identical or greater magnitude if not vaccinated. Mass exposure of US troops to VEE would result in an incapacitating illness of several weeks duration, characterized by severe headache, nausea, and vomiting that may lead to lethal encephalitis. Current therapies are limited by (a) lack of anti-viral treatments and (b) lack of knowledge about the pathophysiology of VEE. Therefore, evaluating the efficacy of novel therapeutic strategies is important to develop an effective agent, which can be used in the treatment of VEEV infection

Research Gaps, Hypothesis and Goals

Epidemiological studies with VEEV have been extensive, virus prevalence in nature, transmission cycle, host range and disease emergence has been well documented [reviewed in Weaver and Barrett 2004]. Importance of interferon in protection against

VEEV and detrimental effect of host immune response has also been studied [Charles et al 2001, Grieder et al 1997, White et al 2001, Schoneboom et al 2000]. It is also well studied that death following VEEV infection is due to neurological complications and virus from peripheral organs is efficiently cleared by healthy matured immune system of host. Detailed studies into the molecular mechanisms of VEEV infection and following inflammatory damage in brain are lacking. These studies are important to better understand the mechanisms of inflammatory reaction in brain and to determine the specific molecular targets for therapeutic purposes. Further, since there is no licensed vaccine for VEEV and conventional methods of VEEV inactivation and attenuated strains have failed to provide a solution, it is necessary to look for novel strategies of virus inactivation to generate vaccine candidates. This research has undertaken experiments to study the molecular mechanisms of VEEV pathogenesis in mice brain.

Earlier our laboratory has shown that Tunicamycin (TM), an antibiotic produced by *Streptomycis,* inhibit the infectivity of enveloped viruses that replicate by budding out such as vesicular somatitis virus (VSV), HSV and SFV. TM also enhanced the anti-viral activity of IFN [Maheshwari et al 1983, 1985]. This action of TM was found limited to *in vitro* studies and was speculated to be due to modification of viral envelope glycoprotein [Maheshwari et al 1983, 1980]. *In vivo*, semliki forest virus (SFV) and encephalomyocarditis virus (EMCV) virulence was increased when mice were treated with TM [Singh et al 1987, Maheshwari et al 1983]. Recently our laboratory has shown that TM also enhances the neuroinvasion of virulent and non virulent strains of VEEV [Steele et al 2006]. TM is known to alter the blood brain barrier (BBB) [Finnie and O'Shea 1990, Steele et al 2006] and therefore the plausible action of TM *in vivo* in

increasing the neurovirulence may be due to modulation of BBB, which may facilitate the increase of virus and peripheral immune cell load in the brain. This assumption is further strengthened by the observations that VEEV after initial appearance in olfactory lobe appears simultaneously at multiple places in various regions of the brain. Based on these observations it appears that BBB as such plays a crucial role in the pathogenesis of VEEV and importantly in the neuroinvasion of VEEV. The role of BBB and the factors that facilitate the modulation of BBB are poorly understood in VEEV pathogenesis of CNS. Therefore it is important to study the various factors that modulate BBB in VEEV infection. The central hypothesis of this aim is that the VEEV infection may result in the modulation and disruption of the BBB thus facilitating the VEEV neuroinvasion and the migration of immune cells into the brain. This may result in the extensive inflammatory response in brain resulting in the neuronal damage. To examine this hypothesis, experiments were designed to study the modulation of adhesion molecules in the brains of VEEV infected mice and their affect on the inflammation in brain.

As described earlier in pathogenesis section, inflammation in brain contributes to the neuronal damage in brain. Though inflammation has been widely reported in brains of the VEEV infected animals, specific molecular mechanism of virus recognition and inflammatory reaction in brain are lacking. As discussed before in the pathology, importance of IFN and host immune system is well studied. Expression of IFN, iNOS and TNF has been reported but broad spectrum inflammatory reaction and signaling is not yet studied in VEEV infection of brain. Lack of such knowledge is reflected in the missing targeted therapy for VEEV infection. By determining the molecular basis of inflammation in brain it may be possible to develop targeted therapy for the treatment of

VEEV infection in CNS. The central hypothesis of this aim is that VEEV infection of brain may modulate multiple mechanisms of inflammatory reactions resulting in the release of cytokine and chemokines that are cytotoxic to neurons. To examine this hypothesis, gene expression kinetics in VEEV infected mice brain was studied using mouse microarray panel for global gene expression. Further this study was extended to specifically study toll like receptor (TLR) and its signaling specific pathways in VEEV infected mice brain. By analogy in other viruses such as SFV, West Nile virus etc… TLR signaling is a key pathway of virus recognition and is responsible for the induction of multiple cytokines and chemokines in response to virus infection. TLRs and associated signaling has not been studied in VEEV infection and therefore it is important to examine various TLRs and their signaling to gain knowledge about the specific TLRs that may be modulated in brain upon VEEV infection. This knowledge will further be useful in developing targeted molecular therapy for treatment of VEEV infection in brain.

As described earlier in vaccine section, there is currently no FDA approved vaccine for VEEV prophylaxis and current experimental vaccines have several drawbacks. It is to be noted that various conventional methods such as formalin inactivation and live attenuated strains have failed to provide desirable immunity against VEEV. Other advanced approaches such as chimeric virion particles expressing VEEV proteins have also failed to give desirable results. Therefore, there is a need to develop non-conventional strategies for developing vaccine candidates for VEEV. A novel compound, 1-5 iodonaphthylazide (INA) has been reported to efficiently block the infectivity of various enveloped viruses such as HIV and influenza [Raviv et al 2005]. Efficacy of INA to inhibit VEEV infectivity was evaluated. The central hypothesis of this

project is that hydrophobic photoactive aryl azides like INA selectively penetrate into the hydrocarbon core of biological membranes. Upon irradiation, with UV light, these compounds directly bind to proteins and lipids embedded in the bilayer. The high partition coefficient targets and concentrates INA into the hydrophobic core of the membrane and selectively inactivates cellular or viral functions that are associated with this domain at the same time not affecting the extracellular domains protein or lipid protruding outside the membrane. Since, VEEV is enveloped viruses, INA in principal should concentrate in the hydrophobic domain of the virus envelope and upon irradiation with light should bind to and inactivate the virus glycoprotein. Since the extracellular domain of the glycoproteins shall not be affected with INA treatment followed by light irradiation, such inactivated virus particles should be able to elicit the immune response and protect the host from the virulent virus challenge. Studies were designed to test if INA can successfully inactivate virulent VEEV and if this treatment maintains the structural integrity of VEEV.

These studies therefore attempt to study the basic molecular mechanisms of VEEV infection and inflammation in mice brain to identify specific therapeutic targets for treatment of VEEV infection. Furthermore a novel strategy of VEEV inactivation will be tested to evaluate the efficacy of using INA for inactivation of VEEV for vaccine candidate development.

Chapter 1

Role of Adhesion Molecules in Venezuelan Equine Encephalitis Virus Pathogenesis in Mice Brain

Abstract

Entry of VEE virus into the brain is a major event in its pathogenesis. Route of entry into the brain is primarily through the olfactory tract, VEEV infects the olfactory neurons and migrate into the olfactory lobe by axonal transport. Virus entry into brain has also been reported through trigeminal nerve in the tooth pulp and through brain microvessels by BBB disruption. As shown with other alphaviruses such as sindbis and SFV, BBB disruption is important for the virus entry and inflammatory cell response in brain. Molecular events leading to the disruption of BBB are poorly understood in the VEEV pathogenesis. In this study, the expression kinetics of adhesion molecules in brains of mice infected with VEEV was studied. Intercellular adhesion molecule 1 (ICAM-1), and several other adhesion molecules expression increased with the progression of disease and were concomitant with the virus appearance in the brain. In ICAM-1 knock out ($ICAM1^{-/-}$) infected mice onset of clinical symptoms of disease was delayed and mortality was reduced by 10-20%. Inflammation in brain was reduced and delayed as compared to the wild type (WT) controls, whereas virus appearance was similar in between the two groups i.e. $ICAM1^{-/-}$ and WT mice. Microarray analysis of inflammatory gene expression showed reduced inflammatory gene expression in $ICAM1^{-/-}$ mice brain at 96 hr post infection over the WT mice brain. These findings are significant as it for the first time demonstrate the induction of adhesion molecules in the VEEV pathogenesis and delayed inflammation in absence of ICAM1 expression. These adhesion molecules may play a key role in the modulation of BBB and inflammation in

brain of VEEV infected mice.

Key words: Venezuelan Equine Encephalitis Virus, Adhesion molecules, Blood Brain Barrier, Encephalitis.

Introduction

BBB is a monolayer of cells that regulates the passage of solutes between the CNS and the blood. The restrictive properties of the BBB are formidable, essentially equaling that of the continuous cell membrane. This barrier (Figure 3) governs the entry and exit of the metabolic fluid, neurotransmitter precursors, and essential nutrients into the CNS [Xiang et al 2003, Dickstein et al 2000, DeLange 2004, Peters et al 2004, Kastin 2002, Sharp et al 2003, Stover et al 1997]. The endothelial cells forming the BBB are also enzymatically active and are source of cytokines, nitric oxide and can also secrete toxic factors [Redzic et al 2001, Johnson and Anderson 1996, Omari et al 2004, Mark et al 2004]. Each diverse aspects of BBB have been associated with disease, either being altered by disease or producing it [Webb and Muir 2000]. BBB largely defines the operating environment of the CNS by regulating the movement of substances between the blood, the cerebrospinal fluid and the brain. BBB both restricts and regulates the exchange of substance like cytokines and adrenocorticotropin (ACTH)-related compounds between the blood and the CNS and is involved in the pathophysiology of many diseases such as AIDS, viral encephalitis, Alzheimer's and experimental encephalitis [Callahan and Ransohoff 2004, Dallasta et al 1999, Eugenin and Berman 2003].

Adhesion molecule on the surface of the endothelial cells of BBB plays an important role in the pathogenesis of many encephalopathies like multiple sclerosis (MS)

[Hartung et al 1995, Muller et al 2004], viral encephalitis [Hartung et al 1993] or cerebral malaria [Turner et al 1994, Gray et al 2003].

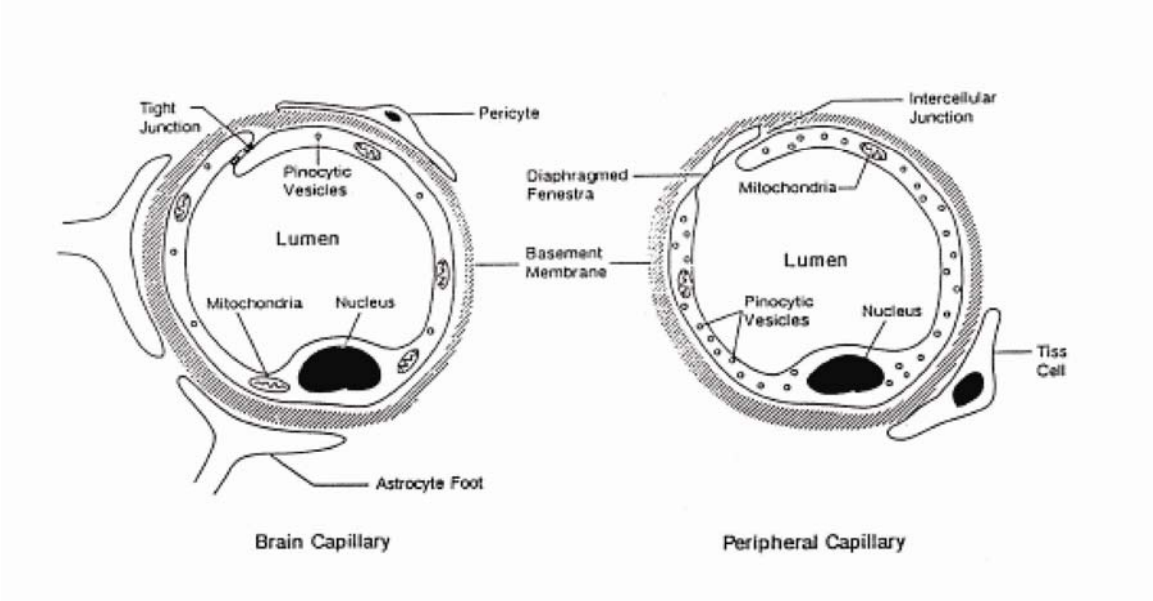

Figure 3: ***Diagrammatic representation of brain and peripheral capillaries***. There are distinctive morphological differences between the brain and peripheral capillaries. Peripheral capillaries are fenestrated and have loose intercellular junctions in between the capillary endothelial cells where as brain endothelial cell junctions are tight junctions and are held together by tight junction proteins. Brian capillary walls are thick and are not fenestrated. Pinocytic vesicles in the endothelial cell of peripheral capillaries are abundant as compared to the brain capillaries have where as brain capillaries endothelial cells has more mitochondrial count over the peripheral capillaries. Further brain capillaries are supported by the astrocytic processes and pericytes from the brain side of the capillary wall that further contribute to the structural integrity of the brain capillary wall or BBB. (*Figure adopted from Donald W Miller. Immunobiology of the blood-brain barrier. Journal of NeuroVirology (1999) 5, 570- 578*).

Intercellular adhesion molecule-1 (ICAM1) is a member of immunoglobulin superfamily [Greenwood et al 2002]. It has an extracellular N` terminal domain, a hydrophobic transmemebrane domain and a cytoplasmic C` terminal domain. ICAM1 was originally described as an adhesion molecule on the surface of the endothelial cells but recent studies have implicated it in cell signaling in endothelial and lymphoid cells [Hubbard and Rothlein 2000, reviewed in Greenwood et al 2002]. The cytoplasmic domain interacts with α-actin cytoskeleton, β-tubulins of cellular microtubles and GAPDH [Frederic et al 1996]. Binding of extracellular domain of ICAM1 with its ligands such as Anti-ICAM1 antibodies or activated leucocytes induces dimerisation of ICAM1 [Casasnovas et al 1998, Durien-Trautmann et al 1994]. This dimerisation increases the activity of non-receptor tyrosine kinases (src) and phosphorylation of the actin binding domain (cortactin). ICAM1 mostly has a constitutive expression and is widely distributed especially in leucocytes, brain microvessels endothelial cells and many other tissues [reviewed in Roebuck and Finnegun 1991, Dietrich 2002]. ICAM1 expression increases on the brain endothelium linings in neuroinflammatory manifestation of brain under the influence of interleukins, tumor necrosis factor (TNF) and interferon gamma (IFNγ) in MS, experimental autoimmune encephalitis (EAE) and Alzheimer's disease [Sobel et al 1990, O'Neill et al 1991, Perry et al 1997]. ICAM1 signaling is implicated and plays an essential role in the transmigration of activated leucocytes into the CNS during brain inflammation [Whalen et al 2000]. Activated leukocytes attaches to the brain microvessel endothelium by a ligand-receptor interaction. Activated leukocyte that are tethering and rolling on the vascular endothelium, under the influence of chemokines, lipid mediators and other proinflammatory cytokine, express lymphocyte functional associated antigen-1

(LFA1). ICAM1 is a ligand for this receptor and thus binding of LFA1 to ICAM1 results in the adhesion of activated leukocytes onto the brain endothelium [Marlin and Springer 1987]. Once adherent, leucocytes migrate across the endothelium and enter into the inflamed tissue [Dietrich et al 2002]. Binding of ICAM1 to its receptor induces dimerisation and these homodimers may then further localize and cluster on the cell membrane [Adamson et al 1999]. ICAM1 dimerisation induces cytoskeletal rearrangement through actin stress mediated by increased GTP-rho protein inside the cells [Adamson et al 1999]. ICAM1 activation also increases src kinase activation [Durien-Trautmann et al 1994]. Activated tyrosine kinase phosphorylates focal adhesion kinases (FAK), paxillin a focal adhesion-associated, phosphotyrosine-containing protein [Schaller MD 2001] and p130 (130-kDa tyrosyl-phosphorylated species) [Timms JF et al 1998] that are localized at the cell-cell junction of the brain endothelial cells [Etienne et al 1998]. Disruption of cytoskeleton of endothelial cells and treatment with C3 transferases, that inhibits rho protein results in inhibition of monocyte adhesion to endothelial cells, clustering of ICAM1 on endothelial cell surface, actin fiber stress , phosphorylation of FAK, paxillin and p130 and ultimately inhibition of lymphocyte migration [Wojeiak-Stothard et al 1999, Adamson et al 1999]. Dimerisation and cross linking of ICAM1 also induces increase in cellular Ca^{++} concentration which may activate src through protein kinase C (PKC) [Pfau et al 1995, Etienne et al 1998]. This Ca^{++} increase occurs due to VCAM cross linking [Lorenzon et al 1998]. Treatment of endothelial cells with Ca^{++} chelators results in inhibition of lymphocyte transmigration through endothelial cells [Eitenne-Manneville et al 2000]. PKC is also known to regulate epithelial junction complexes via phosphorylated Vinculin [Perez-Monero et al 1998] or

accludin [Sakakibara et al 1997]. Increased Ca^{++} in the endothelial cells results in the release of nitric oxide (NO) and other cytokines. NO and cytokines may directly act at the endothelial cell junction and thus participate in the opening of the cell-cell junction [Durien-Trautmann et al 1994]. Therefore, activation of ICAM1 due to binding of activated lymphocytes induces several signaling pathways that converge with each other and results in the opening of the tight junction of brain endothelial linings and transmigration of lymphocytes into brain. This model is described in Figure 4. Once inside the brain leukocytes then engage ICAM1 molecules on the surface of the brain astrocytes resulting in the release of TNF and other chemokines and cytokines [Greenwood et al 2002]. This results in a cycle where more and more leukocytes enter into the brain resulting in a strong inflammatory reaction inside the brain. Similar to ICAM1 vascular cell adhesion molecule 1 (VCAM-1) is also essential for the transendothelial migration of the T cells [Reiss and Engelhardt 1999]. BBB breakdown and ICAM-1 expression on brain endothelium are observed during other encephalitic alphavirus such as SFV infection [Eralinna et al 1996]. Circulating leucocytes from MS patients express higher levels of LFA-1, a ligand of ICAM-1, than the leucocytes in the normal individuals. AIDS encephalitis also involves the upregulation of the ICAM-1 and VCAM –1 expression in BBB. These molecules are also synthesized in the astrocytes and are induced in a dose and time dependent manner by HIV-1 derived Tat protein [Woodman et al 1999, Wu et al 2000]. HIV-tat protein also induces the expression of the ICAM-1, VCAM-1 and endothelial-leukocyte adhesion molecule 1 (ELAM-1) in human endothelial cells, which allowed the adhesion of the human pro-myelomonocytic HL-60 cells to the endothelial cells [Dhawan 1997]. Activated microglial cells also express the

ICAM-1 expression in the moloney murine leukemia virus (ts-1) mediated neurodegeneration.

Once the VEEV is inside the brain there is no physiological barrier that can stop the further spread of the virus into the brain as it spreads from the point of entry into the brain to other parts of the brain, though it does not follow the neuronal path and virus appears in brain randomly in different regions of brain [Steele et al 2006] indicating virus entry into brain though other route that could be safely assumed to be BBB. Also the immune response produced by the host cells itself become detrimental as it becomes the cause of the neuronal damage in the VEEV free areas of the brain [White et al 2001, Schoneboom et al 2000]. Thus understanding how the VEEV modulates the BBB can give insight into the virus and virus infected immune cells entry into the brain and can identify the therapeutic target in VEE pathogenesis. In this study differential regulation of the adhesion molecules was evaluated by cDNA microarray and ICAM-1 gene expression was identified along with several other adhesion molecules. ICAM-1 and VCAM-1 expression in brain was further studied by immunohistochemistry. Role of adhesion molecule in VEEV pathogenesis was then evaluated using ICAM1 knock out (ICAM1-/-) mice. Onsets of disease were delayed and the mean survival time increased in ICAM1-/- mice. This was accompanied by delayed and reduced inflammation and down regulation of several chemokines and interleukins in the brains of ICAM1-/- mice. These results further strengthens the observations that extensive immune/inflammatory response towards VEEV in brain results in damage to brain tissue contributing to the severity of disease and therefore, balanced immune response is critical for better outcome for host following CNS infection of VEEV.

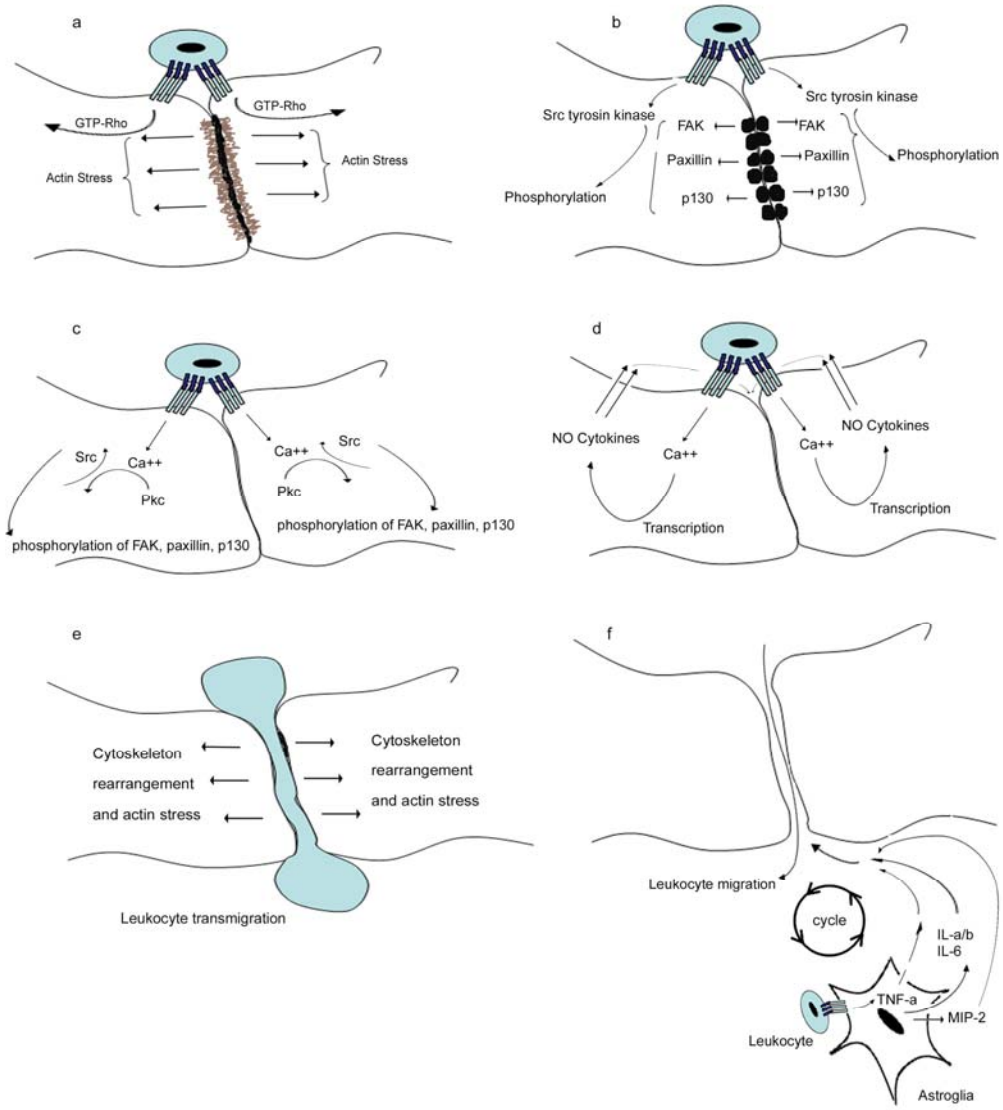

Figure 4: ***Modulation of BBB by ICAM-1***. Engagement of ICAM-1 on the endothelial cells of the brain capillaries by its receptor LFA-1 induces dimerization and clustering of the ICAM-1 resulting in following multiple molecular changes. (a) GTP-rho complexes are formed which then induces stress on the cytoskeleton and participates in the opening of tight junction between endothelial cells. (b) Src tyrosine kinase is activated which then further phosphorylates the proteins that are localized at the cell-cell junctions and modulates opening of these junctions. (c) Cellular Ca^{++} level is increased which results in activation of src kinase via PKC activation resulting in further phosphorylation of junction proteins. (d) Increased cellular Ca^{++} level results in induction of nitric oxide (NO) and cytokines, which further act individually at the cell-cell junctions. (e, f) the above modulations results in the opening of the tight junctions between the endothelial cells and leukocytes transmigrate into the brain. Inside brain they can further engage the ICAM-1 expressed on the astrocytes resulting in the cytokines such as interleukins and TNF-α, which then further act upon the tight junctions of BBB and result in more and more leukocyte transmigration into brain. *Information extracted from Greenwood et al)*

Materials and Methods

Animals

Following animal strains were used for this study.

1.) Five to six week old male CD-1 mice were obtained from Charles River Laboratories, Wilmington, MA, USA.

2.) Five to six week old male B6.129S4-Icam1tm1Jcgr/J and C57BL/6J 000664 mice were obtained from Jackson Laboratories Bar Harbor, Maine, USA. B6.129S4-Icam1tm1Jcgr/J mice are homozygous for the *Icam1*^{tm1Jcgr} targeted mutation. This strain was generated by insertion of a vector containing the *neo* resistance gene into exon 4 of the *Icam1* gene. The 129-derived J1 ES cell line was used. (Stock No. 002867, Jackson mice database). The background strain for these mice is C57BL/6 mice.

Mice were housed in micro isolator cages and were provided food and water ad libitum with a 12hr light/dark cycle. For VEE study animals were housed in animal biosafety level 3 (BSL-3) facility and all the experiments were carried out in accordance to Guide for the Care and Use of Laboratory Animals (Committee On Care And Use Of Laboratory Animals Of The Institute Of Laboratory Animal Resources, National Research Council, NIH Publication No. 86-23, revised 1996) and university protocol for handling animals in ABSL3 facility.

Virus and Challenge Procedure

Molecularly cloned, virulent strain of VEEV, V3000 was used (Grieder FB et al, 1995). This is a complementary DNA clone of the full length virulent Trinidad donkey strain of VEEV genome, generated in an expression plasmid downstream of a T7

promoter, resulting in the virulent parental strain. VEEV was kindly provided by Dr. Franziska B Grieder, Uniformed Services University of The Health Sciences (USUHS), Bethesda, MD, USA. Working dilutions of virus were made by diluting stock virus solution in 1 X Dulbecco's phosphate buffered saline (DPBS) (Gibco, Invitrogen Corporation, Carlsbad, CA) that supplemented with 0.1% fetal bovine serum (FBS) (Mediatec) (VWR, West Chester, PA 19380). Mice were given mild inhalation anesthesia using, methoxyflurane and 1000 pfu of V3000 in 25µl volume was inoculated in the left rear footpad using sterile 26G(3/8) intradermal bevel needle on 1cc sterile syringe (Becton Dickinson and Company, Franklin Lakes, NJ 07417).

Brain Tissue Isolation

Three animals from each group were anesthetized using isoflurane and sacrificed at 6, 24, 48, 72 & 96 hr post infection. Brain was isolated and right hemisphere was fixed in 10% buffered neutral formalin (BNF) for 3-4 weeks. Half of left hemisphere was put in Trizol and immediately stored at -80^{0}C. Other half was put in 1X DPBS supplemented with 0.1% FBS and stored on dry ice and later homogenized. Homogenized brain was then centrifuged at high speed for 5min and supernatant was stored at -80^{0}C. Formalin fixed tissues were transferred into fresh 10%BNF and taken out from BSL-3 facility, routinely processed, and embedded in paraffin sections.

In ICAM-1 knock out mice experiments, 6 mice were euthanized at 48, 72 and 96 hr post infection and brains were isolated and processed as described above.

Total RNA Preparation

Frozen tissues were minced over ice using sterile RNase free polypropylene pestle (Kimble/Knotes, Vineland, New Jersey, USA) and motor in 1.5 ml microfuge tubes and

total RNA was extracted using TriZol kit (Invitrogen life technologies Carlsbad, CA) as per the manufacturer's directions. Briefly, homogenized tissues were mixed and incubated in Trizol for 5 min at room temperature (RT). 0.2 ml of chloroform (Fisher Scientific, Pittsburgh, PA 15275) for every 1ml of Trizol used was added. Mixing was done vigorously by hand and samples were incubated for 3 min at RT. Samples were then centrifuged (TOMY MTX-150, Tomy Tech USA, Inc. Palo Alto, CA- 94303, USA) at 12000g/15min/4^0C. Top aqueous phase was transferred to new 1.5 ml microfuge tubes and 0.5 ml of Isopropyl alcohol was added for every 1 ml TriZol used in order to precipitate RNA. Samples were mixed and incubated at RT for 10 min. RNA was palette by centrifuging at 12000g/10min/4^0C. Supernatant was removed and RNA palette was allowed to air dry for 5 min. RNA palette was then solublilized in 50µl of RNase/DNase free water (GIBCO, Invitrogen Corporation, Carlsbad, CA). Total RNA was quantitated using Beckman DU640 spectrophotometer (Beckman instruments Inc., Columbia, MD, USA) and RNA quality was determined by electrophoresis on 1% agarose formaldehyde gel.

cDNA Microarray

cDNA microarray was performed for the mouse extracellular matrix and adhesion molecule panel using cDNA microarray kit (Superarray Bioscience Corporation, Fredrick, MD) as per the manufactures protocol. Briefly, procedure can be divided into three steps; Step I: Probe synthesis, step II: Hybridization and step III: Detection. Briefly, probe was synthesized using Ampolabeling kit (Superarray Bioscience Corporation, Fredrick, MD). Annealing mix was incubated at 70^0C for 3min, cooled and maintained at 37^0C for 10 minutes. RT cocktail was added to the annealing mix and reverse

transcription was carried out at 37^0C for 30min. Reaction was stopped by incubating at 85^0C for 5 min. LPR cocktail was added to the RT reaction and PCR was carried out using following cycles: initial denaturation of 85^0C for 5 min, then denaturation at 85^0C for 1 min; annealing at 50^0C for 1 min; extension at 72^0C for 1 min for 26 cycles, a final extension was done at 72^0C for 5 min. Probe was denatured by adding buffer D to the reaction mixture and incubating at 68^0C for 20 min followed by neutralization with Buffer E and incubation for 10 minutes. Pre-hybridization was done for 2 hr at 60^0C with GEAhyb Hybridization solution supplemented with 100µg/ml of denatured salmon sperm DNA (Invitrogen life technologies Carlsbad, CA) followed by overnight hybridization with hybridization solution (probe re-suspended in 750ul of pre-hybridization solution). Detection was done using Chemiluminescence detection kit (Superarray Bioscience Corporation, Frederic, MD). After Hybridization array membranes were washed twice for 10 min at 60^0C each with pre-warmed wash solution 1 (2XSSC, 1% SDS) followed by wash solution 2 (0.1XSSC, 0.5%SDS. Blocking was done for 2hr, 10-20rpm at room temperature with 2ml of blocking solution Q followed by incubation with 2ml of binding solution (1:15000 Ap-strep in 1xBuffer F). Membranes were then washed four times using 4ml 1X buffer F followed by rinsing 4 times with 2ml buffer G. Detection was done using CDP star substrate supplied with the kit. Membranes were incubated with 1ml of CDP star substrate for 3min, 10-20 rpm at room temperature. CDP star substrate was discarded and excess was blotted off the membranes. Membranes were immediately put in between clean plastic sheet. X-ray films (Kodak Scientific Imaging Film, Eastern Kodak Company, Rochester, NY-14650) were exposed to the membrane for different time period and films were developed using Kodak Image developer (Eastern Kodak

Company, Rochester, NY-14650). X-ray images were scanned and converted to digital image for further analysis.

Image development and analysis: Image analysis was done using GEArray Expression Analysis Suite (Superarray Bioscience, Frederic, MD). Gene densities were expressed as average density (total density divided by number of pixels). Background detection was done locally i.e. each expression value was individually subtracted with value from the area outside the capture grid but within the spot cell area. Data normalization was done with non-modulating house keeping gene, Glyceraldehyde-3-phosphate dehydrogenase (GAPDH). A gene was considered "absent" where the average density of the spot was less than the mean value of the local backgrounds of the lower 75 percentile of all non-bleeding spots. All other spots were considered “present”.

Immunohistochemical Staining for ICAM-1, VCAM-1 & VEE Virus Antigen

Primary antibodies used were hamster anti mouse ICAM-1 IgG (BD Biosciences Pharmingen San Diego, CA), goat polyclonal anti mouse VCAM-1 IgG (Santa Cruz Biotechnology, Inc. Santa Cruz, CA 95060) and rabbit polyclonal anti serum raised against VEEV kindly provided by Franziska B Grieder, USUHS. Immunostaining was performed using an indirect avidin-biotin-immunoperoxidase technique (Vectastain ABC Elite, Vector laboratories, Burlingame, CA) as specified by the manufacturer. Briefly, Tissue sections were de-paraffinized by three passages through clearing agent Citrosolv (Fisher Scientific, USA) for 5 min each. Sections were then hydrated by sequential washes of absolute (200 proof) ethanol followed by 95% ethanol and then one wash of 70% ethanol 5 min each. Sections were then washed in PBS for 10min. Antigen retrieval was done by boiling in citrate buffer. Tissue sections were incubated in 10M sodium

citrate, Ph 6.0, at 98^0C for 20 min and then were allowed to cool for 25 min RT while still immersed in the citrate buffer. Antigen stabilization was done by incubating tissue sections in 3% Glycine (Mallinckrodt, Inc. Paris, Kentuky) for 10min at RT. Intracellular peroxidase was blocked by incubating tissue sections in 3% hydrogen peroxide (H_2O_2) for 10 min at RT. Blocking was done with 2.5% normal horse serum and tissue sections were overlaid with serum and incubated for 1 hr at RT. Excess serum was blotted off and tissue sections were then overlaid with primary antibodies i.e. hamster anti mouse ICAM-1 IgG (BD Biosciences Pharmingen San Diego, CA) or goat polyclonal anti mouse VCAM-1 IgG (Santa Cruz Biotechnology, Inc. Santa Cruz, CA 95060) or rabbit polyclonal anti serum raised against VEEV. Sections were incubated overnight at 4^0C in a humidified chamber. As a negative control, sections from each test were incubated with normal serum IgG separately. Brian sections from the saline injected controls were also included as background controls. Sections were then washed three times in 1X PBS, for 5 min each and were overlaid with biotin labeled anti-rabbit IgG secondary antibody, and incubated for 10 min at RT followed by three washes in 1X PBS for 5 min each. Tissue sections were then incubated with streptavidin-peroxidase enzyme complex for 5 min at RT followed by three washes with 1X PBS for 5 min each. Sections were then incubated with enzyme substrate, diamine benzidine (DAB) solution, (DAB:H_2O_2:Buffer::1:2:1) for 7 min at RT for color development and were then washed 3 times with 1X PBS for 5min each and counter stained with Harris hematoxylin for 10min at RT followed by rinsing under tap water for three to five min. Sections were then dehydrated by passing through the gradients of ethanol in following sequence: 70% ethanol for 5 min followed by 5 min incubation in 95% and 100% ethanol , three times

each. Sections were then washed three times for 5 min each in citrasolv. Excess citrasolv was blotted off and slides were mounted with mounting medium and covered with coverslips. Slides were allowed to dry overnight at RT and sections were analyzed by bright field microscopy.

Oligo Microarray

Pathway focused Oligo GEArray® Mouse Inflammatory Cytokine and Receptors and Toll Like Receptor Microarray kit (Superarray Bioscience Corporation, Frederick, MD) was used and experiments were carried out as per the manufacture's protocol. RNA was converted to cDNA and that cDNA was used to make cRNA probe. Array membranes were hybridized with this probe and detected with chemiluminscence detection kit.

Probe synthesis: Probe was synthesized using Ampolabeling-LPR 2.0 kit (Superarray Bioscience Corporation, Frederick, MD). Annealing mixture was prepared by mixing 2-3 µg RNA with 1µl of buffer G1 and RNase DNase free water was added to make final volume to 10µl. This mix was incubated at 70^0C for 10 min followed by 4^0C for 2 min. Simultaneously, cDNA synthesis master mix was prepared by mixing 4µl of RNase free water, 4µl of 5X cDNA Synthesis buffer mix (G3), 1µl RNase Inhibitor (RI) and 1µl cDNA Synthesis Enzyme mix (G2) per reaction. cDNA synthesis was carried out by mixing 10µl of Annealing mix with 10µl of cDNA synthesis master mix per reaction and incubating at 42^0C for 50 min. cDNA synthesis reaction was stopped by incubating samples at 70^0C for 5min. Samples were then kept on ice. cRNA synthesis master mix was prepared by mixing 16µl of 2.5X cRNA Amplification Buffer (G24), 2µl of 10mM Biotin UTP (Roche Applied Science, Indianapolis, IN 46250), 2µl Amplification Enzyme

mix (G25) per reaction. cRNA amplification was carried out by mixing 20µl of cDNA synthesis reaction (pre-warmed to 37^0C) with 20µl of cRNA synthesis master mix per reaction and incubating at 37^0C for 5 hours. This cRNA probe was then stored at -20^0C. cRNA Purification was done by using cRNA purification kit (Superarray Bioscience Corporation, Frederick, MD). Each cRNA probe sample was made to 100µl volume by adding 60µl of RNase DNase free water and was transferred to new 1.5ml microfuge tubes. 350µl of Buffer G6 and 350µl of 100% room temperature ethanol was added to each cRNA probe and mixed. This solution was then loaded onto a spin column provided with the kit and columns were placed in a collection tube. Columns were centrifuged at 8000x*g* for 30sec and flow through was discarded. Now 600µl of buffer G17 (ethanol added to it) was loaded onto the column and centrifuged at 8000x*g*. Flow through was discarded and 200µl of Buffer G17 was again loaded onto the column and centrifuged at 11000x*g*. Flow through was discarded and columns were rotated dry at 11000x*g* for 2min. Collection tube was discarded and columns were placed in the elution tubes. Immediately 50µl of room temperature RNase DNase free water was loaded at the center of the column and columns were incubated at room temperature for 2min followed by centrifugation at 8000x*g* for 1min. Columns were discarded and eluted cRNA probe was stored at -20^0C. 1µl of cRNA was used to quantitate the yield of cRNA probe using Beckman DU640 spectrophotometer (Beckman instruments Inc., Columbia, MD, USA).

Array Membrane Pre-Hybridization: For both pre-hybridization and hybridization, hot air, rotating hybridization chamber (Techne Hybridiser HB-1D, Techne Inc., Burlington, NJ-08016) was used. Microarray membranes were purchased from Superarray Bioscience Corporation, Frederic, MD in polypropylene tubes. These tubes containing microarray

membranes will be called array tubes through out the protocol. Array membranes were made wet with 5ml of RNase DNase free water (GIBCO, Invitrogen Life Technology, Carlsbad, CA) and incubating at 60^0C for 5min with 10-20 rpm in hybridization chamber. Array membranes were then pre-hybridized with 2ml of GEA Hyb hybridization buffer pre-warmed to 65^0C, incubated at 60^0C/10-20 rpm for 2hr.

Hybridization: Hybridization solution was made by mixing 4µg of cRNA probe with 750µl of GEA Hyb hybridization buffer pre-warmed to 65^0C. Pre-hybridization buffer from the array tubes was discarded and hybridization solution was added to the array tubes. Array tubes were then placed in the hybridization chamber and overnight hybridization was carried out at 60^0C/ 10-20 rpm.

Washing: Hybridization solution was removed and microarray membranes were washed for 15 min at 60^0C/10-20 rpm each with pre-warmed wash solution 1 (2XSSC, 1% SDS) and wash solution 2 (0.1XSSC, 0.5%SDS) respectively.

Chemiluminescence's development and detection: All the steps from here onwards were carried at room temperature and shaking was done on rotating shaker, Roto-Shake Geine (Scientific Industries, Inc. Bohemia, NY-11716). Blocking was done for 2hr/10-20 rpm with 2ml of blocking solution Q followed by incubation with 2ml of binding solution (1:15000 Ap-strep in 1x buffer F) for 10min/10-20 rpm. Array membranes were then washed four times at 10-20 rpm with 4ml of 1X buffer F for 5min each. Following washing array membranes were rinsed four times with 3ml of buffer G for 3min each at 10-20 rpm. Chemiluminescence's detection was done by incubation membranes with 1ml of CDP star substrate supplied with the kit for 3min, 10-20 rpm. Array membranes were then immediately removed from the array tubes and excess CDP star substrate was

blotted off. Array membranes were then kept in between clear transparent plastic sheet. Care was taken not to dry the array membranes.

Image development: X-ray films (Kodak Scientific Imaging Film, Eastern Kodak Company, Rochester, NY) were exposed to the membrane for different time period and films were developed using Kodak Image developer (Eastern Kodak Company, Rochester, NY). X-ray images were scanned and converted to digital image for further analysis.

Analysis: Image analysis was done using GEArray Expression Analysis Suite (Superarray Bioscience, Frederic, MD). Gene densities were expressed as average density (total density divided by number of pixels). Background detection was done locally i.e. each expression value was individually subtracted with value from the area outside the capture grid but within the spot cell area. Data normalization was done with non-modulating house keeping gene, Glyceraldehyde-3-phosphate dehydrogenase (GAPDH). A gene was considered "absent" where the average density of the spot was less than the mean value of the local backgrounds of the lower 75 percentile of all non-bleeding spots. All other spots were considered “present”.

Reverse Transcription (RT)

cDNA was synthesized by RT using the first strand synthesis kit (Invitrogen Life Technology, Carlsbad, CA.) as per the manufactures protocol. Briefly, primer mixture was prepared by mixing 1µg of RNA with 1µl of 10mM dNTP mix and 1µl of oligo dt and incubation at 65°C for 5 min. Reaction mixture (2 µl 10X PCR buffer, 4 µl 25mM $MgCl_2$, 2 µl 0.1MDTT, 1 µl of RNase inhibitor per reaction) was prepared separately and 9 µl of reaction mixture was mixed with primer mix from each sample. Samples were

preheated to 42°C for 2 min and 1 µl of reverse transcriptase enzyme (SSII) was added to each reaction tube. Reverse transcription was carried out 42°C for 50 min and reaction was stopped by incubating samples at 70°C for 15 min. Residual RNA was digested by 1 µl of *E. coli* RNase H at 37°C for 20 min and samples were stored at -20°C.

Polymerase Chain Reaction (PCR)

PCR was done using PCR supermix (Invitrogen Life Technology, Carlsbad, CA) as per the manufacturer's protocol. Briefly, for each reaction 45 µl of PCR supermix was mixed with 30ng of each forward and reverse primers each, one to 2 µl of cDNA from RT reaction and final volume was made to 49µl with RNase DNase free water (GIBCO, Invitrogen Life Technology, Carlsbad, CA). Primers for PCR were: ICAM-1 forward primer (5' CAACTGGAAGCTGTTTGAGCTG 3'), ICAM-1 reverse primer (5' GTGTTCACAGTCTTGCTCCAT-3'). VCAM-1 forward primer (5'-CCTCACTTGCAGCACTACGGGCT-3'), VCAM-1 reverse primer (5'-TTTTCCAATATCCTCAATGACGGG-3'). GAPDH forward primer (5' CCATCACCATCTTCCAGGAGCGAG 3'), GAPDH reverse primer (5' CACAGTCTTCTGGGTGGCAGTGAT 3'). ICAM-1 cDNA amplification was performed according to following protocol: initial denaturation at 94°C for 3min; then 35 cycles of denaturation at 94°C/1min, annealing at 60°C/1min, extension at 72°C/ 2min and a final extension was done at 72^0C/5 min. VCAM-1 cDNA amplification was performed according to following protocol: initial denaturation at 94°C for 4min; then 40 cycles of denaturation at 94°C/1min, annealing at 61°C/1min, extension at 72°C/1min and a final extension was done at 72^0C/10 min. GAPDH cDNA amplification was performed according to following protocol: initial denaturation at 94°C for 3min; then 30

cycles of denaturation at 94°C/ 30 sec, annealing at 62°C/ 45 sec, extension at 72°C/30 sec. PCR product was visualized by electrophoreses on 1.2% agarose gel and staining with ethidium bromide. Specific amplification was determined by comparing the size of product on gel relative to known DNA molecular weight marker.

Results

VEEV Pathology in Brain

Following the challenge with the virus animals became sick as early as 24 hour post infection as evident by ruffled fur and hunched back. VEEV specific antigen staining shows virus appearance in the brain by 72 hour post infection. VEEV was scattered through out the brain at 72 hour post infection and at 96 hour post infection virus was widely spread though out the brain (Figure 5). Virus antigen was primarily localized in the neurons but could also be found in brain glial cells and cells of lymphoid origin (Figure 6f). Inflammation started appearing at 48hr post infection in the meninges and the olfactory lobe. Inflammation was extensive by 72hr post infection and extends into the midbrain. By 96hr post infection inflammation is extensive and through out the brain (Figure 6a and e). Inflammation was observed localized both within the regions of brain associated with and with out the viral antigen (Figure 6a and d, Figure 7). At 96hr post infection cells of lymphoid origin were seen infiltrating the brain around the inflamed blood vessels and have traveled some distance form the site of infiltration (Figure 6e and Figure 8a). Neurophagia (association of glial or lymphoid cells with dying neurons) was seen in the inflamed regions with or with out VEEV antigens (Figure 7c and Figure 8c, d). Staining of serial sections for H&E, fibrinogen, VEEV antigen and ICAM1 revealed localization/leakage of fibrinogen around inflamed brain microvessels indicating BBB

disruption (Figure 6c). Inflamed vessels endothelium was positive for ICAM1 staining and the region around the vessels was extensively infected with VEEV virus (Figure 6b and d). Hyperchromatic neurons (a hallmark of dying neurons) were observed both associated only with the inflammation and with VEEV antigen (Figure 6f and Figure 7). Region around the inflamed blood vessels also revealed inflammatory damage such as demylenation (Figure 6g) was observed around the inflamed vessels.

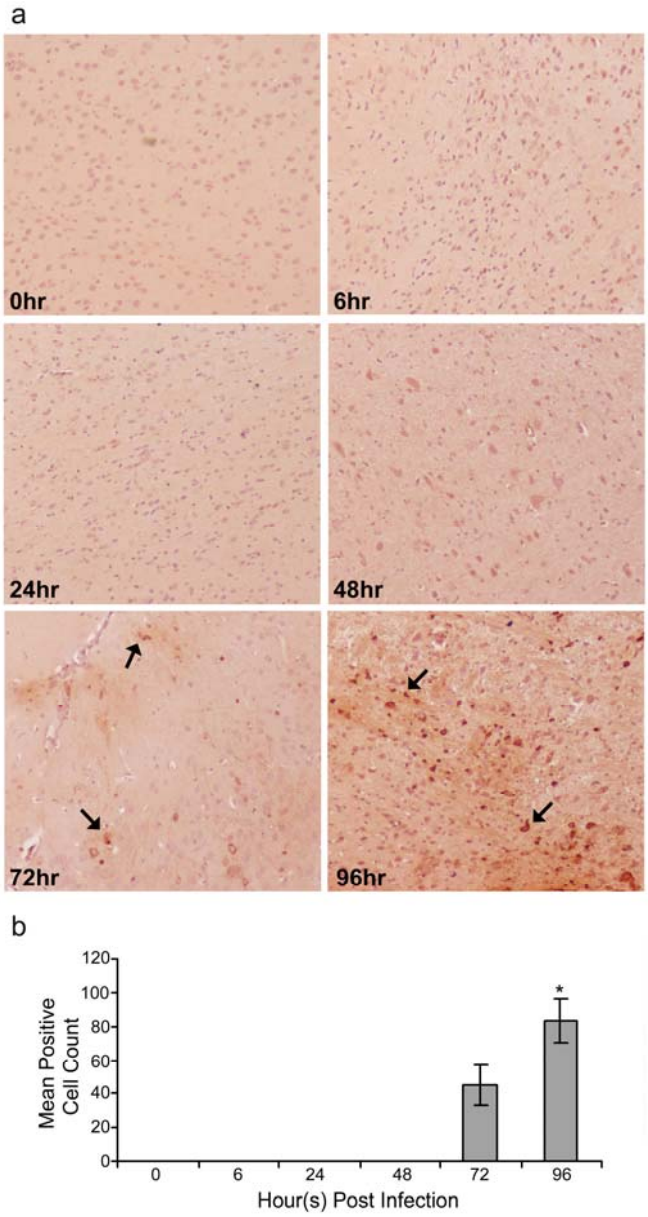

Figure 5: ***Localization of VEEV antigen in mice brain.*** (a) Paraffin embedded formalin fixed tissue sections were studied for VEEV antigen using immunohistochemistry. VEEV appeared in brain at 72 hr post infection and at 96 hour post infection virus was present through out the brain. (b) Number of the cells showing positive staining for VEEV was counted in seventeen fields (20X). Cell counts were significantly higher at 96 hr post infection as compared to 72 hour post infection. Values are expressed as mean ± SEM. * $p< 0.007$.

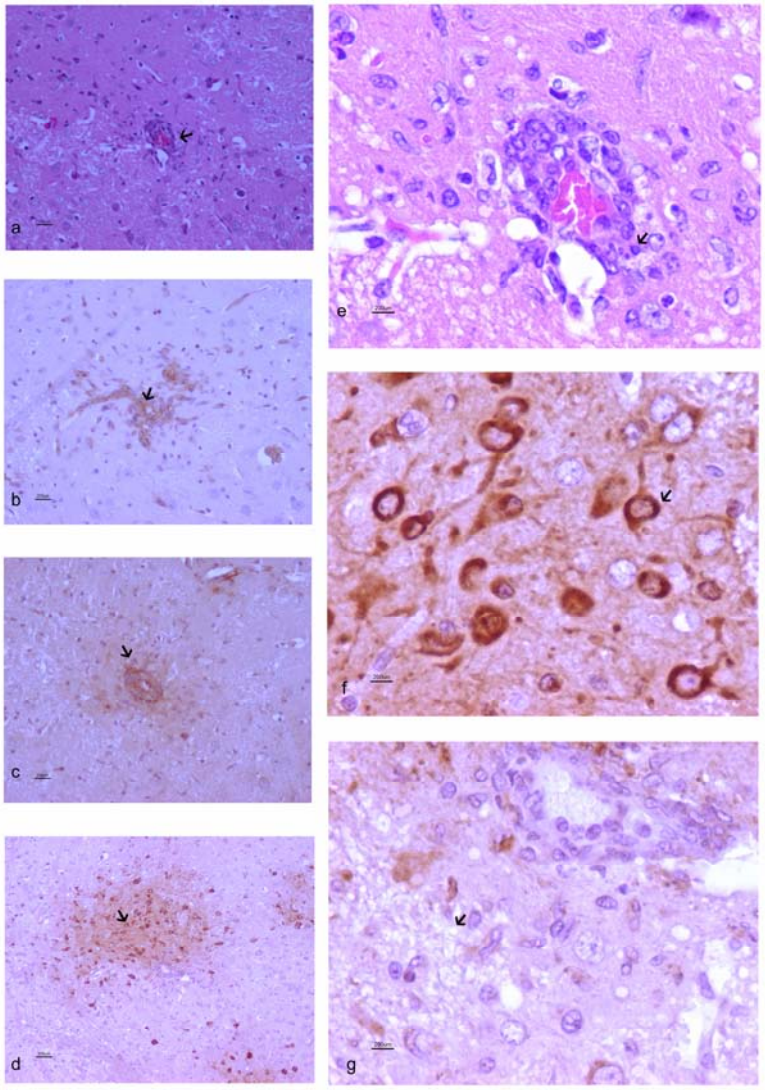

Figure 6: ***Histological evaluation of VEEV pathogenesis in mice brain at 96 hr post infection.*** (a) H & E staining of VEEV infected mice brain showed multiple foci of inflammation through out the brain. (b) Endothelial lining of inflamed vessels were thick and positive for ICAM-1 staining in serial section of the brain. (c) Fibrinogen staining of the serial sections localized fibrinogen leakage indication BBB disruption around the inflamed vessels. (d) Extensive VEEV specific staining revealed numerous cells infected with VEEV around the inflamed vessels. (e) Neutrophils and other cells of lymphoid origins were observed escaping from the walls of inflamed vessels. (f) Neurons were primarily infected with VEEV. VEEV antigen was also localized in glia and cell of lymphoid origin. (g) Demylination was observed around the inflamed vessels.

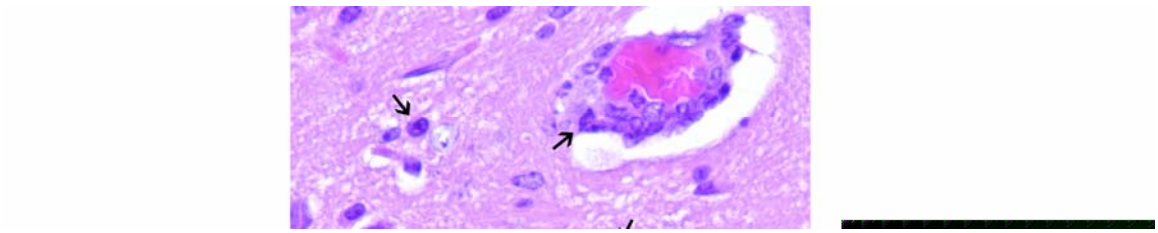

Figure 7: ***Inflammation associated with hyper chromatic neurons in regions free of VEEV antigen.*** (a, b) Hyper chromatic neurons (hall mark of dying neurons) were observed around the inflamed vessels. (c) Serial sections stained for VEEV antigen showed no staining for VEEV antigen in these areas. Neurophagaia (association of lymphocytes with dying neurons) was also observed in these areas.

Modulation of Adhesion Molecules in VEEV infected Mice Brain

cDNA microarray analysis revealed several adhesion molecules being modulated in brain upon VEEV infection (Figure 9). These genes are further classified based on there biological function (Table 2). 1.) Cell Adhesion Molecules genes: a.) *Transmembrane molecules*: *Cdh5*, and *Pecam1* expression was upregulated in VEEV infected mice brain over control as the disease progressed. Where as *Cdh3*, *Cdh4* and *Ncam1* expression was down modulated in VEEV infected mice brain as compared to control; b.) *Cell-Cell Adhesion*: *ICAM1* expression was differentially regulated as disease progressed. Its expression was absent as was in control in VEEV infected mice brain at 6 and 12 hr post infection. *ICAM1* expression was induced at 24 and 48hr post infection and again was absent at 72 and 96hr post infection. Its expression was again detected at 120hr post infection. *VCAM1* expression was upregulated as early as 6hr post infection. Its expression was down modulated at 24 and 48hr post infection and again upregulated at 72, 96 and 120 hr post infection; c.) *Cell-Matrix adhesion*: *Ceacam1*, *Itga7*, *Itga8*, *ItgaX* and *Itgb1* expression was down modulated in VEEV infected mice brain as compared to the control. *Itga3*, *Itga5* and *ItgaE* expression was differential modulated in VEEV infected mice brain. Their expression was down modulated at 6 and 12 hr post infection but increased several folds at 24 and 48hr post infection and was again down modulated there after till 120 hr post infection; d.) Other adhesion molecules; *Ctnnd2* expression was upregulated through out the study; 2.) Extracellular Matrix (ECM) proteins genes: e) *Basement Membrane constituents*: *Laminin B1* and *procollagen* expression was down modulated through out the study; f.) *ECM proteases*: *Adamts8* and *MMP16* expression was differentially regulated in VEEV infected mice brain. Their expression was absent at 6 and 12 hr post infection and was upregulated several fold

(*Admats8*) and was induced (*MMP16*) at 24 and 48hr post infection. Their expression again was down modulated and was absent at 72, 96 and 120hr post infection. *CatsB* and *CatsD* expression was also differentially regulated. Their expression was induced at 6 and 12 hr post infection then down modulated at 24 and 48 hr post infection and was again induced at 72, 96 and 120hr post infection. *MMP24* expression was down modulated through put the study. *MMP19* expression was down modulated early in the study but latter increase and was similar to the control; g.) *ECM protease inhibitor*: *CladeE* expression was down modulated through out the study. Other two MMP inhibitor *Timp1* and *Timp2* expression was absent early in the study. Their expression was induced in the VEEV infected mice brain latter in the infection; h.) *Other ECM molecules gene*: *Extracellular matrix protein 1* and *fibronectin* expression was down regulated through out the study. *Thrombospondin 1* expression was differentially regulated. Its expression was absent in the VEEV infected mice brain at 6 and 12hr post infection and was upregulated several fold at 24 and 48hr post infection. Its expression was again down modulated and was absent at 72, 96 and 120hr post infection.

ICAM-1, VCAM-1, Cathepsin B, Cathepsin E, Timp1 and MMP2, MMP9 and MMP8 gene expression by RT-PCR

Randomly selected genes were validated by PCR analysis. Basal level of *ICAM1* expression was seen in saline controls and 6hr post VEEV infection in mice brain. Expression of *ICAM1* increased as the disease progressed and was highest at 120hr post infection. Upregulation of *ICAM 1* was statistically significant ($P \leq 0.5$) at 12, 48, 96 and 120 hr pots infection. Similarly, *VCAM1* expression increased as the disease progressed. Basal level of *VCAM1* expression was detected in saline control and 6hr post VEEV infection. Expression was highest at 120hr post infection and was statistically significant

at 96hr post infection (Figure 10). Basal level expression of *TIMP1* was seen at 6, 12 and 24hr post infection and then its expression increased as the disease progressed. *Timp1* expression was significantly upregulated at 72 and 96hr post infection. Basal level of *Cathepsin B* and *E* expression was detected at 6hr post infection, their expression increased as the disease progressed but was not statistically significant. *MMP2*, *MMP8* expression was also studies. *MMP2* expression was not modulated post VEEV infection and remained approximately same through out the infection in mice brain. *MMP8* expression was similar to basal expression till 72hr post infection but was significantly higher at 96 and 120hr post infection (Figure 10).

ICAM-1 and VCAM1 Protein Expression in the VEEV Infected Mice Brain

ICAM1 and VCAM1 protein expression was evaluated by immunohistochemistry using ICAM1 and VCAM1 specific antibodies. ICAM-1 expression in the brain of the infected mice increased with the progress of the disease. Immunohistochemical localization revealed ICAM1 and VCAM expression specific to the brain microvessel endothelial linings ICAM-1 expression was not detected in saline control and at early time point of 6 hour post infection. Its expression appeared at 24 hour post infection and was specific to the endothelial cell linings of the blood vessels in the brain. ICAM-1 expression increased significantly by 48 hour post infection and remained significantly higher all through the infection (Figure 11). VCAM-1 expression was induced at 24 hour post infection which then increased with the progress of the disease and virus appearance in the brain. VCAM-1 expression reached peak at 72 hour post infection and remained elevated by 96 hour post infection (Figure 12).

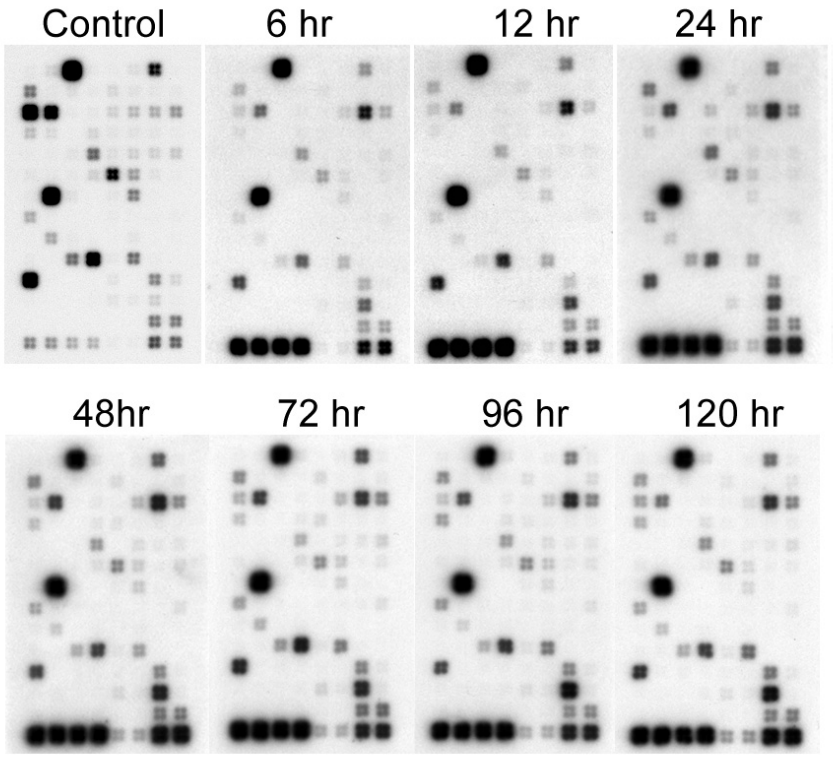

Figure 9: ***cDNA Microarray for extracellular matrix and adhesion molecules in VEEV infected mice brain.*** cDNA microarray was done as described in methods and X-ray images were developed and converted to digital images. These images were then quantified using GEArray analysis suite software.

Table 2: ***Differential regulation of adhesion and extracellular matrix proteins genes in VEEV infected mice brain***.

UniGene ID	Functional Grouping (Gene)	Hours Post Infection						
		6	12	24	48	72	96	120
	Cell Adhesion Molecules							
	Transmembrane molecules							
Mm.21767	Cadherin 5 (Cdh5)	(A)	(A)	P. I.	P. I.	1.7	P. I.	P. I.
Mm.343951	Platelet/endothelial cell adhesion molecule 1 (Pecam1)	0.82	0.82	49.98	53.16	0.82	2.14	2.34
Mm.4658	Cadherin 3 (Cdh3)	(A)	(A)	(A)	(A)	(A)	(A)	(A)
Mm.184711	Cadherin 4 (Cdh4)	(A)	(A)	(A)	(A)	(A)	(A)	(A)
Mm.4974	Neural cell adhesion molecule 1 (Ncam1)	0.34	0.26	0.9	0.85	0.81	0.56	0.65
	Cell Cell Adhesion							
Mm.90364	Intercellular adhesion molecule 1 (ICAM1)	(A)	(A)	P. I.	P. I.	(A)	(A)	P. I.
Mm.76649	Vascular cell adhesion molecule 1 (VCAM1)	5.89	7.41	(A)	(A)	5.89	5.66	6.27
	Cell Matrix Adhesion							
Mm.322502	CEA-related cell adhesion molecule 1 (Ceacam1)	0.21	0.19	0.49	0.6	0.35	0.23	0.42
Mm.57035	Integrin alpha 3 (Itga3)	(A)	(A)	2.17	2.5	(A)	(A)	(A)
Mm.16234	Integrin alpha 5 (fibronectin receptor alpha) (Itga5)	(A)	(A)	13.21	9.36	(A)	(A)	(A)
Mm.179747	Integrin alpha 7 (Itga7)	(A)	(A)	(A)	(A)	(A)	(A)	(A)
Mm.329997	Integrin alpha 8 (Itga8)	0.48	(A)	(A)	(A)	1.05	(A)	0.73
Mm.96	Integrin, alpha E, epithelial-associated (ItgaE)	(A)	(A)	1.88	2.96	(A)	(A)	(A)
Mm.22378	Integrin alpha X (Itgb3) (ItgaX)	0.44	0.42	(A)	(A)	0.48	0.51	0.54
Mm.263396	Integrin beta 1 (fibronectin receptor beta) (Itgb1)	0.29	0.25	(A)	(A)	0.67	0.66	0.38
	Other adhesion molecules							
Mm.218891	Catenin (cadherin associated protein), alpha-like 1(Ctnna1)	(A)	(A)	1.2	1	(A)	(A)	(A)
Mm.321648	Catenin (cadherin associated protein), delta 2	4.84	5.51	3.66	3.91	3.47	3.63	3.51

	(Ctnnd2)							

Table Cont…

	Extracellular Matrix (ECM) Proteins							
	Basement membrane constituents							
Mm.172674	Laminin B1 subunit 1	0.29	0.41	(A)	(A)	0.38	0.26	0.29
Mm.181021	Procollagen, type IV, alpha 2	(A)	(A)	(A)	(A)	(A)	(A)	(A)
	ECM Proteases							
Mm.100582	A disintegrin-like metallopeptidase with thrombospondin type 1 motif, 8 (Adamts8)	(A)	(A)	16.21	23.73	(A)	(A)	(A)
Mm.236553	Cathepsin B	P. I.	P. I.	(A)	(A)	P. I.	P. I.	P. I.
Mm.231395	Cathepsin D	P. I.	P. I.	(A)	(A)	P. I.	P. I.	P. I.
Mm.230249	Cathepsin E	(A)	(A)	(A)	(A)	(A)	(A)	(A)
Mm.204820	Matrix metallopeptidase 16	(A)	(A)	P. I.	P. I.	(A)	(A)	(A)
Mm.131266	Matrix metallopeptidase 19	(A)	0.37	(A)	(A)	1.09	0.54	0.81
Mm.330707	Matrix metallopeptidase 24	(A)	(A)	(A)	(A)	(A)	(A)	(A)
	ECM Protease Inhibitor							
Mm.250422	Serine (or cysteine) peptidase inhibitor, clade E, member 1	(A)	(A)	(A)	(A)	(A)	(A)	(A)
Mm.8245	Tissue inhibitor of metalloproteinase1	(A)	(A)	P.I.	P.I.	P.I.	P.I.	P.I.
Mm.206505	Tissue inhibitor of metalloproteinase2	(A)	(A)	(A)	(A)	P.I.	P.I.	P.I.
	Other ECM molecules							
Mm.3433	Extracellular matrix protein 1	(A)	(A)	(A)	(A)	(A)	(A)	(A)
Mm.193099	Fibronectin 1	(A)	(A)	(A)	(A)	(A)	(A)	(A)
Mm.4159	Thrombospondin 1	(A)	(A)	7.49	7.85	(A)	(A)	(A)

(A) = Absent; P.I. = Present in VEEV infected. ;
Yellow = same expression as control = No modulation;
Green = Down regulation; Red = Up-regulation; In Yellow Box = Absent in control;
(A) In Green Box = Present in control

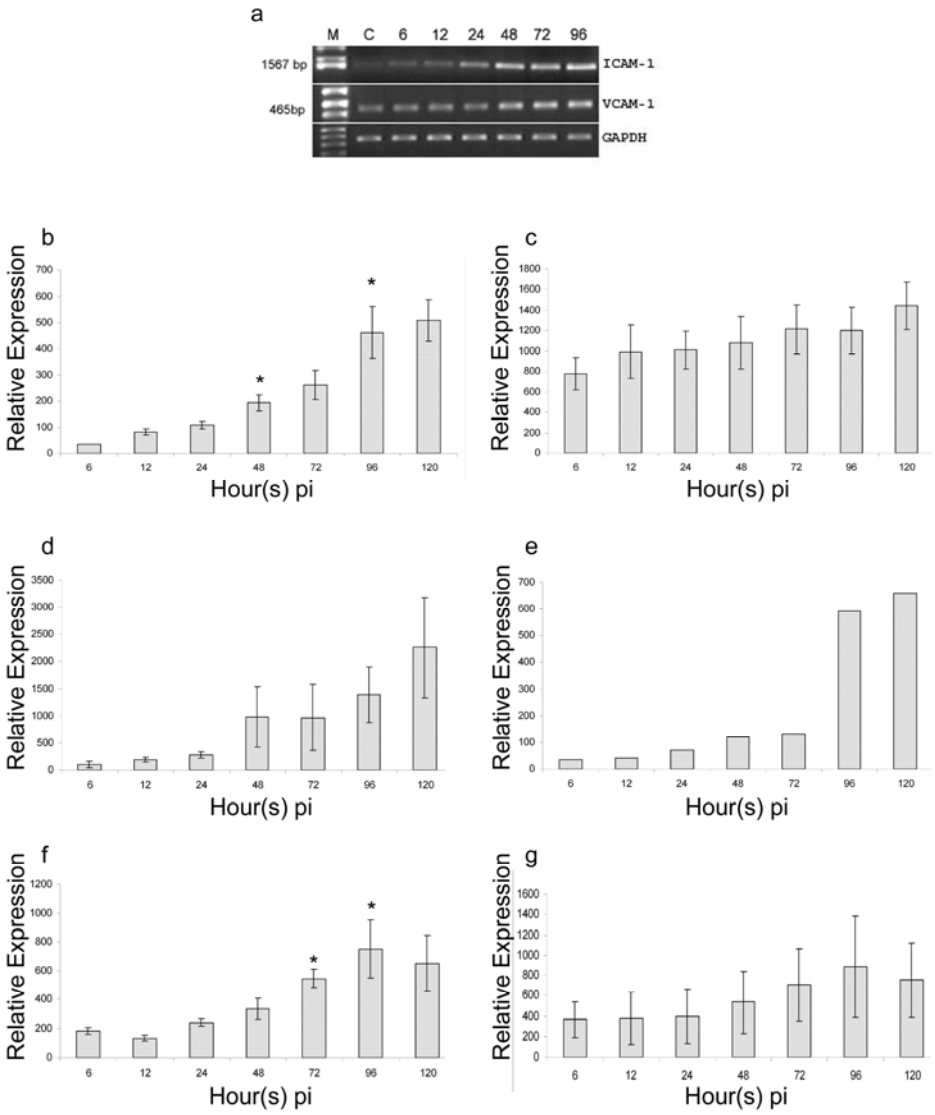

Figure 10: ***Expression of ICAM-1and VCAM-1 mRNA in VEEV Infected mice brain.*** (a) Total RNA was extracted from the brain and 1µg of RNA was subjected to RT-PCR analysis. Lanes: M-DNA Marker; C- Saline injected control; 6- Six hour; 12-twelve hour; 24- Twenty four hour; 48- Forty eight hour; 72- Seventy two hour; and 96- Ninety six hour post infection (pi). Equal amount of RNA in RT-PCR expression was determined by analyzing GAPDH as shown in the lower panel. This is the representative of three repeats with similar results. Quantitative estimation was done by densitometry analysis of the PCR product. Values were normalized to the corresponding values of the house keeping genes for individual samples: b- ICAM-1; c- MMP2; d- VCAM-1; e- MMP8; f-Timp1; and g-cathepsin E. Values are expressed as mean ± SEM. * $p < 0.05$

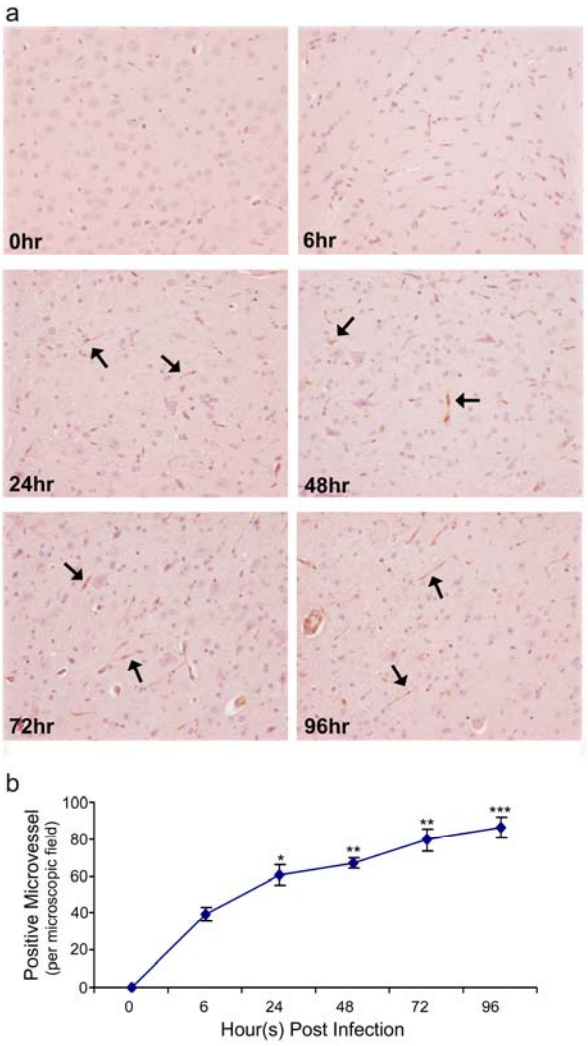

Figure 11: ***Immunohistochemistry for ICAM-1 Expression in VEE virus infected mice brain.*** (a) Paraffin embedded formalin fixed tissue sections were studied for ICAM-1 expression using immunohistochemistry as described in materials and methods. ICAM-1 expression was absent at 0 hr and 6 hr post infection. Its expression increased at 24 hr post infection and was specific to endothelial cell lining of blood vessels in brain. There after it continued to increase till 96 hr post infection. ICAM-1 expression profile was concomitant with the progress of disease and appearance of virus in the brain. Objective used 20X. (b) Number of the cells showing positive staining for ICAM-1 were counted. Mean number of the positively stained cells per eleven fields (20X) was counted. Cell counts were significantly higher at all the time points as compared to six hour post infection. Values are expressed as mean ± SEM. * $p < 0.006$, ** $p < 0.0002$, *** $p < 0.000004$.

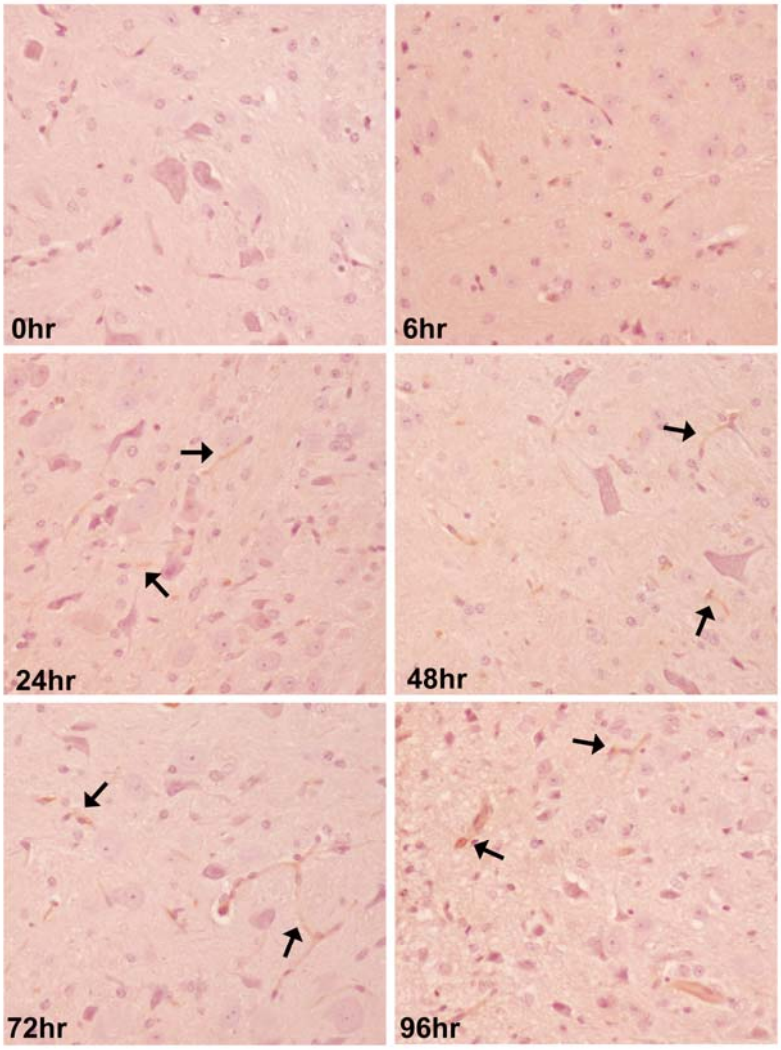

Figure 12: ***Immunohistochemistry for VCAM-1 Expression in VEE virus infected mice brain.*** Paraffin embedded formalin fixed tissue sections were studied for VCAM-1 expression using immunohistochemistry as described in materials and methods. VCAM-1 expression was absent in control. Its expression increased at 24 hr post infection and was specific to endothelial cell lining of blood vessels in brain. There after it continued to increase till 72 hr post infection and then small decrease at 96 hr post infection. ICAM-1 expression profile was concomitant with the progress of disease and appearance of virus in the brain. Objective used 20X.

Onset of Disease was Delayed in ICAM-1 Knock Out Mice.

***Survival study1*:** n=5 each group. 8-10 week old ICAM1 wild type (WT) and ICAM1 knock out (KO) were infected with 1000 pfu of virulent V3000 strain of VEEV. Thereon disease onset and percent mortality was calculated. All the animals in both the groups were hunched and had ruffled fur by day 4 post infection. At day six post infection one of the five mice in WT group showed hind limb paralysis (HLP) while none of the five KO mice showed any symptoms of HLP. Other three WT mice were rough, lethargic and shivering while one had only ruffled fur. Four KO mice had ruffled fur but were not lethargic while one of the KO mice was rough, lethargic and shivering. At day 7 post infection four of five WT mice had full blown disease, were dehydrated, eyes closed and had complete HLP. One WT mice was normal. One of the KO mice was completely paralyzed and was similar to WT mice. Three of the four remaining mice were hunched, lethargic but did not show HLP. Remaining one mouse was normal. At day 9 post infection, four out of five WT mice were moribund, had complete paralysis and were only breathing while three out of five KO mice were sick but had only partial HLP. One of the remaining two KO mice was lethargic but did not show symptoms of HLP and remaining one mouse was normal. Over the next five days all the sick mice gradually died in both the WT and KO groups. One out of 5 WT mice survived till day 14 post infection when the study was terminated. One of the KO mice that fell sick after VEEV infection recovered from the disease and two out of 5 mice survived the infection (Figure 13). Total mortality was 80% in WT and 60% in KO.

***Survival study 2*:** All the animals (5-6 weeks old) in both the groups i.e. WT (n=5) and KO (n=5) were infected with 1000pfu of V3000 as described before. All the animals in WT group were hunched and ruffled at day 4 post infection. Seven out of 8

WT mice showed initial symptoms of HLP and remaining one mouse was rough, hunched and lethargic. All the 5 KO mice were rough but did not have any symptom of HLP. At day 6 post infection 5 WT mice were completely paralyzed. At day 7 post infection all the 5 WT mice were completely paralyzed, non responsive and were moribund. Three out of five KO mice were completely paralyzed but were responsive and were visually better than WT. Remaining two KO mice had partial paralysis. By day 12 post infection all the 5 WT mice and four out of 5 KO mice died. One of the remaining KO mouse survived the 14 day period of the study but had HLP at day 14 and was euthanized (Figure 13). There was 100% mortality in WT and 80% mortality in KO mice group.

In both the study there was 20% less mortality in the KO mice and the onset of the encephalitic disease was delayed on an average by 48hr post infection.

Inflammation is Reduced and Lagging Behind in ICAM-1 Knock Out Mice

Pathological manifestation in the VEEV infected mice brain of WT and KO mice was evaluated in H&E stained sections of brains. Pathological manifestations such as endothelial swelling, perivascular cuffing, and inflammation of meninges and around the brain microvessels were evaluated. Infected KO mice brain exhibited reduced inflammation early in the infection which appeared to be lagging behind as compared to the inflammation in the infected WT mice brain. Initiation of meningial inflammation was lagging in the brains of infected KO mice. Meningial inflammation was established in WT mice brain at 48hr post infection (Figure 14b) while it was negligible in infected KO mice brain. Olfactory and post olfactory lobe has extensive inflammation and neutrophil infiltration in infected WT mice brain where as it was negligible in infected

KO mice brain (Figure 14c). Endothelial swelling and perivascular cuffing was extensive in infected WT mice brain and had only initiated in the infected KO mice brain at 48hr post infection (Figure14a). Meningial inflammation was extensive at 72hr post infection in WT mice brain whereas it started to establish in the infected KO mice brain (Figure 14b).

Inflammatory Cytokines are down Modulated in Brains of ICAM-1 Knock out Mice as Compared to WT Mice

Inflammatory cytokine array of RNA samples from 96 hr post infection mice brain was performed. These results are described in table 3 in detail. Several inflammatory cytokine and chemokine gene expression was differentially regulated between KO and WT mice. These results are depicted in scatterplot analysis (Figure 15) and hierarchical clustering (Figure 16). Relative expression of genes among samples is shown by Venn diagram (Figure 17).

In both WT and KO mice brain several chemokine ligands such as *C3*, *Ccl2*, *Ccl4*, *Ccl19*, *Cxcl10*, *Cxcl11* were upregulated over their respective saline controls. *C3*, *IL12b* and *Fcer1g* were also upregulated in both WT and KO mice over their respective controls. *Ccl12* and *Il10rb* were upregulated only in WT mice brain while inducible cytokine Scye1 was upregulated only in infected KO mice brain.

Chemokine ligand *Cxcl14*, Interleukins *Il6st*, *Il12a* and *Il18*, Fc receptor *Fcgr1* and toll interacting protein *Tollip* were down regulated in both WT and KO infected mice brain as compared to their respective saline controls. Chemokine ligand *Ccl22*, *Syce1* and secreted phosphoprotein *Spp1* were down regulated in infected WT mice brain. Chemokine receptor *Ccr2* and *Cx3cr1*, chemokine ligand *Cx3cl1* and interleukin *Il10*, *Il13* were down regulated in infected KO mice brains.

Comparison of WT and KO infected samples with each other revealed down regulation of chemokine ligand *Ccl12*, *Ccl19* and *Cxcl11*, interleukin *12b* and Fc receptor *Fcgr1* in VEEV infected mice brain as compared to WT. While expression of interleukin *Il6st*, toll interacting protein *Tollip* and secreted phosphoprotein *Spp1* was upregulated in infected KO mice brain over infected WT mice brain.

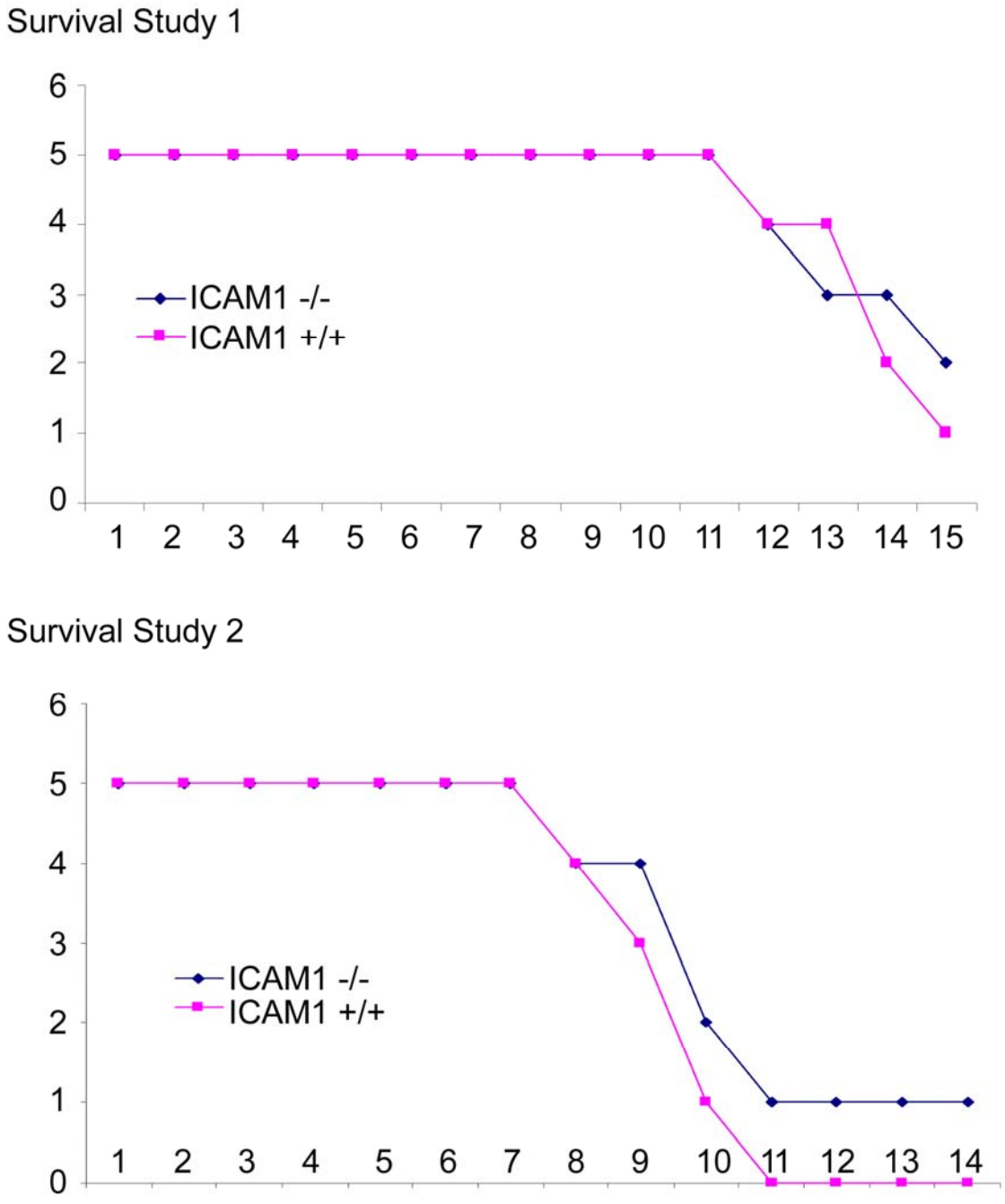

Figure 13: ***Survival study in VEEV infected ICAM-1 KO Mice.*** Two separate survival studies were done in ICAM-1 KO mice for VEEV infection. ICAM-1 knock out mice were generated on a balb/c background therefore, corresponding age matched balb/c mice served as controls in these studies. There was a 20% reduction in mortality in ICAM-1 KO mice over their wild type controls in both the studies.

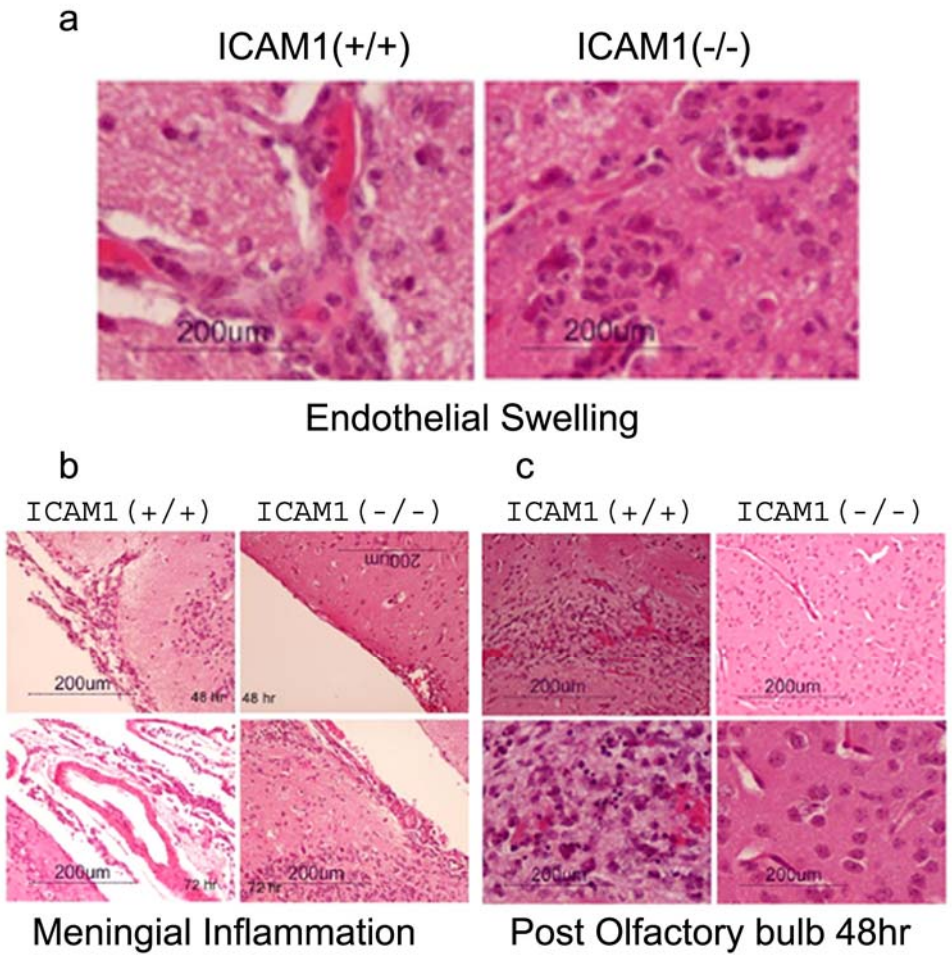

Figure 14: ***Pathogenesis in ICAM-1 KO mice brain.*** (a) Degree of endothelial swelling and edema was significantly reduced in. (b) Minengial inflammation was also significantly less in ICAM-1 KO mice as compared the wild type. (c) Inflammation in olfactory lobe was also significantly less in ICAM-1 KO mice as compared wild type mice.

Table 3: **Inflammatory cytokines and receptors gene expression analysis in ICAM-1 KO mice brain over WT mice**.

UniGene ID	Functional Grouping (Gene)	Expression		Fold Difference
		WT	KO	
	Chemokines and Cytokines			
Mm.867	Ccl12 (Chemokine (C-C motif) ligand 12)	351.071 ± 264.17	51.96 ± 41.95	0.13 ± 0.02
Mm.379051	Ccl19 (Chemokine (C-C motif) ligand 19)	421.04 ± 361.68	195.49 ± 185.49	0.33 ± 0.16
Mm.31505	Ccl24 (Chemokine (C-C motif) ligand 24)	42.13 ± 32.13	(A)	(PWT)
Mm.341574	Ccl7 (Chemokine (C-C motif) ligand 7)	57.22 ± 47.22	(A)	(PWT)
Mm.131723	Cxcl11 (Chemokine (C-X-C motif) ligand 11)	1233.54 ± 405.15	317.05 ± 305.78	0.38 ± 0.37
Mm.10116	Cxcl13 (Chemokine (C-X-C motif) ligand 13)	125.38 ±115.38	(A)	(PWT)
Mm.30211	Cxcl14 (Chemokine (C-X-C motif) ligand 14)	313.76 ± 303.76	(A)	(PWT)
Mm.766	Cxcl9 (Chemokine (C-X-C motif) ligand 9)	324.17 ± 314.17	43.42 ± 33.42	0.56 ± 0.44
Mm.240327	Ifng (Interferon gamma)	(A)	20.83 ± 10.38	(PKO)
Mm.103585	Il22 (Interleukin 22)	20.10 ± 10.10	(A)	(PWT)
Mm.288474	Spp1 (Secreted phosphoprotein 1)	412.10 ± 395.80	834.94 ± 262.48	18.24 ± 16.88
	Chemokine Receptors and Cytokine Receptors			
Mm.6272	Ccr2 (Chemokine (C-C motif) receptor 2)	160.98	(A)	(PWT)
Mm.44065	Cx3cr1 (Chemokine (C-X3-C) receptor 1)	(A)	20.39 ± 10.39	(PKO)
Mm.2856	Il6ra (Interleukin 6 receptor, alpha)	(A)	40.72 ± 30.72	(PKO)
Mm.4364	Il6st (Interleukin 6 signal transducer)	413.80	629.36 ± 467.15	2.48 ± 1.07
	Interleukins and Receptors			
Mm.4154	Il10rb (Interleukin 10 receptor, beta)	232.22	17.04 ± 7.04	0.53 ± 0.47
Mm.103783	Il12a (Interleukin 12A)	414.66	176.34 ± 166.34	0.71 ± 0.29
Mm.239707	Il12b (Interleukin 12B)	512.62	311.52 ± 282.73	0.43 ± 0.29
Mm.222830	Il1b (Interleukin 1 beta)	353.02	116.73 ± 106.73	0.66 ± 0.34
Mm.1349	Il1r2 (Interleukin 1 receptor 2)	47.92	(A)	(PWT)
Mm.103551	Tollip (Toll interacting protein)	486.13	729.33 ± 367.46	1.76 ± 0.40
	TNF Ligands and Receptors			
Mm.1293	Tnf (Tumor necrosis factor alpha)	27.21	(A)	(PWT)

Table 3 Cont…

	Other Factors Involved in Inflammatory Response			
Mm.150	Fcgr1 (Fc receptor, IgG, high affinity I)	132.54	40.65 ± 30.65	0.36 ± 0.30
Mm.292510	Rac1 (RAS-related C3 botulinum substrate 1)	(A)	19.18 ± 9.18	(PKO)
Mm.23979	Tlr7 (Toll like recptor 7)	(A)	52.70 ± 42.70	(PKO)

Inflammatory cytokines and receptor gene expression was studied at 96 hour post infection in brains of VEEV infected ICAM-1 knock out (KO) and wild type (WT) mice. "A"- absent; "PWT"- expressed only in WT; and "PKO"- expressed only in KO.

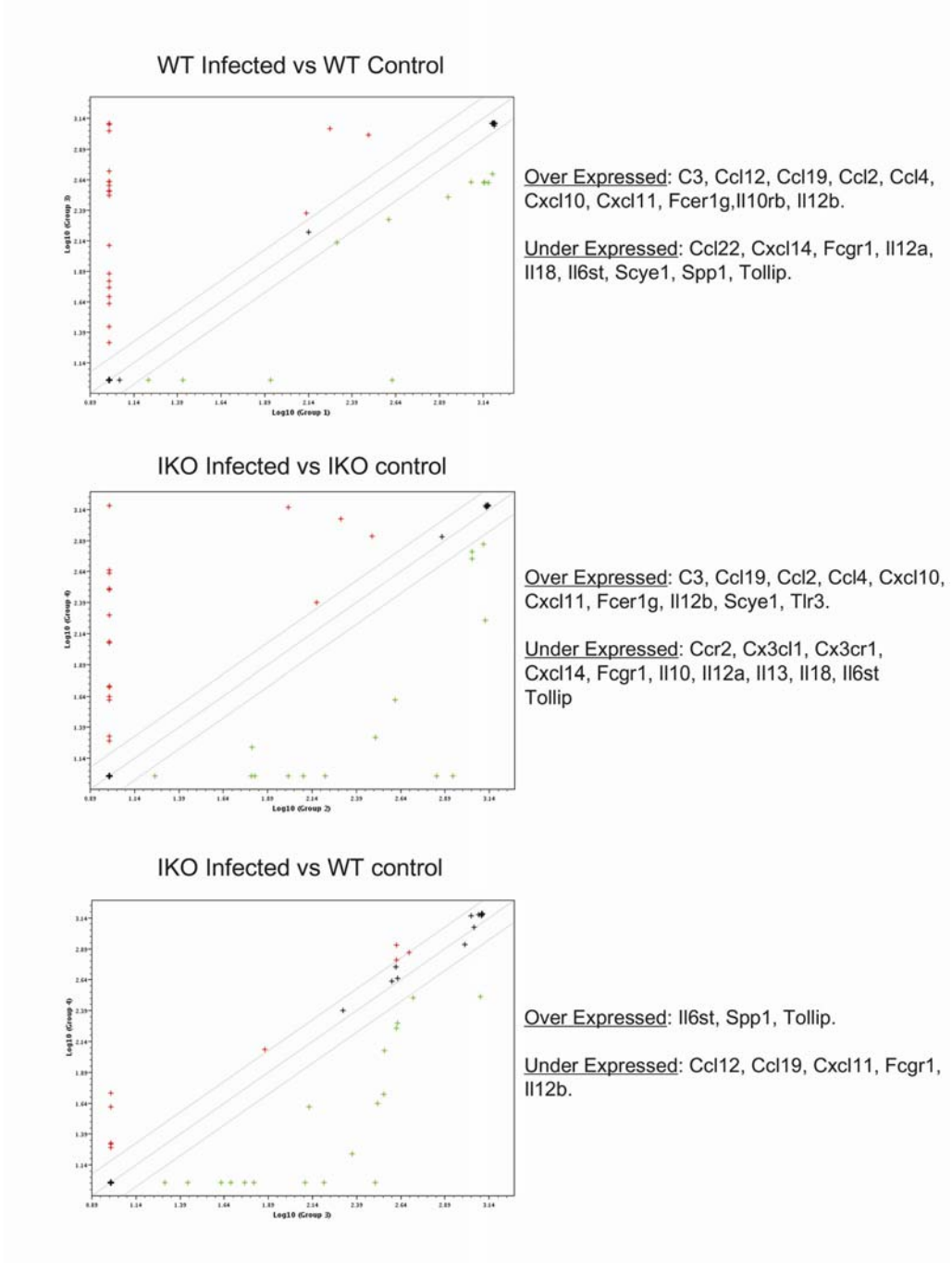

Figure 15: ***Scatterplot analysis for ICAM-1 KO and wild type mice infected with VEEV***. Scatterplot analysis was done to identify differential regulated genes between ICAM-1 KO and wild type (WT) mice. Genes that are identified to be up or down regulated in the ICAM-1 KO mice brain may be considered for further study towards developing therapeutic targets for VEEV treatment.

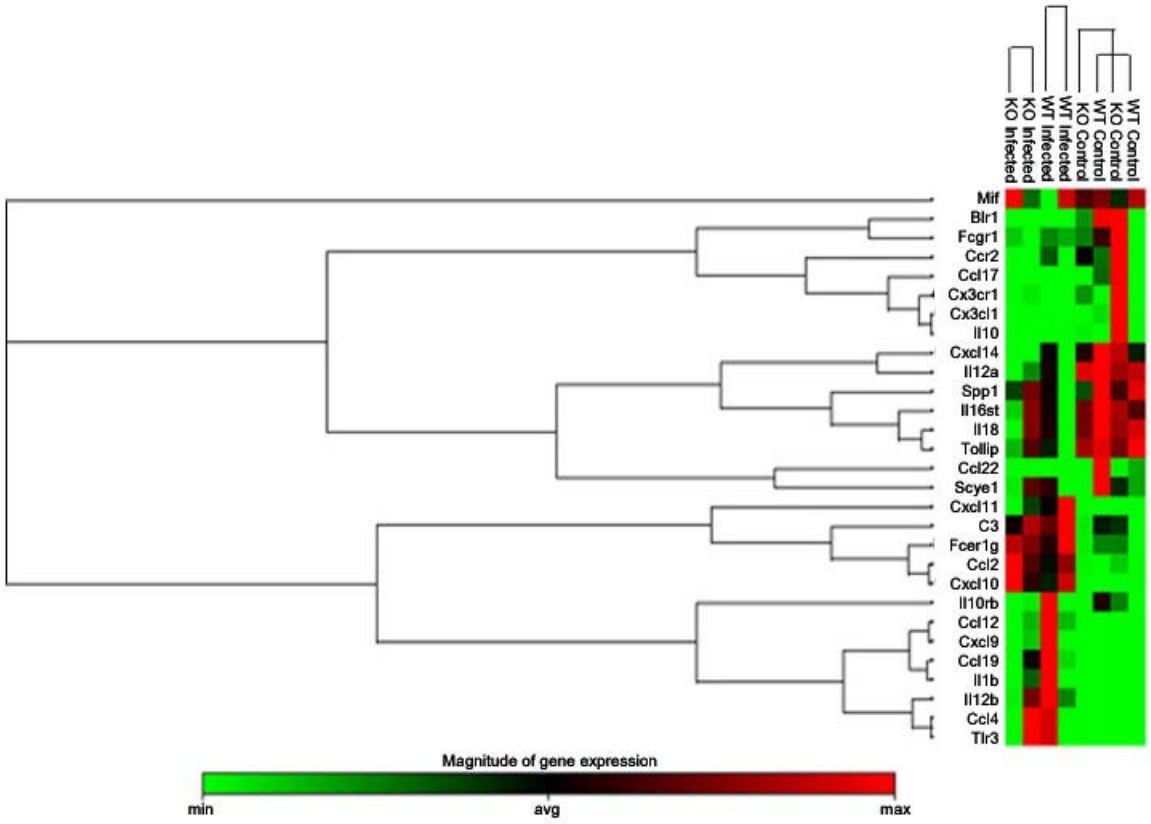

Figure 16: ***Hierarchical clustering of gene expression in mouse brain after VEEV infection***. All genes modulated by 1.5 fold at 96hr post infection were clustered. Color indicates the relative expression level of each gene, with red indicating higher expression, black indicating average expression and green indicating minimum expression.

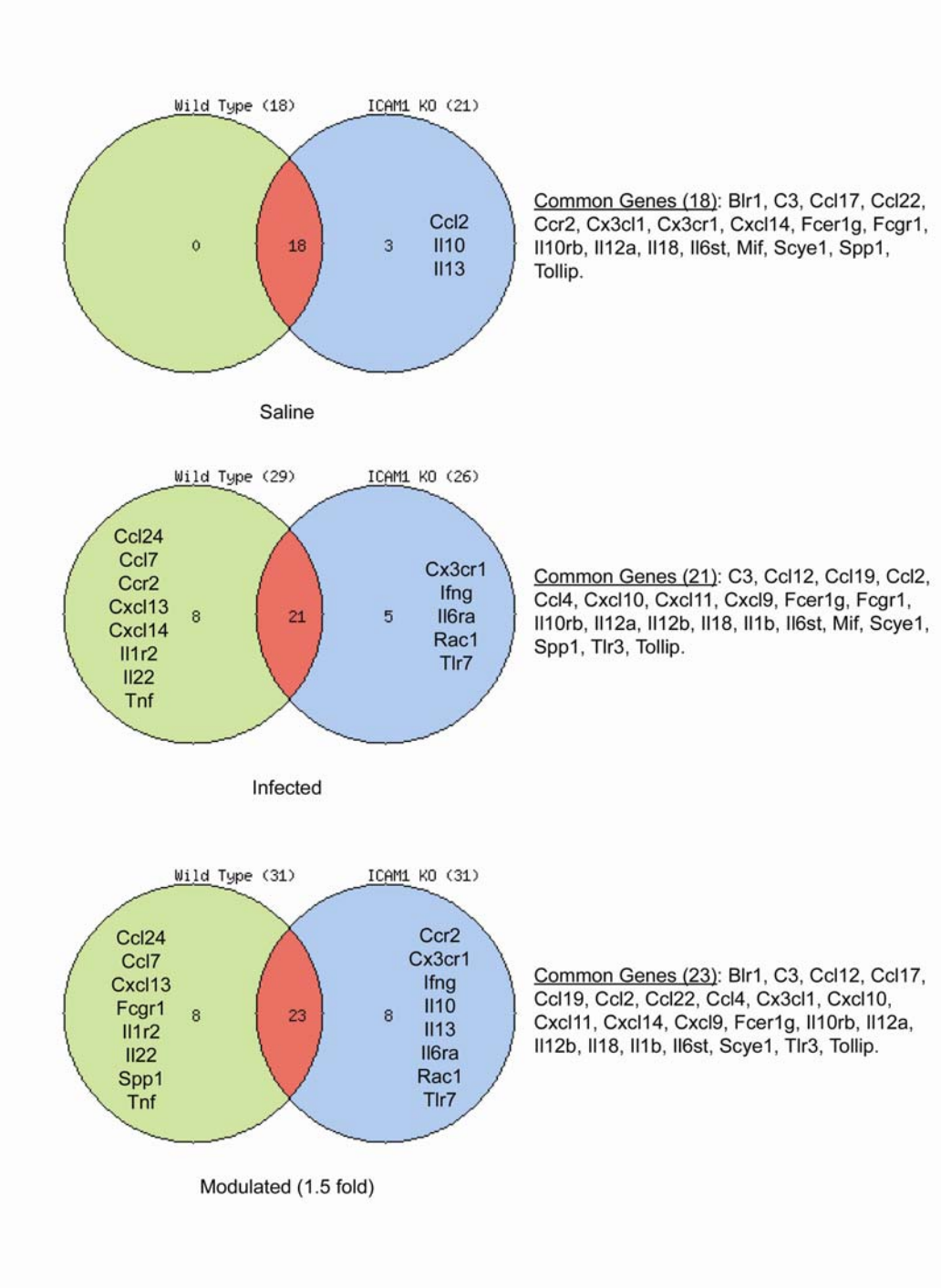

Figure 17: ***Venn diagram relating gene expression between VEEV infected or saline injected ICAM-1 KO and wild type mice brain.*** Venn diagram was constructed to identify common and unique gene expression in different sample groups. This relation distinctly identify genes that are unique expressed in ICAM-1 KO or wild type mice brain under normal and VEEV infected conditions. The genes expressed uniquely in ICAM-1 KO mice brain may be explored for the therapeutic treatment of VEEV infection.

Discussion

BBB is the target for many viruses and is modulated to gain entry into the CNS. It is the first line of defense of brain to protect itself from the invading pathogens. Viruses over the time have developed various mechanisms to break this barrier [Soilu-Hanninen et al 1994] and or to go around the barrier for instance, the olfactory route as used by VEEV to get entry in to the brain [Vogel et al 1996]. Extensive inflammatory response to the presence of VEEV in the brain causes the pathological conditions resulting in neuronal deaths observed to be associated with the inflammation or reactive microglial cells in the region of brain free from virus antigens [Schoneboom et al 2000] that was also seen in our results. Inflammatory response results in modulation and the infiltration of the inflammatory cells like neutrophils, T cells & monocytes into the brain [Eugenin and Berman 2003, Kim et al 2004, Pu et al 2003]. These cells may themselves be infected with viruses and can result in increasing the virus load in brain. Thus, the breakage of the BBB can be of great importance in the pathogenesis of VEEV. In this study, we looked into the expression of adhesion molecules which play an important role in the modulation of the BBB. Adhesion molecules such as ICAM-1 and VCAM-1 have been shown to be upregulated in various virus infections involving BBB modulation *e.g.* SFV and HIV or by viral proteins such as HIV tat protein [Eralinna et al 1996, Pu et al 2003, Woodman et al 1999]. Our study shows the induction and upregulation of the ICAM-1 and VCAM-1 in the VEEV infected mice brain. ICAM-1 and VCAM-1 induction was concomitant with the disease progression and virus appearance in the brain. ICAM-1 and VCAM-1 expression was induced as early as 6 hour post VEEV infection, which may be a component of generalized systemic immune response towards VEEV, and their expression increased with the disease progression and peaked at the time of virus entry

into the brain. Virus appearance in the brain at 72 hour post infection coincided with the peak expression of and ICAM-1 and VCAM-1. Indirect indication of increased neutrophil migration thus increasing transmigration of immune cells through BBB came from the increased expression of neutrophil specific collagenase, MMP8. MMP8 has been reported to increase in the inflammatory conditions in CNS and BBB disruption such as EAE and bacterial meningitis (Nygardas and Hinkkanen 2002, Leppert et al 2000). Further fibrinogen leakage and associated inflammation and VEEV antigen further strengthen the possibility of BBB modulation and its importance in VEEV induced CNS pathology.

Further, pathological manifestations such as inflammation was reduced in ICAM-1 KO mice as compared to WT mice at earlier time points though there was no significant difference in the VEEV antigen staining and distribution through out the brain. This reduced inflammation coincided with the late onset of the encephalitic conditions such as excitability, seizures and hind limb paralysis in the ICAM-1 KO mice. Reduced inflammation also reflected in the microarray data which showed reduced expression of several chemokines and cytokines such as *Ccl12*, *Ccl19*, *Cxcl11* and *IL12b.* Evidence is emerging that chemokine receptors are involved in neuronal death and hence neurodegenerative diseases (reviewed in Cartier et al 2005). *Il12b* cause local inflammatory injury in the brain in EAE and Alzheimer's disease (Ahemad et al 2001, 2003, Mehlhorn et al 2000). *Il16* that was upregulated in ICAM-1 KO mice is differentially upregulated by microglial cells in response to different stimuli such as EAE or viruses (Guo et al 2004). This observation of Il16 is interesting as it may be either playing a role in the reduced inflammation and delayed encephalitis or acting just opposite and that's why delayed encephalitis and death in ICAM-1 KO mice. Studying

the exact role of Il16 may provide a therapeutic target for VEEV infection. Reduced mortality (20% below WT background controls) thus may be a result of this reduced inflammatory reaction in brains of the ICAM-1 KO mice and thus further strengthens the assumption that inflammation plays a crucial role in the neuronal damage seen in VEEV induced pathogenesis in brain and thus a balanced inflammatory response is needed for a better outcome from VEEV infection.

These findings are significant as it for the first time shows the upregulation of the adhesion molecules in the VEEV infection, which may be responsible for the reduced inflammation and mortality as seen in VEEV infection of ICAM-1 KO mice. These molecules thus have a potential to be developed as therapeutic targets in the VEEV infection.

Chapter 2

Toll Like Receptors are Modulated in Venezuelan Equine Encephalitis Virus infected Mice Brain: Implication in Inflammatory Response

Abstract

Toll-Like Receptors (TLR) recognize conserved microbial sequences and induce specific biological response in the form of proinflammatory cytokine induction. In this study, 3-5 weeks old mice were infected with 1000 pfu of V3000, a neurovirulent strain of VEEV. VEEV infection resulted in up regulation of *Tlr 1*,*2*,*3*,*7* and *9*, chemokines, inflammatory cytokines and interferon and interferon regulatory factors and genes involved in TLR signal transduction. Our results for the first time suggest that TLRs are upregulated following VEEV infection and thus may play an important role in VEEV pathogenesis.

Key Words: Encephalitis, Toll like Receptors, Inflammation, Neurodegeneration.

Introduction

Toll-Like Receptors (TLR) recognizes conserved sequences in the microbial components and induces specific biological response [Kaisho and Akira 2006, Horner 2006]. At least 11 mammalian TLRs have been identified (Reviewed in Horner 2006). TLR2 interacts with peptidoglycan (PGN), a constituent of all bacterial cell walls; TLR3 recognize viral dsRNA such as Lang reovirus and West Nile virus (WNV) [Alexopoulou et al 2001, Wang et al 2004]; TLR4 recognizes LPS; TLR5 recognizes bacterial flagellin; TLR7 (mouse and human) and TLR8 (human) recognize several synthetic imidizoquinolones, as well as viral single-stranded RNA sequences; TLR9 is activated by

DNA sequences that are rare in mammalian genomes but common in the genetic material of bacteria, fungi, and DNA viruses. TLR9 and TLR3 are both involved in immunity against mouse cytomegalovirus infection [Tabeta et al 2004]; and TLR11 (mice) recognizes an undefined PAMP associated with uropathogenic bacteria and a pro- filin-like protein associated with Toxoplasma gondii. Certain TLRs (ie, TLR1, TLR2, TLR3 and TLR6) are also recruited into the phagosome, where they heterodimerize with other TLRs. Such interactions between different TLRs might serve to expand the variety of PAMPs that can be recognized by this family of proteins and therefore the number of microbes to which the innate immune system can respond.

TLRs have not been studied in VEEV pathogenesis and it will be safe to assume that, by analogy in other RNA viruses such as SFV, TLRs will be modulated in VEEV infection. Since mortality is due to neurological complications we examined the expression kinetics of TLRs and their downstream signaling genes in VEEV infected mice brain by microarray and PCR. Our results demonstrate that several TLRs such as *Tlr 1, 2, 3, 7* and *9*, and associated downstream signaling genes such as TLR interacting adaptors (*Myd88* and *Ticam1*), kinases (*IRAK1* and *Tbk1*) were up regulated. Transcription factors such as *Nfkb1, Irf1* and *7* and target genes such as *IFN* α */β*, *Mcp-1*, *IP10*, *Casp8*, *Il12 α /β* were also up regulated. The results confirm that TLRs are modulated in mice brain infected with VEEV and may be important part of inflammatory response in brain against VEEV infection.

Materials and Methods

Animals;Virus, Challenge Procedure and Survival Study; Histopathology and Immunohistochemistry for VEEV antigen; and Isolation of RNA

These procedures were same as described in chapter 1.

Toll Like Receptor (TLR) Signaling Pathway Specific Gene Expression

Pathway focused Oligo GEArray® Mouse Toll-Like Receptor Signaling Microarray kit (Superarray Bioscience Corporation, Frederick, MD) was used and experiments were carried out as per the manufacture's protocol. Each array has 128 genes spotted on the array membrane. Briefly, cRNA probe was synthesized from 1µg of RNA using TrueLabeling- AMP Linear RNA Amplification Kit, SuperArray Bioscience Corporation, Frederick, MD. The amplified cRNA was purified using spin column (ArrayGrade™ cRNA Cleanup Kit, SuperArray Bioscience Corporation, Frederick, MD) and quantitated by spectrophotometer. Array membranes were prehybidized for 2hr/60^0C/ 10-20 rpm with GEAHyb hybridization solution followed by overnight hybridization with 4µg of cRNA mixed in 750µl of hybridization buffer at 60^0C/10-20 rpm in hybridization chamber. Array membranes were then washed for 15 min each at 60^0C/10-20 rpm with pre-warmed wash solution 1 (2XSSC, 1% SDS) and wash solution 2 (0.1XSSC, 0.5%SDS) respectively. Blocking was done for 2hr/10-20 rpm at room temperature (RT) with 2ml of blocking solution Q followed by incubation with 2ml of binding solution (1:15000 AP-Strep in 1xBuffer F). Array membranes were then washed with 1X buffer F and rinsed with buffer G. Detection was done by incubation membranes with 1ml of CDP star substrate supplied with the kit for 3min, 10-20 rpm/ RT. X-ray films (Kodak Scientific Imaging Film, Eastern Kodak Company, Rochester, NY) were exposed to the membrane for different time period and films were developed using Kodak Image developer. X-ray images were scanned and converted to digital image (Supplementary Fig. 1) for further analysis.

Analysis: Image analysis was done using GEArray Expression Analysis Suite (Superarray Bioscience, Frederick, MD). Gene densities were expressed as average density (total density divided by number of pixels). Background detection was done locally i.e. each expression value was individually subtracted with value from the area outside the capture grid but within the spot cell area. Data normalization was done with non-modulating house keeping gene, Glyceraldehyde-3-phosphate dehydrogenase (*GAPDH*). A gene was considered "absent" where the average density of the spot was less than the mean value of the local backgrounds of the lower 75 percentile of all non-bleeding spots. All other spots were considered “present”.

Reverse Transcription (RT) and Polymerase Chain Reaction (PCR)

cDNA was synthesized using the Superscript first strand synthesis system for RT-PCR kit (Invitrogen Inc. Carlsbad, CA). Briefly, Primer mix (1ugRNA, dNTP, oligo dts) was incubated at 65°C for 5 min then mixed with reaction mixture (10X PCR buffer, 25mM $MgCl_2$, 0.1M DTT, RNase inhibitor) and incubated at 42°C for 2 min. cDNA synthesis was done using RT enzyme (SSII) at 42°C for 50 min. Reaction was stopped by incubating at 70°C for 15 min. Residual RNA was digested by E. *coli* RNase H at 37°C for 20 min and samples were stored at -20°C.

PCR was performed to validate all the genes that were modulated 2 fold and above in the microarray. Primers and conditions used for the different genes are described in table 4. For TLR PCR one additional step of non-specific amplification was carried for 5-10 cycles of 95^0C/60sec, 45^0C /90sec, 72^0C /90sec followed by specific amplification. PCR products were visualized by electrophoreses over 1.2% agarose gel and staining with ethidium bromide. Further PCR products were sequenced and checked for specific

amplification by blasting the sequence in the NCBI genome database and aligned against known gene sequences using Clone Manager Professional Suite Version 8 software. Briefly, PCR products were pooled from 72 and 96 hr for each sample and purified using spin QIAprep Spin Miniprep kit (Qiagen Inc. USA, Valencia, CA). Sequencing reaction was done using BD BigDye Version 3.1 (Applied Biosystems, Foster City, CA). Product was then purified using Performa® DTR Gel Filtration Cartridges (Edge BioSystems, Gaithersburg, MD). Sequencing was done in in-house facility on DNA Sequencer 3100 (Applied Biosystems, Foster City, CA) at USUHS.

Table 4: ***PCR primers and amplificatio***

Gene	Primers	Anneal Temp	Product size	Cycles
Il12a	Sense 5'-GGTAGCATCTATGAGGAC-3' Anti Sense 5'-GACCACCTGACTCTTATG-3'	54	365	32
Il12b	Sense 5'-GTAGAGGTGGACTGGACT-3' Anti Sense 5'-GGTGCTTCACACTTCAGG-3'	56	296	30
Pkr	Sense 5'-CCAGTTTATGAATGTGAAAG-3' Anti Sense 5'-AATGTCCAACCACGTTCGT-3'	54	481	28
Map2k6	Sense 5'-AGCCTCAGACCAGTTCCAC-3' Anti Sense 5'-TGTGTAAATGTTCTAACGC-3'	56	448	27
Mapk12	Sense 5'-GTCATTGGGCTACTGGATG-3' Anti Sense 5'-CTCACTGTCTGCCTGCCTG-3'	58	287	31
IRF 1	Sense 5'-TGTCGTCAGCAGCAGTCTCT-3' Anti Sense: 5'- ACTCACTCAGGAGGGCAAGA-3'	61	467	25
IRF7	sense: 5'-CCAGGAGCAAGACCGTGTTTA-3' Anti Sense: 5'-GGTAGATGGTGTAGTGTGGTG-3'	61	688	25
Nfkb1	Sense: 5'-CGATTCCG CTATGTGTGTG-3' Anti sense: 5'-CTCCGCCTTCTGCTTGTAG - 3'	58	384	28
Jun	Sense: 5'-GCCTCGTTCCTCCAGTCCG-3' Anti sense: 5'-GTCTGCGGCTCTTCCTTC-3'	58	657	22
Casp8	Sense: 5'-GTATCTTACGACGACTGCAC-3' Anti sense: 5'-GCTCTGGCAAAGTGACTG-3'	56	441	30
Fos	Sense: 5'-GAGGAAGAGAAACGGAGAATC-3 Anti sense: 5'-CTCCCAGTCTGCTGCATAG-3	59	506	28
MCP-1	Sense 5'-CTCTTCCTCCACCACCATGCAG-3' Anti-sense 5'-GAAAAATGGATCCACACCTTGC-3'	62	582	27
Cd86	Sense 5′ATCGCCAACTTCAGTGAA CC3′ Anti sense 5′TCTCACTGCCTTCACTCTGC3′	55	544	35
Cd14	Sense 5'GTCCTTAAAGCGGCTTACGG3' Anti sense 5'GCGCTAAAACTTGGAGGGCT3'	58	399	32
IP-10	Sense 5'-CCTATCCTGCCCACGTGTTGAG-3' Anti-sense 5'-CGCACCTCCACATAGCTTACAG-3'	65	430	26
IFN-β	Sense 5' GGAGATGACGGAGAAGATGC 3' Anti sense 5' CCCAGTGCTGGAGAAATTGT 3'	58	102	32
MyD88	Sense 5'-CCAGAGTGGAAAGCAGTGTC-3' Anti-sense 5'-GTCCTTCTTCATCGCCTTGT-3'	58	365	28
IRAK1	Sense 5'-GACCTCGTTCACATCCTCAC-3' Anti-sense 5'- ACCACCCTCTCCAATCCTGA -3'	59	422	32
TICAM1	Sense 5'- GCTGGGGAGTCTGTGTTCA -3' Anti-sense 5'- TGTCAATGGGACGAGGCTG-3'	59	463	32
IFNα	Sense 5'- AGGATGTGACCTGCCTCAG -3' Anti-sense 5'- AGACTTCTGCTCTGACCAC -3'	57	448	30
TLR1	Sense 5-TACAGTTCCTGGGGTTGAGC-3' Anti-sense 5-TAGTGCTGACGGACACATCC-3'	56	215	18
TLR2	Sense 5-CGTTGTTCCCTGTGTTGCT-3' Anti-sense 5-AAAGTGGTTGTCGCCTGCT-3'	56	118	21
TLR3	Sense 5'-CAGTTCAGAAAGAACGG-3' Anti-sense 5'-AGCCTTATACCATAAAAGC-3'	50	596	25
TLR7	Sense 5-GCTGTGTGGTTTGTCTGGTG-3' Anti-sense 5-CCCCTTTATCTTTGCTTTCC-3'	56	269	21
TLR9	Sense 5-GAAAGCATCAACCACACCAA-3' Anti-sense 5-ACAAGTCCACAAAGCGAAGG-3'	56	303	21

PCR primers were designed using NCBI and UCSC Genome Bioinformatics database. Primers were checked for hairpin loop formation and primer dimmer formation using OPERON oligo tool kit. Amplicon sizes were determined by blasting in NCBI database. Ann Temp- Annealing Temperature

Results

Development of Disease and Mortality

Roughening was visible as soon as day two post infection in five out of nine mice on day two post infection. All nine mice were lethargic, shivering and one mouse had hind limb paralysis on day four post infection. At day five post infection mice stopped feeding, were immobile with varying degree of hind limb paralysis and one mouse died on this day. Three mice died on day six, four mice died on day seven and one remaining mouse died on day nine post infection. Mortality was 100% with mean survival time of 6.6 days. Disease progression and mortality is documented in table 5.

VEEV Appearance and Inflammation in Brain

VEEV specific antigen staining was detected in few cells in olfactory and prefrontal areas of brain at 48hr post infection. Many more VEEV infected cells were present at 72 hr post infection and VEEV antigen was present through out the brain by 96hr post infection (Figure 18) Inflammation corresponded to the max density of viral infected cells. Inflammation started with perivascular cuffing and meningeal inflammation at 48h and was established at 72h, especially in olfactory and frontal area of the brain. By 96 hr post infection inflammation was extensive and had spread through out the brain. This experiment was repeated twice with similar results and these observations are consistent with the published literature.

Table 5. ***Progression of disease and mortality in VEEV infected mice.***

Disease Progression	**Day(s) Post Infection**									
	0	**1**	**2**	**3**	**4**	**5**	**6**	**7**	**8**	**9**
Roughening of Fur	0	0	5	9	-	-	-	-	-	-
Hunched Posture/ Lethargic/Shivering	0	0	0	0	8	-	-	-	-	-
Hind Limb Paralysis	0	0	0	0	1	8	5	1	1	-
Death	0	0	0	0	0	1	3	4	0	1
Total died/ Total No.	0/9	0/9	0/9	0/9	0/9	1/9	4/9	8/9	8/9	9/9
% Mortality	0	0	0	0	0	11.1	44.4	88.8	88.8	100
MST (Day)	6.66									

Mice were infected with 1000 pfu of V3000 in left rear foot pad at day 0 and were monitored for the clinical symptoms of disease thereafter. All the animals exhibited hind limb paralysis, a hallmark of VEEV infection and succumbed to disease by day 9 post infection. Mortality was 100% with a mean survival time of 6.6 days.

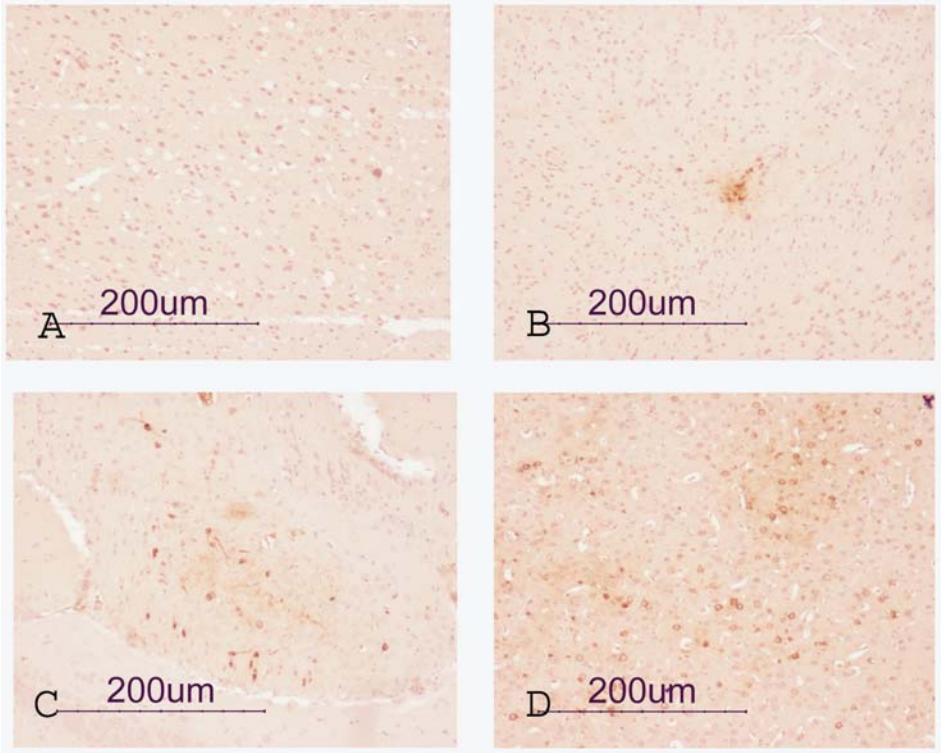

Figure 18: ***VEEV antigen staining in brain of infected mice.*** A.) Saline injected mice brain;. B.) Brian section at 48hr post infection: olfactory bulb and post olfactory region of brain show VEEV positive staining; C.) Brian section at 72hr post infection: there was more infiltration of VEEV into the cortex region of the brain; D.) Brian section at 96hr post infection: VEEV antigen was found through out the brain.

Modulation of Toll Like Receptor (TLR) Signaling Pathway Specific Gene Expression

Microarray analysis for brain RNA samples infected with VEEV at 96 hr post infection showed 43 genes being modulated by ≥1.5 fold. These genes have been grouped according to their function in TLR signaling specific pathway for the ease of understanding (Table 6). These groups are (1) *Toll Like Receptors*: *Tlr3* was up regulated by 10 folds and *Tlr7* expression was induced upon VEEV infection; (2) *Downstream Pathways and Target Genes*; Nfkb Pathway: *Ccl2* or *Mcp1*, *Ifn-β1*, *Ifn-γ*, *Il1β*, *Il1r1*, *Il12β*, *Map3k14*, *Nfkb2*, *Nfkbie* and *Rela* expression was induced upon VEEV infection. *Chuk*, *Hrb*, *Nfkb1* and *Nfkbil1* expression was up regulated in VEEV infected mice brain. JNK/p38 Pathway: *Fos, Jun*, *Map2k3* expression was up regulated and *Map2k6*, *Mapk10* and *Mapk12* was down regulated in VEEV infected mice brain. NF/ IL6 Pathway: *Cebpb*, *Il6* and *Ptgs2* expression was induced upon VEEV infection and *Ptges* expression was up regulated in VEEV infected mice brain. IRF Pathway: *Cxcl10* or *IP10*, *Irf1*, *Irf7* expression was induced upon VEEV infection and *Tbk1* expression was up regulated in VEEV infected mice brain; (3*) Adaptors and TLR Interacting Proteins*: *Cd14* and *Pglyrp1* expression was induced upon VEEV infection, *Hmgb1*and *Mydd88* expression was upregulated. *Hspd1*, *Mal* and *Tollip* were down regulated; (4) *Effectors*: *Casp8* and *Map3k7* expression was induced upon VEEV infection. *Irak1* and *Prkr* expression was upregulated and *Pkr* expression was down regulated in VEEV infected mice brain; (5) *Regulation of Adaptive Immunity*: *Cd86* was up regulated in VEEV infected mice brain.

Table 6. ***Differential regulation of TLR signaling pathway specific genes in VEEV infected mice brain at 96hr post infection.***

UniGene ID	Functional Grouping (Gene)	Expression		Fold Difference
		Control	Infected	
	Toll Like Receptors			
Mm.33874	Tlr3 (Toll like receptor 3)	13.59 ± 2.07	151.74 ± 81.69	10.28 ± 4.17 (p= 0.16)
Mm.23979	Tlr7 (Toll like receptor 7)	(A)[!]	59.04± 22.06	(PI)[$]
	Downstream Pathways and Target Genes			
	NFkB Pathway			
Mm.290320	Ccl2/MCP-1(Chemokine {c-c motif} ligand 2)	(A)[!]	345.31 ± 34.88	(PI)[$]
Mm.3996	Chuk (Conserved helix-loop-helix ubiquitous kinase)	132.36 ± 57.84	268.62 ± 47.29	5.47 ± 4.12 (p= 0.14)
Mm.6461	Hrb (HIV-1 Rev binding protein)	51.72 ± 17.47	223.02 ± 37.05	4.76 ± 1.09 (p= 0.07)
Mm.1245	Ifnb1 (Interferon beta 1, fibroblast)	(A)[!]	375.24 ± 29.69	(PI)[$]
Mm.240327	Ifng (Interferon gamma)	(A)[!]	57.59 ± 32.57	(PI)[$]
Mm.222830	IL1b (Interleukin 1 beta)	(A)[!]	41.86 ± 16.83	(PI)[$]
Mm.896	Il1r1 (Interleukin 1 receptor type 1)	(A)[!]	37.22 ± 9.07	(PI)[$]
Mm.239707	Il12b (interleukin 12B)	(A)[!]	249.98 ± 19.94	(PI)[$]
Mm.158981	Map3k14 (Mitogen activated protein kinase 14)	(A)[!]	41.72 ± 26.78	(PI)[$]
Mm.256765	Nfkb1 (Nuclear factor of kappa light chain gene enhancer in B-cells 1)	22.91 ± 3.30	106.72 ± 63.43	4.40 ± 2.16 (p= 0.25)
Mm.102365	Nfkb2 (Nuclear factor of kappa light polypeptide gene enhancer in B-cells 2)	(A)[!]	79.56 ± 56.17	(PI)[$]
Mm.57043	Nfkbie (Nuclear factor of kappa light polypeptide gene enhancer in B-cells inhibitor, epsilon)	(A)[!]	15.15 ± 4.90	(PI)[$]
Mm.300795	Nfkbil1 (Nuclear factor of kappa light polypeptide gene enhancer in B-cells inhibitor-like 1)	12.35 ± 1.27	19.54 ± 5.24	1.65 ± 0.48 (p= 0.25)
Mm.249966	Rela (V-rel reticuloendotheliosis viral oncogene homolog A {avian})	(A)[!]	19.86 ± 8.93	(PI)[$]
	JNK/p38 Pathway			
Mm.246513	Fos (FBJ osteosarcoma related oncogene)	68.07 ± 34.71	342.22 ± 56.58	10.23 ± 6.60 (p= 0.01)*
Mm.275071	Jun (Jun oncogene)	47.77 ± 9.91	296.33 ± 44.40	6.85 ± 2.09 (p< 0.01)*
Mm.18494	Map2k3 (Mitogen activated protein kinase 3)	102.87 ± 27.75	224.67 ± 37.81	2.941± 1.40 (p= 0.06)
Mm.14487	Map2k6 (Mitogen activated protein kinase 6)	15.12 2.93	(A)[!]	(PC)^
Mm.39253	Mapk10 (Mitogen activated protein kinase 10)	923.54 ±121.30	460.99 ± 62.61	0.51 ± 0.09 (p= 0.02)*
Mm.38343	Mapk12 (Mitogen activated protein kinase 12)	41.98± 17.06	18.19 ± 5.05	0.43 ± (p= 0.25)
	NF/ IL6 Pathway			
Mm.347406	Cebpb (CCAAT/ enhancer binding protein {C/EBP}, beta)	(A)[!]	251.34 ± 11.76	(PI)[$]
Mm.1019	Il6 (Interleukin 6)	(A)[!]	69.79 ± 32.59	(PI)[$]
Mm.28768	Ptges (Prostaglandalin E synthase)	17.71 ± 4.35	44.28 ± 6.83	3.10 ± 1.26 (p= 0.03)*
Mm.292547	Ptgs2 (Prostaglandin-endoperoxide synthase 2)	(A)[!]	53.59± 26.04	(PI)[$]
	IRF Pathway			
Mm.877	Cxcl10/IP-10 (Chemokine {C-X-C motif} ligand 10)	(A)[!]	244.46 ± 39.33	(PI)[$]
Mm.105218	Irf1 (Interferon regulatory factor1)	(A)[!]	464.08 ± 68.71	(PI)[$]
Mm.3233	Irf7 (Interferon regulatory factor 7)	(A)[!]	234.44 ± 36.12	(PI)[$]

Table 6 cont….

Mm.34580	Tbk1 (Tank binding kinase 1)	52.84 ± 18.81	156.00 ± 95.84	3.92 ± 1.81 (p= 0.35)
	Adaptors and TLR Interacting Proteins			
Mm.3460	Cd14 (CD14 antigen)	(A)!	253.97 ± 79.55	(PI)$
Mm.313345	Hmgb1 (High mobility group box 1)	30.24 ± 9.77	49.29 ± 31.13	2.54 ± 1.22 (p= 0.44)
Mm.371564	Hspd1 (Heat shock protein 1 {chaperonin})	942.09± 86.44	425.68 ± 41.34	0.45 ± 0.05 (p< 0.01)*
Mm.39040	Mal (Myelin and lymphocyte protein, T-cell differentiation protein)	917.52 ± 85.02	434.32 ± 69.28	0.48 ± 0.09 (p= 0.01)*
Mm.213003	Myd88 (Myeloid Differentiation primary response gene 88)	15.77 ± 4.24	261.54 ± 5.07	18.94 ± 4.44 (p< 0.01)*
Mm.21855	Pglyrp1 (Peptidoglycan recognition protein 1)	(A)!	53.62 ± 33.08	(PI)$
Mm.103551	Tollip (Toll interacting protein)	944.84 ± 111.69	452 ± 61.47	0.50 ± 0.10 (p= 0.01)*
	Effectors			
Mm.38241	IRAK1 (Interleukin 1 receptor associated kinase 1)	33.46 ± 23.46	69.54 ± 31.02	5.28 ± 3.80 (p= 0.40)
Mm.336851	Casp8 (Caspase 8)	(A)!	189.81 ± 45.64	(PI)$
Mm.258589	Map3k7 (Mitogen activated protein kinase 7)	(A)!	15.90 ± 3.20	(PI)$
Mm.378990	Eif2ak2/PRKR (Protein kinase, interferon-inducible double stranded RNA dependent)	34.84 ± 16.57	344.69 ± 37.85	13.79 ± 6.70 (p= 0.02)*
Mm.277250	Prkra/PKR (Protein kinase, interferon-inducible double stranded RNA dependent activator)	443.10 ± 119.47	230.51 ± 40.75	0.66 ± 0.30 (p= 0.16)
	Regulation of Adaptive Immunity			
Mm.1452	Cd86 (CD86 antigen)	13.36 ± 1.86	174.24 ± 24.01	14.14 ± 4.09 (p< 0.01)*

* These values were statistically significant.
! No expression i.e. absent (A)
$ Expressed only in Infected (PI)
^ Expressed only in Control (PC)

Microarray was performed for 96hr post infection brain RNA samples as extensive inflammation and VEEV antigen was observed in brain at 96 hr post infection. Total RNA was isolated and array was performed as described in methods. Three biological replicates were taken from two different experiments. Values are expressed as Mean ± SEM. Two tail-students t-test was done to determine statistical significance.

Genes either involved in the TLR signaling or are target of the TLR signaling that were modulated in microarray were validated and there expression kinetics was studied using semi quantitative RT-PCR.. In addition we performed PCR for all the TLRs included on the membrane, *Ticam1*, an adaptor in TLR signaling that was not included on microarray. All the expression with $p<=0.05$ were considered statistically significant. Genes that were sequenced (data not shown) have accession number in parenthesis. *Tlr 1*(**NM_030682.1**)*, 2, 3* (**NM_126166.2**)*, 7* (**NM_133211.2**) and *9* (**NM_031178.1**) expression was significantly upregulated in VEEV infected mice brains (Figure 19 and 20a). *Tlr 4*, *5* and *6* (**NM_011604.2**) did not show any statistically significant difference from controls (data not shown). TLR interacting proteins gene, *Ticam1* (**NM_174989.2**) expression increased at 72hr post infection with some decrease at 96hr post infection. *Myd88* (**NM_010851.2**), *Cd14* expression was significantly upregulated in VEEV infected mice brain (Figure 19 and 20b). Target genes such as *Il12α/β*(**NM_008351.1**/**NM_008352.1**), *IP10* (**NM_021274.1**), *Mcp1* (**NM_011333.1**)*, IFN α* (**NM_010502**) and *Ifn β* were also significantly upregulated upon VEEV infection in mice brain over controls (Figure 19 and 20c). Expression of effector molecules such as *Casp8* (**NM_009812.1**), and *Cd86* (**NM_019388.2**) expression increased with the progress of disease and was significantly upregulated at 72hr and 96hr post infection while *Pkr* expression was down modulated as the disease progressed (Figure 19 and 20d). Transcription factors such as *Irf1* (**NM_008390.1**), *Irf7* (**NM_016850.1**), *Nfkb1* (**NM_008689.1**) was significantly upregulated over controls in VEEV infected mice brain (Figure 19 and 20e). Genes involved in the pathway downstream to TLR activation such as *Fos* (**NM_010234.2**), *Jun* (**NM_010591.1**), *Map2k6* (**NM_011943.1**), *Mapk12*,

Nfkb1 and *Irak1* (**NM_008363.1**) was also detected in VEEV infected mice brains. *Fos*, *Jun* and *Irak1* was significantly up regulated in VEEV infected mice brain. Map2k6 expression down regulated with the progress of disease and was significantly down modulated at 96hr post infection. Mapk12 level showed some down modulation at 48hr post infection and its expression level were comparable to controls at 72hr and 96hr post infection (Figure 19 and 20e).

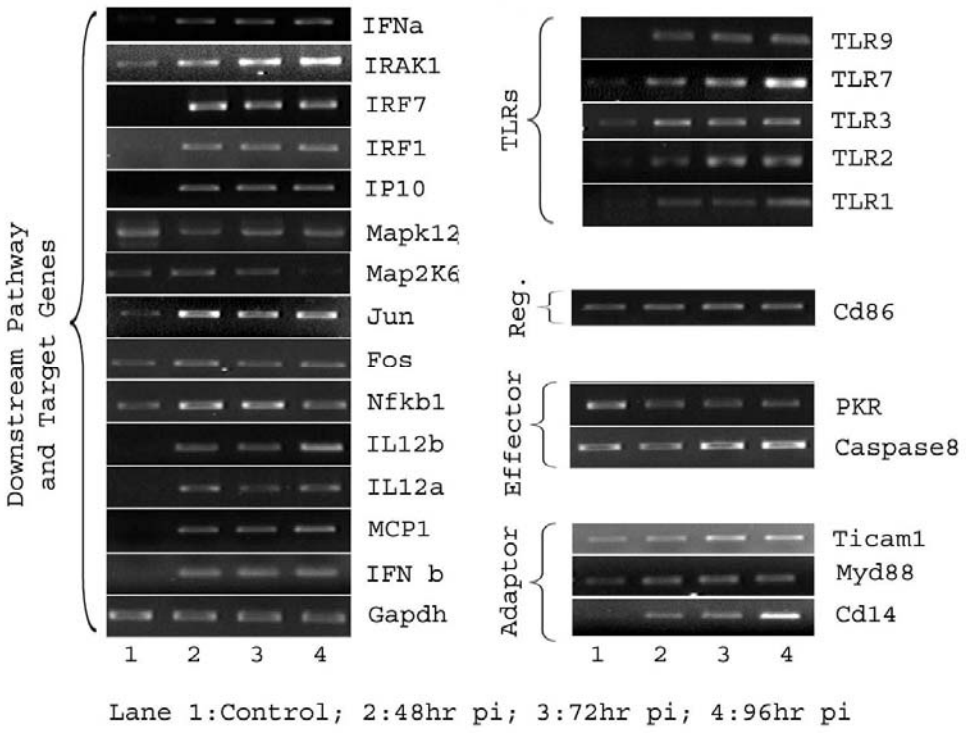

Figure 19: ***Expression kinetics of genes in VEEV infected mice brain***. Semi quantitative RT-PCR was performed using PCR supermix (Invitrogen life technologies, Carlsbad, CA). Expression was normalized with housekeeping gene GAPDH. Lane 1: Saline injected control, Lane 2: 48hr post infection, Lane 3: 72hr post infection, Lane 4: 96hr post infection.

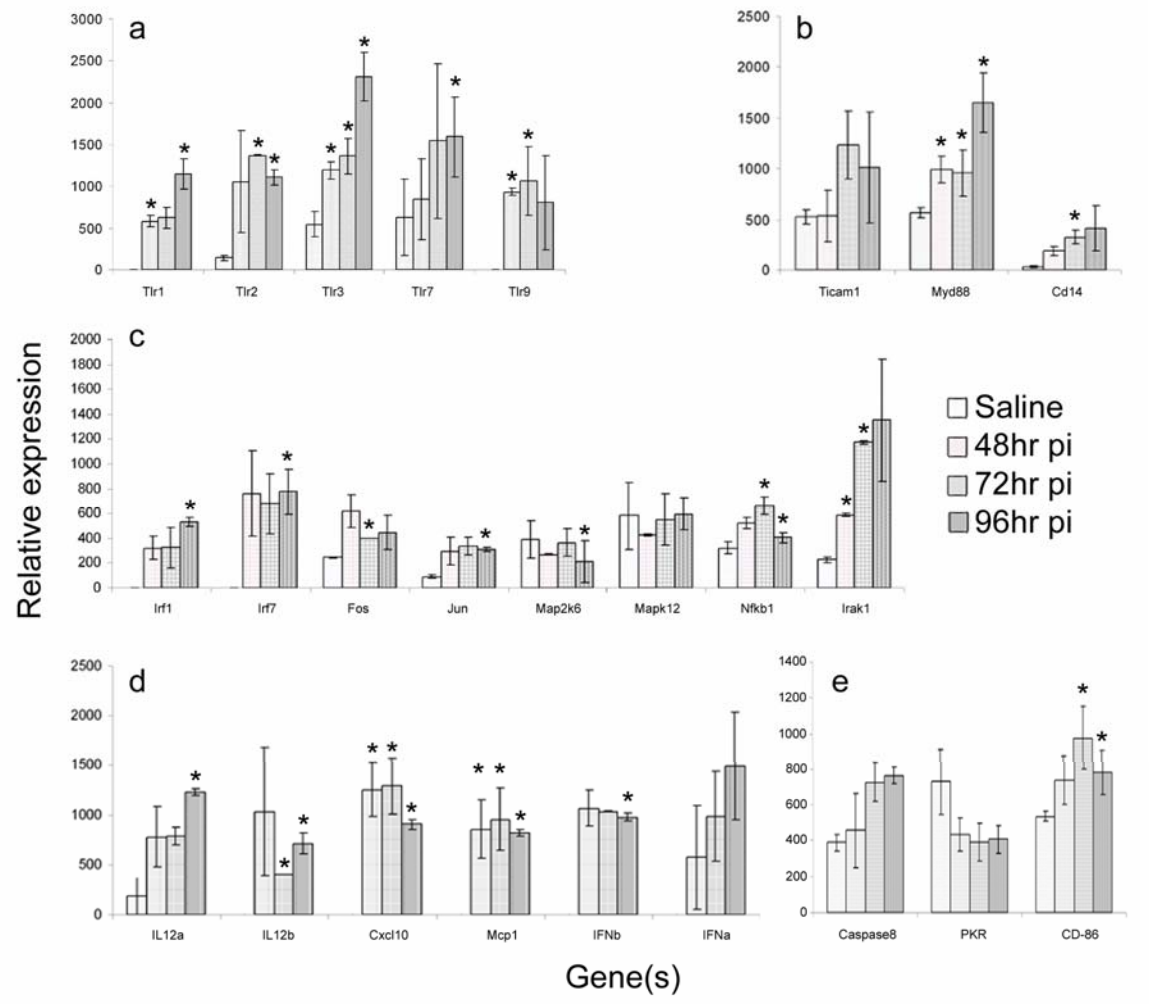

Figure 20: ***Quantitation of gene expression in VEEV infected mice brain***. Quantitative estimation was done by densitometry analysis of the PCR product shown in Figure 2. Values were normalized to the corresponding values of the house keeping genes for individual samples. Values are expressed as mean ± SEM. * $p \leq 0.05$. a) Toll Like Receptors; b) Adaptors and TLR interacting proteins; c) Target genes of TLR signaling; d) Effectors in TLR signaling; e) TLR pathway downstream signaling genes.

Discussion

TLRs are membrane bound receptors that recognize pathogen associated molecular pattern. Several reviews describe these molecules and their importance in innate immunity [Kaisho and Akira 2006, Olson et al 2004, Takeda and Akira 2005]. Normal resting mouse brain have basal level of TLR 1, 2, 3, 4, 5, 6, 7, 8 and 9 expression and their expression is up regulated in response to virus invasion of brain [McKimmie et al 2005, Bottcher et al 2003]. In our study, *Tlr1*, *2*, *3*, *7* and *9* were significantly up regulated following VEEV appearance in brain and their expression closely followed progression of inflammation and VEEV appearance in brain. TLR3 mediated peripheral inflammation and alteration of blood brain barrier (BBB) is demonstrated in response to WNV infection [Wang et al 2004]. RABV infected neurons produces TLR3, *CxCl10* and *IFN-β* [Prehaud et al 2005] and mice lacking functional IFN system are unable to up regulate TLR3 and *9* following infection with SFV [McKimmie et al 2005]. Natural killer (NK) and $CD56^{+}$ T cells express higher level of TLR3 and *4* following infection with VEEV replicons [Saikh et al 2003].

Genes that are involved in the downstream TLR signaling were also up regulated in our study and their expression was concomitant with VEEV appearance and inflammation in brain. Several reviews describe in detail TLR signaling [Takeda and Akira 2004, Moynagh 2005, O'Neill 2006]. Myd88 and Ticam1 are two important adaptors that interact directly with TLRs and initiate downstream signaling. Myd88 signaling is utilized by all the TLRs except TLR3 [O'Neill 2006]. TLR3 utilizes Ticam1 dependent signaling [Oshiumi et al 2003]. Both *Myd88* and *Ticam1* were significantly up regulated in our study. Myd88 dependent signaling results in Nfkb mediated gene expression of target cytokine and chemokines such as IFNβ, IL12, MCP-1, CxCl10 etc.

IRAK1 mediates the activation of Nfkβ by interacting with TLR-Myd88 complex [Takeda and Akira 2004]. Mice that lack *Myd88* are highly susceptible to lethal encephalitis following infection with HSV1 [Mansur et al 2005]. Both *Irak1* and *Nfkb1* were up regulated in our study. Target genes of Myd88 and Nfkβ pathway i.e. *Mcp1*, *Il12a*, *Il12b*, *Ifnβ1* were also significantly up regulated in our study. Ticam1 mediated signaling involves transcriptional factors Irf3 and Irf7. Irf3 being involved early in the signaling resulting in the Irf7 expression which later on replaces Irf3 thus creating a positive feedback [Moynagh 2005]. Irf7 is also activated by Myd88 dependent pathway probably by interacting with Irak1 [Honda et al 2004]. Activated Irfs carry out transcription of *Ifnα*, *Cxcl10* (*IP10*) etc. In our study, *Irf7* and target genes *Ifnα* and *Cxcl10* were significantly up regulated. These results suggest that both Myd88 dependent Nfkb mediated and Ticam1 dependent Irf mediated signaling is activated in VEEV infected mice brain.

Other genes that are associated with the TLR signaling were also modulated. *Cd14*, a co receptor for TLR4 [Rolland et al 2006] was significantly up regulated at 72 hr post infection. *Cd86*, which is a co-stimulatory molecule and is upregulated following activation of antigen presenting cells by viruses [Ahmed et al 2006] or TLRs [Takeda and Akira 2005] was also up regulated. *Mcp1* that has been shown to directly alter the BBB and induce chemotactic signal for leukocytes and macrophages in CNS inflammation [Eugenin et al 2006, Stamatovic 2005, Song and Pachter 2004] was also up regulated in VEEV infected mice brain.

These results for the first time suggests that multiple TLRs may recognize VEEV antigens and induce downstream signaling pathways resulting in expression of both *Nfkb*

and *Irf* transcription factor mediated gene expression i.e. type I IFN and inflammatory cytokine and chemokine expression that may contribute to antiviral response in brain and secondary neuronal damage. These findings add to our present knowledge of VEEV pathogenesis. Further the identified TLRs and their downstream signaling may be explored for therapeutic targets for treatment of VEEV induced encephalitis.

Chapter 3

Venezuelan Equine Encephalitis Virus Infection Causes Modulation of Inflammatory and Immune Response Genes in Mouse Brain

Abstract

Neurovirulent *Venezuelan Equine Encephalitis virus* (VEEV) causes lethal encephalitis in equines and humans. Molecular mechanisms of VEE pathogenesis are poorly understood. Lack of appropriate vaccine for VEEV and its use as a potential bio-warfare agent makes it an important pathogen to study from military and civilian standpoint. To understand the molecular pathways of pathogenesis, we have investigated the differential gene expression in VEEV infected mice brain by microarray analyses. Our study is designed to investigate a molecular framework of changes in gene expression associated with progression of the disease. Among overall changes were over expression of genes related to some of the important immune pathways such as antigen presentation, inflammation and virus response. The number of transcripts that were upregulated (>1.5 fold), out of 35,852 analyzed, increased as the disease progressed and were 197, 296, 400, 1086 at 24, 48, 72 and 96 hours post infection respectively. Several important genes including *Cxcl10*, *CxCl11*, *Ccl5*, *Ifr7*, *Ifi27 Oas1b*, *Fcerg1*, *Mif*, *Clu and MHCII* were found to be modulated and thus may play an important role in VEEV pathogenesis of brain. Identification of these modulated genes will help in the selection of marker genes for diagnosis and for targeted therapies against VEEV induced neurodegenration.

Key Words: Venezuelan Equine Encephalitis, neuroinflammation and Cytokines

Introduction

Venezuelan Equine Encephalitis virus (VEEV) is an alphavirus in the family togaviridae. It causes a highly virulent CNS disease in horses and other equines that is transmitted by mosquitoes to humans. Outbreak of VEEV occurs at intervals of 2 to 10 years, which has resulted in VEEV being included on the list of emerging pathogens (Weaver 2004). VEEV has also been developed as a bio-warfare agent, making its use more likely than other non weaponized agents in the event of use of a bio-weapon or bio-terrorism agent (Hawley and Eitzen 2001). VEEV is endemic in rodents and infection in mice induces the bi-phasic disease observed in humans thus making it a good model to study VEEV pathogenesis (Bigler et al 1974, Jackson et al 1991). VEE spreads from the site of inoculation through the locally draining lymph nodes, causes viremia, and disseminates to other lymphatic organs (Grieder et al 1995). Viremia is followed by neuronal phase (Grieder et al 1997, Charles et al 1995, 2001). VEEV enters into the CNS primarily through the olfactory neuroepithelium, via brain capillary endothelial cells and trigeminal nerve (Charles et al 1995, Ryzhikov et al 1995). In CNS, VEEV infects neurons and glial cells and causes subsequent cellular degeneration. Infection by VEEV results in neuronal cell death, active gliosis and intense inflammatory response characterized by perivascular and interstitial mononuclear infiltrate (Jackson et al 1991, Grieder et al 1995, Schoneboom et al 1999, 2000, Steele et al 2006). Viral antigens can be localized in a subset of dead neuronal cells, suggesting a direct association of VEE-infection and neurodegeneration, astrocytes and other glial cells of the granular cell layer (Jackson and Rossiter 1997). However, in another subset of dying neurons associated with the astrogliosis, no VEEV antigens can be found, indicating an alternate, indirect

mechanism of neuronal degeneration (Jacskon and Rossiter 1997, Schoneboom et al 2000).

As mechanism(s) underlying the inflammatory response to VEEV infection in brain and subsequent neurodegenration are poorly understood, it becomes important to characterize the cellular molecular pathways to understand the immune response and inflammation in CNS following VEEV infection. Therefore, in this study, we have studied gene expression changes in VEEV infected mouse brain using global microarrays containing 35,852 genes transcripts. We demonstrate that gene modulation increases both in numbers and fold as the disease progresses. Many of the overall changes were associated with important immune pathways such as antigen presentation, inflammation and viral response. Gene Expression changes were confirmed by RT-PCR analysis and brain pathology changes by H&E analysis.

Materials and Methods

Animals

Eight to Ten week old male CD-1 mice were obtained from Charles River Laboratories, Wilmington, MA. Details are same as described in chapter 1.

Virus and Challenge Procedure

Same as described in chapter 1

Survival study

Infected animals (n=9) were observed twice a day for clinical symptoms of disease i.e. roughening of fur, hunched back, lethargic, hind limb paralysis and mortality.

Histopathology and Immunohistochemistry (IHC) for VEEV antigen

Two animals from each group (n=10) were anesthetized using isoflurane and

sacrificed at 24, 48, 72 and 96 hr post infection (pi), control mice were sacrificed at 96hr pi. Detailed procedure is same as described in chapter 1

Isolation of total RNA

Same as described in chapter 1

Microarray studies

High quality oligonucleotide glass arrays were produced containing a total of 35,852 seventy-mer oligonucleotides chosen from 750 bases of the 3' end of each ORF (Operon Inc. Valencia, CA). The high quality microarrays were produced in house (at CBER microarray laboratory) by spotting 70-mer oligonucleotides on poly-L-lysine coated glass slides by Gene Machines robotics (Omnigrid, San Carlos, CA). The quality of printed arrays was confirmed as described (Yang et al 2006, communicated). Only high quality arrays that passed our quality control tests were used for these experiments. We have followed the MIAME (minimum information about a microarray experiment) guidelines for the presentation of our data (Brazma et al, 2001). Microarray was performed as described earlier (Bhattacharya et al, 2004). Various steps involved in the microarray are as follows.

i) Probe preparation: Labeled cDNA probes were produced as described (Risinger JI et al, 2003, Han et al 2005). Briefly, 5µg of total RNA was dissolved in 12µl of DEPC water and incubated at 70°C for 5 minutes along with 1µl of aminoallyl-oligo dT (5' amino-modified) primer and quickly chilled for 3 minutes. Then, 2µl 10× first strand buffer, 1.5µl Stratascript RT enzyme (Stratagene, La Jolla, CA), 1.5µl 20× aminoallyl dUTP and 2µl of 0.1 M dithiothreitol (DTT, Invitrogen, Carlsbad, CA) were added and

incubated for 90 minutes at 42°C. After incubation, volume of the reaction mixture was raised to 60µl with 40µl of DEPC water.

cDNA was purified by MinElute column (Qiagen, Valencia, CA). 300µl of Binding buffer PB was added to the coupled cDNA and mixed thoroughly. The mixture was applied to the MinElute column, and centrifuged for 1 min at max speed. After discharging the flow-through, 600µl of washing buffer PE was added to the column, and centrifuged for 1 min at max speed. The flow-through was discharged and the washing repeated. The columns were then placed into a fresh eppendorf tube and 10µl elution buffer added to the center of the membrane, incubated for 1 min at room temperature, centrifuged for 1 min at max speed and probes were collected. Finally, 3µl of 2× coupling buffer (1M NaHCO3, pH 9.0) and 5µl Cy3 and 5µl Cy5 (Amersham Biosciences, UK) dye mixed into eluted buffers derived from both saline and VEE infected samples respectively and incubated at room temperature in dark for 90 minutes. Saline control probes were labeled with Cy3 and probe from VEEV infected samples were labeled with Cy5. After incubation, the volume was raised to 60µl by DEPC water and then cDNA was purified by MinElute column and eluted with 13µl elution buffer by centrifugation.

ii) Hybridization: For hybridization, 36µl hybridization mixture [26µl cDNA mixture, 1 µl (10µg) COT-1 DNA, 1 µl (8–10µg) poly(dA), 1 µl yeast tRNA (4µg), 6µl 20× SSC and 1µl 10% SDS] was pre-heated at 100°C for 2 minutes and cooled for 1 minute. Total volume of probe was added on the array and covered with cover slip (22 mm × 40 mm). Slides are placed in hybridization chamber (Genemachines) and 20µl water was added to far end of slide (to maintain humidity), and incubated overnight (10–

16 hr) at 65°C. Slides were then washed for 2 minutes each into 2× SSC, 1× SSC and 0.1× SSC and spin-dried.

iii) Data filtration, normalization, and analysis: Microarray slides were scanned in both Cy3 (532 nm) and Cy5 (635 nm) channels using Axon GenePix 4000B scanner (Axon Instruments, Inc., Foster City, CA) with a 10-micron resolution. Scanned microarray images were exported as TIFF files to GenePix Pro 5.1 software for image analysis. The raw images were collected at 16-bit/pixel resolutions with 0 to 65,535 count dynamic range. The area surrounding each spot image was used to calculate a local background and subtracted from each spot before Cy5:Cy3 ratio calculation. The average of the resulting total Cy3 and Cy5 signal gave a ratio that was used to normalize the signals. Each microarray experiment was globally normalized to make the median value of the log2-ratio equal to zero. The normalization process corrects for dye bias, PMT (Photo multiplier tube) voltage imbalance, and variations between channels in the amounts of the labeled cDNA probes hybridized. The data files representing the differentially expressed genes were then created.

For advanced data analysis, data files (in gpr format) and image (in jpeg format) were imported into mAdb (microarray database, Center for Information Technology, National Cancer Institute, Bethesda, MD, USA), and normalized by software tools provided by National Institutes Health, Center for Information Technology. Spots with ≥1.5 fold higher expression with at least 150-fluorescence intensity in either channel or 30μm spot size were considered as good quality spots for analysis with additional filtration. These advanced filters prevented the potential effect of the poor quality spots in data analysis. All VEE infected samples from four different time points were hybridized

in duplicates (biological replicate). The data were further analyzed by Gene Ontology for Functional Analysis (GOFFA) Library of Arraytrack software (Sun et al 2006).

Reverse Transcription (RT) and Polymerase Chain Reaction (PCR)

cDNA was synthesized using the Superscript first strand synthesis system for RT-PCR kit (Invitrogen Inc. Carlsbad, CA). Briefly, Primer mix (1ugRNA, dNTP, oligo dts) was incubated at 65°C for 5 min then mixed with reaction mixture (10X PCR buffer, 25mM $MgCl_2$, 0.1M DTT, RNase inhibitor) and incubated at 42°C for 2 min. cDNA synthesis was done using RT enzyme (SSII) at 42°C for 50 min. Reaction was stopped by incubating at 70°C for 15 min. Residual RNA was digested by E. *coli* RNase H at 37°C for 20 min and samples were stored at -20°C. PCR was performed to validate few of the genes that were identified in the microarray. Primers and conditions used for the different genes are as follows. Clu: forward primer (BC075668.1: 36-52) 5`GACTCCAGATTCCAAGG`3, reverse primer (BC075668.1: 419-401) 5'GGTATGCTTCAGGCAGGGC'3 (95^0C/30s, 50^0C/45s, 72^0C/45s: 20 cycles), ; Oas1b: forward primer (BC012877.1: 250-266) 5'GCTCAAGGGCAGGTCAG'3, reverse primer (BC012877.1: 652-635) 5'GGTTGGGCGACAGTTCAG'3 (95^0C/30s, 52^0C/45s, 72^0C/45s: 22 cycles); Mif: forward primer (NM_010798.2: 19-37) 5'CTGGCTTGGGTCACACCGC'3, reverse primer (NM_010798.2: 383-367) 5'CGTAATAGTTGATGTAG'3 (95^0C/30s, 45^0C/45s, 72^0C/45s: 23 cycles); Fcer1g: forward primer (NM_010185.4: 207-225) 5'TATGGTATTGTCCTTAC'3, reverse primer (NM_010185.4: 429-412) 5'CCAAGAGGGCTCGGAGAG'3 (95^0C/30s, 49^0C/45s, 72^0C/45s: 23 cycles); CxCl11 primer mix was purchased from Superarray Bioscience Corporation, Frederic MD, RefSeq Accession # NM_019494.1, position 693-713

(95^0C/30s, 55^0C/45s, 72^0C/45s: 23 cycles); GAPDH: forward primer 5'CCATCACCATCTTCCAGGAGCGAG'3, reverse primer 5'CACAGTCTTCTGGGTGGCAGTGAT'3 (95^0C/30s, 52^0C/45s, 72^0C/45s: 25 cycles). PCR products were visualized by electrophoreses over 1.2% agarose gel and staining with ethidium bromide. Specific amplification was determined by comparing the product size on gel relative to known DNA molecular weight marker. Further PCR products were sequenced and checked for specific amplification by blasting the sequence in the NCBI genome database. Briefly, PCR products were pooled from 72 and 96 hr for each sample and purified using spin QIAprep Spin Miniprep kit (Qiagen Inc. USA, Valencia, CA). Sequencing reaction was done using BigDye Version 2.1(Applied Biosystems, Foster City, CA). Product was then purified using Performa® DTR Gel Filtration Cartridges (Edge BioSystems, Gaithersburg, MD). Sequencing was done in in-house facility on DNA Sequencer 3100 (Applied Biosystems, Foster City, CA).

Results

Survival of Animals Post VEEV Infection

Animals began showing roughening of fur and hunched back by two day four post infection and by day five, all the animals were lethargic. Two out of 6 mice showed hind limb paralysis (HLP) on day six post infection and remaining four exhibited initial symptoms of HLP. All the six mice were completely paralyzed on day seven post infection. Two mice died on day eight post infection and all other animals were very sick with little or no movement and animals appeared fragile. All the animals died by day 12 post infection. Mortality was 100% and mean survival time was 9.8 days. Animal mortality is documented in table 7.

Histopathology and IHC for VEEV antigen

Mouse brain sections obtained for day 2 to day 4 infected mice were analyzed by H&E and IHC. VEEV specific antigen staining showed virus antigen presence in few cells in olfactory and prefrontal areas of brain at 48hr post infection. Many more VEEV infected cells were present and VEEV was scattered through out the brain at 72hr post infection. VEEV antigen was present through out the brain at 96hr post infection and inflammation corresponded to the max density of viral infected cells. Inflammation started with perivascular cuffing and meningeal inflammation at 48hr. Inflammation had established at 72hr post infection, especially in olfactory and frontal area of brain and by 96hr post infection inflammation was extensive and has spread through out the brain (Figure 21).

Table 7: ***Progression of disease and mortality in VEEV infected mice***

Disease Progression	Day(s) Post Infection									
	3	4	5	6	7	8	9	10	11	12
Dead	0	0	0	0	0	2	1	1	0	2
Cumulative death	0	0	0	0	0	2	3	4	4	6
% Mortality	0	0	0	0	0	33.3	50.0	66.6	66.6	100
MST (Day)	9.8									

Mice were infected with 1000 pfu of V3000 in left rear foot pad at day 0 and were monitored for the clinical symptoms of disease thereafter. All the animals exhibited hind limb paralysis, a hallmark of VEEV infection and succumbed to disease by day 12 post infection. Mortality was 100% with a mean survival time of 9.8 days.

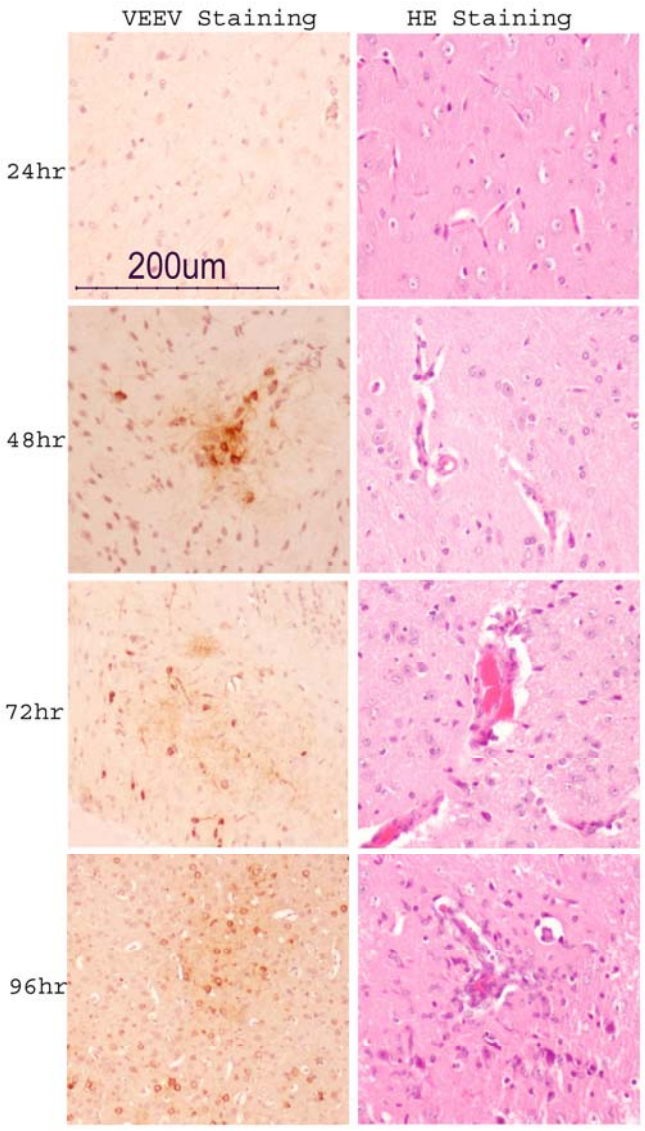

Figure 21: ***Evidence of the VEEV infection and inflammation in mice brain.*** Mice brains at various time points after VEEV infection were analyzed by H&E and IHC staining. VEEV appeared in brain at 48 hr post infection, which was accompanied by the initiation of inflammation in brain as evident by vessel thickening and endothelial cuffing. At 72 hr post infection VEEV antigen can be detected through out the mid brain and inflammation has established as evident by increased endothelial cuffing and neutrophil infiltration. Inflammation was extensive and through out the brain along with increased VEEV antigen in brain at 96 hr post infection.

Gene Expression Analysis

Microarrays were performed at 24hr, 48hr, 72hr and 96hr post infection on RNA extracted from VEEV infected mice brain (Figure 22). All the biological replicates shared significant homology in gene expression (correlation coefficient $\geq$ 0.80). Mean fold expression was taken from biological replicates and expression of $\geq$ 1.5 fold over control was identified or value was determined to be significant. As shown in table 8, the number of genes upregulated in brain increased as disease progressed. At 96hr post infection highest number of total gene were upregulated in mouse brain.

To analyze similarities and difference between brains at different time points, hierarchical clustering analysis was done for all genes at 4 time points. Genes which showed a distinct pattern of over-expression with the time of VEEV infection are shown in Figure 23. All genes were grouped in two clusters. First cluster contained genes modulated at 24hr and 48hr, whereas second cluster contained genes modulated at 72hr and 96hr post infection. This analysis clearly distinguished the changes in gene expression profile with the progression of VEEV infection. Some genes related to inflammatory response such as *Cxcl10, Clu* and antigen presentations such as *B2m*, *Fcer1g* showed over-expression only at 72 and 96hr post infection but are not expressed or expressed < 1.5 fold at 24 and 48hr post infection (Figure 23).

Functional analysis of the over expressed genes was performed using GOFFA library of the Arraytrack software. Genes belonging to various biological processes modulated by VEEV infection were grouped together. Based on these analyses, a majority of genes (164, 251, 759, 928) were identified to play a role in different biological processes at 24hr, 48hr, 72hr, and 96hr post infection respectively. These genes were further categorized by using Arraytrack software (Figure 24) as follows:

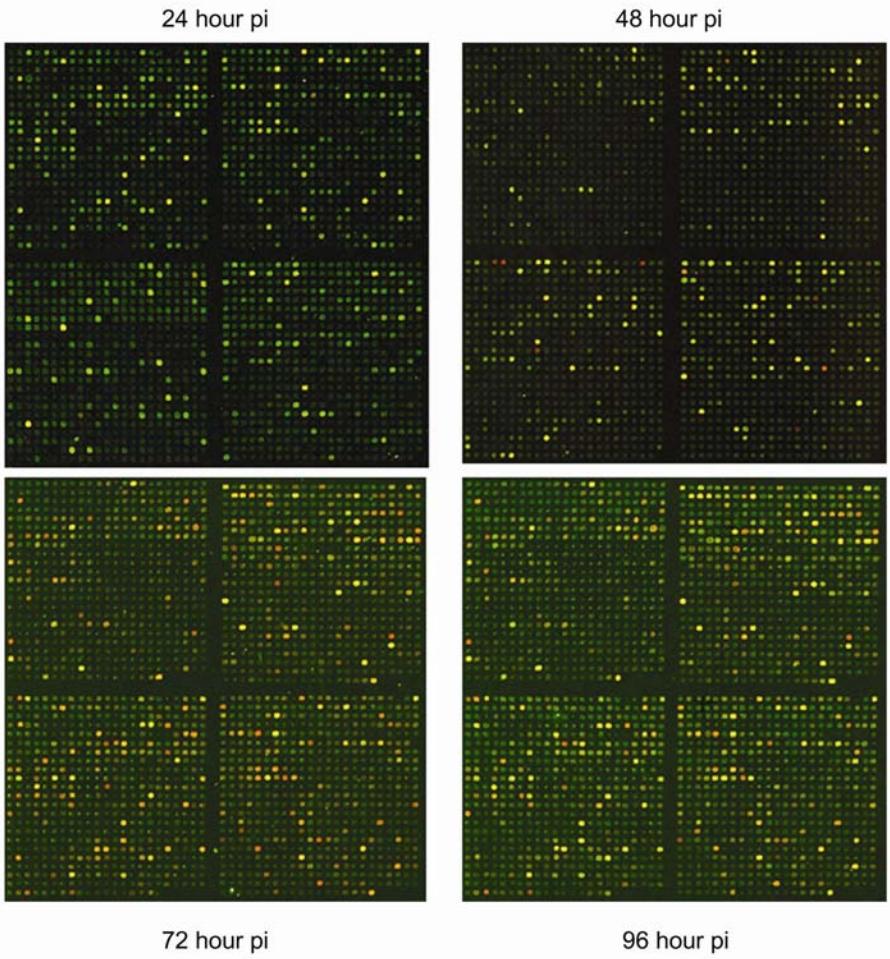

Figure 22: ***Microarray of VEEV infected mice brain at different time points***. Microarray was performed on the total RNA extracted from VEEV infected mice brain at 24, 48, 72 and 96 hr post infection (pi). These are the representative images of the microarray performed. Control RNA from saline injected mice was labeled with Cy3 and green spot represents gene expression in saline controls. RNA from VEEV infected mice brain was labeled with Cy5 and red spot represents gene expression in test. Black regions represent absence of gene expression. Yellow and its shades represents expression in both control and test samples.

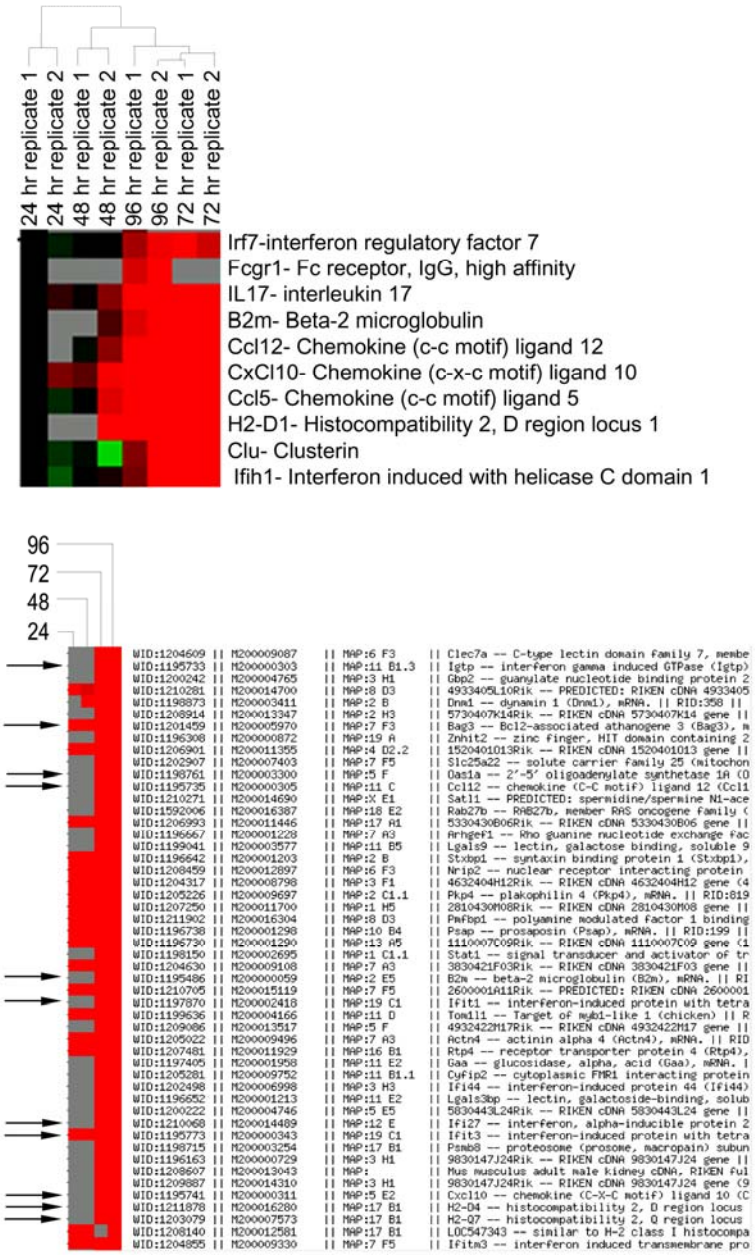

Figure 23: ***Hierarchical clustering of gene expression in mouse brain after VEEV infection***. All genes over expressed were clustered; however, a snap shot of some genes is shown due to space limitation. Genes that are marked with arrows are over expressed >= 2.0 fold in 72 and 96hr. Color indicates the relative expression level of each gene, with red indicating higher expression, grey indicating absence of expression and light red color indicating over expression but at a lower level. Genes labeled with arrows may be considered as marker of VEEV infection.

Table 8: ***Total Genes Upregulated in VEEV Infected Mice brain***.

Time, Hour(s) pi	> 5.0 folds	> 3.0-5.0 folds	≥ 1.5-3.0 folds	Total genes over-expressed
24	**6**	**18**	**183**	**207**
48	**3**	**27**	**292**	**322**
72	**53**	**148**	**212**	**413**
96	**33**	**129**	**960**	**1122**

Total RNA extracted from VEEV infected brain was analyzed by microarray as described in methods. Gene's upregulated =>1.5 folds were considered. Number of genes over expressed increased as the disease progressed with maximum genes over expressed at 96hr post infection.

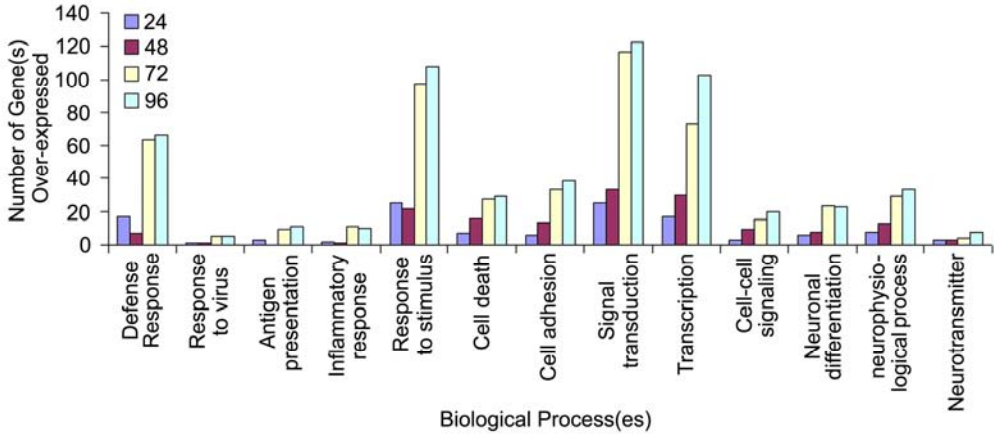

Figure 24: ***Analysis of molecular pathways in VEEV infected brain***. Number of genes involved in various pathways of biological processes was analyzed by GOFFA Library of Arraytrack software. Genes involved in the various biological processes increased with the progress of the disease.

i) Modulation of virus response genes*:* It has been shown that interferon and interferon inducible genes play an important role in the immune response towards virus pathogens. Consistent with this information, several interferon inducible genes were upregulated (Table 9). These include *Ifi27*, *Ifih1*, *Irf7* and *Oas1b* which were upregulated at 72 hr and 96hr post infection except *Becn1* that was over-expressed only at 72hr post infection and *Spn* which was over-expressed at all time points.

ii) Modulation of inflammatory response genes*:* Inflammation constitutes an important part of the immune response towards the invading pathogen. In VEEV infection, brain inflammation is implicated in the secondary neuronal damage leading to morbidity and mortality. Several genes related to inflammatory response were upregulated in the brain following the VEEV infection mostly at 72 hr and 96 hr (Table-3). Most importantly chemokine genes *e.g., Cxcl9, Cxcl10, Cxcl11, Cxcl13*, *Ccl3, Ccl5* and *Ccl12* that exert a chemotactic signal for the immune cell migration at the site of the injury were upregulated at 72hr and 96 hr post infection. In addition inflammation genes *e.g., Fcer1g*, and *Mif* were over-expressed at 72 and 96 hr post infection (Table9)

iii) Modulation of genes involved in antigen presentation (AP)*:* Residential glial cells of the brain are known to act as antigen presenting cells and constitute an important part of immune response against a virus pathogen. Several major histocompatiblity complex (MHC) class II genes *e.g., H2-D1, H2-D4 H2-Q7 and H2-T23* were upregulated at 72hr and 96hr post infection, concomitant with the VEEV antigen appearance in the brain. MHC class I receptors such as *Cd1d1*, *B2m* and *Ap3d1* were also upregulated at 96hr post infection (Table 9).

iv) VEEV infection modulates the apoptotic gene expression in mice brain: Apoptotic neurons are seen in the VEEV infected mice brain in regions associated with VEEV antigen and the regions of gliosis that are free from VEEV antigen. Several apoptotic genes such as caspase recruitment domain (*Card*)14, fas apoptotic inhibitory molecule (*Faim*)2, Apoptosis-associated tyrosine kinase (*Aatk*), eukaryotic translation initiation factor 5 (*Eif5a*) and myeloid cell leukemia sequence 1 (*Mcl1*) were upregulated at 72hr and 96hr post infection (Fig-3). Few genes like amyloid beta (A4) precursor protein (*App*), bcl2/adenovirus e1b interacting protein 3-like (*Bnip3l*), baculoviral IAP repeat-containing 6 (*Birc6*) and *Spn* were upregulated all through out the study and few such as amyloid beta (*A4*) precursor-like protein 1 (*Aplp1*), *Clu*, integral membrane protein 2B (*Itm2b)*, and valosin containing protein (*Vcp*), were upregulated as early as 48hr post infection (Table 10).

Confirmation of Gene Expression

Randomly selected genes identified in the microarrays were analyzed by semi-quantitative PCR analysis in 3-4 biological replicates. Specific amplification was confirmed by sequencing PCR products as described in materials and methods (data not shown). As shown in Fig.4, the expression of these genes (*Oas1b*, *Fcre1g, Mif* and *Clu)* was up-regulated in mice brain infected with VEEV. Although RT-PCR analysis is not quantitative, consistent with microarray analysis, gene expression of *Fcer1g*, *Oas1b* and *Clu* was higher at 48, 72 and 96hr post infection as compared to saline control and 24hr post infection (Figure 25)

Table 9: ***Genes involved in viral response, inflammatory response and antigen presentation.***

UniGene ID	Functional Grouping (Gene)	Expression (Hours post infection) 24	48	72	96
	Virus Response and Inflammation				
Mm.136224	Interferon induced with helicase C domain 1 (Ifih1)	NE	3.59/-	5.21 ± 1.05	4.18 ± 0.31
Mm.3233	Interferon regulatory factor 7 (Irf7)	NE	NE	4.31 ± 1.51	2.01 ± 0.08
Mm.271275	Interferon, alpha-inducible protein 27 (Ifi27)	NE	NE	4.79 ± 0.67	6.62 ± 0.32
Mm.233471	2'-5' oligoadenylate synthetase 1B (Oas1b)	NE	1.89/-	5.12 ± 0.04	2.32 ± 0.08
Mm.867	Chemokine (C-C motif) ligand 12 (Ccl12)	5.03 ± 1.86	4.63/-	7.87 ± 0.54	4.70 ± 0.36
Mm.131723	Chemokine (C-X-C motif) ligand 11 (Cxcl11)	NE	8.76/-	17.02 ± 5.19	13.68 ± 5.51
Mm.877	Chemokine (C-X-C motif) ligand 10 (Cxcl10)	NE	7.49/-	15.45 ± 0.67	8.69 ± 0.37
Mm.284248	Chemokine (C-C motif) ligand 5 (Ccl5)	NE	NE	4.27 ± 1.27	3.56 ± 0.66
Mm.1282	Chemokine (C-C motif) ligand 3 (Ccl3)	NE	NE	2.26/1.83	2.05 ± 0.21
Mm.10116	Chemokine (C-X-C motif) ligand 13 (Cxcl13)	NE	NE	2.06 ± 0.41	1.73/-
Mm.766	Chemokine (C-X-C motif) ligand 9 (Cxcl9)	NE	NE	3.99 ± 1.62	1.85 ± 0.14
Mm.22673	Fc receptor, IgE, high affinity I, gamma polypeptide (Fcer1g)	NE	NE	3.66 ± 0.29	3.38 ± 0.63
Mm.5419	Interleukin 17 (Il17)	NE	NE	NE	2.06 ± 0.33
Mm.2326	Macrophage migration inhibitory factor (Mif)	NE	1.08 ± 0.17	2.25 ± 0.53	2.06 ± 0.07
Mm.24163	PYD and CARD domain containing (Pycard)	NE	NE	1.81 ± 0.165	1.52 ± 0.31
Mm.200608	Clusterin (Clu)	NE	1.74 ± 0.13	4.03 ± 1.54	2.45 ± 0.37
Mm.283714	Sialophorin (Spn)	1.93 ± 0.14	2.50 ± 0.19	2.87 ± 1.63	2.25 ± 0.24
	Antigen Presentation				
Mm.209294	Adaptor-related protein complex 3, delta 1 subunit (Ap3d1)	1.33 ± 0.83	NE	2.17 ± 0.35	1.69 ± 0.01
Mm.163	Beta-2 microglobulin (B2m)	NE	NE	10.39 ± 0.32	6.07 ± 0.25
Mm.1894	CD1d1 antigen (Cd1d1)	NE	NE	NE	1.56 ± 0.01
Mm.22673	Fc receptor, IgE, high affinity I, gamma polypeptide (Fcer1g)	NE	NE	3.66 ± 0.29	3.38 ± 0.63
Mm.33263	Histocompatibility 2, D region locus 1 (H2-D1)	NE	NE	4.88 ± 0.12	9.04 ± 1.15
Mm.387141	Histocompatibility 2, D region locus 4 (H2-D4)	NE	NE	8.92 ± 7.66	9.42 ± 1.34
Mm.35016	Histocompatibility 2, T region locus 23 (H2-T23)	NE	NE	4.72 ± 0.89	3.15 ± 0.83
Mm.296901	Histocompatibility 2, Q region locus 7 (H2-Q7)	4.55 ± 2.49	4.58/-	10.22 ± 4.92	9.50 ± 0.76
Mm.296901	Histocompatibility 2, Q region locus 8 (H2-Q8)	NE	NE	4.45 ± 0.48	NE

Genes that are involved in the virus response and immune response were upregulated at 72 and 96 hr post infection concomitant with the virus appearance in the brain. Several inflammatory response and antigen presentation genes were upregulated and their expression increased with the progression of the disease. Values are expressed as mean ± SEM. NE indicates not expressed and (-) indicates not expressed in biological replicates.

Table 10: ***Genes involved in apoptotic response in VEEV infected mice brain***.

UniGene ID	Functional Grouping (Gene)	Expression [Hour(s) pi] 24	48	72	96
	Apoptosis				
Mm.3336	RIKEN cDNA 1110007C09 gene (1110007C09Rik)	2.66 ± 1.63	3.68 ± 1.14	6.81 ± 4.35	5.22 ± 0.66
Mm.277585	amyloid beta (A4) precursor protein (App)	2.50 ± 0.48	2.54 ± 0.59	4.05 ±1.20	2.87 ± 0.42
Mm.84073	Bcl2-associated athanogene 3 (Bag3)	2.63 ± 0.59	3.30 ± 0.43	4.61 ± 2.37	4.23 ± 0.18
Mm.29820	BCL2/adenovirus E1B 19kDa-interacting protein 3-like (Bnip3l)	1.96 ± 0.11	2.52 ± 0.04	3.88 ± 2.19	3.07 ± 0.14
Mm.290908	Baculoviral IAP repeat-containing 6 (Birc6), mRNA.	1.94 ± 0.33	2.15 ± 0.22	2.54 ± 0.93	2.18 ± 0.04
Mm.283714	Sialophorin (Spn), mRNA.	1.99 ± 0.14	2.50 ± 0.19	2.87 ± 1.63	2.25 ± 0.24
Mm.2381	Amyloid beta (A4) precursor-like protein 1 (Aplp1),	NE	1.90 ± 0.06	3.70 ± 1.15	2.27 ± 0.14
Mm.200608	Clusterin (Clu)	NE	1.74 ± 0.13	4.03 ± 1.54	2.45 ± 0.37
Mm.136224	interferon induced with helicase C domain 1 (Ifih1)	NE	3.59/-	5.21 ± 1.05	4.18 ± 0.31
Mm.4266	integral membrane protein 2B (Itm2b)	NE	1.55 ± 0.20	2.43 ± 0.95	2.46 ± 0.54
Mm.2326	Macrophage migration inhibitory factor (Mif)	NE	1.08 ± 0.17	2.25 ± 0.53	2.06 ± 0.07
Mm.277518	Monocyte to macrophage differentiation-associated (Mmd)	NE	0.59 ± 0.04	2.33 ± 0.45	1.64 ± 0.18
Mm.347546	Inositol 1,3,4-triphosphate 5/6 kinase	NE	1.94 ± 0.02	0.95 ± 0.05	1.83 ± 0.02
Mm.285322	Mitochondrial carrier homolog 1 (C. elegans) (Mtch1)	NE	0.95 ± 0.01	2.08 ± 0.35	1.77 ± 0.23
Mm.687	Ras homolog gene family, member B (Rhob)	NE	1.17 ± 0.03	2.48 ± 0.87	1.59 ± 0.15
Mm.379457	Valosin containing protein (Vcp)	NE	1.68 ± 0.15	2.04 ± 0.77	1.80 ± 0.17
Mm.6826	Apoptosis-associated tyrosine kinase (Aatk)	NE	NE	1.65 ± 0.07	1.20 ± 0.43
Mm.223689	Bifunctional apoptosis regulator (Bfar)	NE	NE	1.83 ± 0.58	1.70 ± 0.08
Mm.130832	Caspase recruitment domain family, member 14 (Card14)	NE	NE	3.23 ± 1.52	2.69 ± 0.08
Mm.29028	Death associated protein 3 (Dap3)	NE	NE	1.87 ± 0.14	0.96 ± 0.03
Mm.280594	Death effector domain-containing DNA binding protein 2 (Dedd2)	NE	NE	1.79 ± 0.66	1.92 ± 0.09
Mm.379461	Eukaryotic translation initiation factor 5A (Eif5a)	NE	NE	2.61 ± 0.49	1.92 ± 0.14
Mm.342392	Engulfment and cell motility 1, ced-12 homolog (C. elegans) (Elmo1), transcript variant 2	NE	NE	1.74 ± 0.21	1.41 ± 0.08
Mm.39760	Fas apoptotic inhibitory molecule 2 (Faim2)	NE	NE	2.85 ± 1.23	2.44 ± 0.12
Mm.281298	Growth arrest and DNA-damage-inducible 45 gamma (Gadd45g)	NE	NE	3.16 ± 0.21	2.12 ± 0.05
Mm.15510	Granzyme A (Gzma)	NE	NE	1.27 ± 0.41	1.94 ± 0.26
Mm.2720	Mitogen activated protein kinase 8 interacting protein 1 (Mapk8ip1)	NE	NE	2.25 ± 0.75	1.16 ± 0.19
Mm.1639	Myeloid cell leukemia sequence 1 (Mcl1)	NE	NE	1.83 ± 0.18	1.56 ± 0.09
Mm.204876	nucleolar protein 3 (apoptosis repressor with CARD domain) (Nol3)	NE	NE	2.02 ± 0.52	1.84 ± 0.09
Mm.24163	PYD and CARD domain containing (Pycard)	NE	NE	1.82 ± 0.17	1.38 ± 0.18

Table Cont…

Mm.276325	Superoxide dismutase 1, soluble (Sod1)	NE	NE	1.74 ± 0.22	1.54 ± 0.24
Mm.200792	Tumor necrosis factor receptor superfamily, member 21 (Tnfrsf21)	NE	NE	2.37 ± 0.84	1.40 ± 0.17
Mm.1894	CD1d1 antigen (Cd1d1)	NE	NE	NE	1.56 ± 0.01
Mm.217764	Phosphoglucomutase 2 (Pgm2)/ Itgb3bp	NE	NE	NE	1.63 ± 0.11
Mm.312628	Serine (or cysteine) proteinase inhibitor, clade A, member 3G (Serpina3g)	NE	NE	NE	2.83 ± 0.18
Mm.218473	Tumor differentially expressed 1 (Tde1)/ Serinc3	NE	NE	NE	1.94 ± 0.01
Mm.338613	Forkhead box O3a (Foxo3a)	1.92 ± 0.17	NE	2.26 ± 1.08	1.57 ± 0.03
Mm.22216	TSC22 domain family 3 (Tcs22d3)	NE	1.63 ± 0.20	NE	NE
Mm.1360	Growth arrest and DNA-damage-inducible 45 beta (Gadd45b)	NE	2.00 ± 0.33	NE	1.85 ± 0.03
Mm.329277	Ubiquitin specific peptidase 14 (Usp14)/ Thoc1	NE	1.90 ± 0.21	NE	2.02 ± 0.18
Mm.347406	CCAAT/enhancer binding protein (C/EBP), beta (Cebpb)	NE	NE	2.01 ± 0.17	NE
Mm.150	Fc receptor, IgG, high affinity 1(Fcgr1)	NE	NE	2.26 ± 0.26	NE
Mm.292100	Fibrinogen-like protein 2 (Fgl2)	NE	NE	1.90 ± 0.27	NE
Mm.368515	Myc-like oncogene, s-myc protein (Mycs)	NE	NE	3.11 ± 0.05	NE

Genes that are modulated in the apoptotic response were upregulated at 72 and 96 hr post infection concomitant with the virus appearance in the brain. Values are expressed as mean ± SEM. NE indicates not expressed and (-) indicates not expressed in biological replicates.

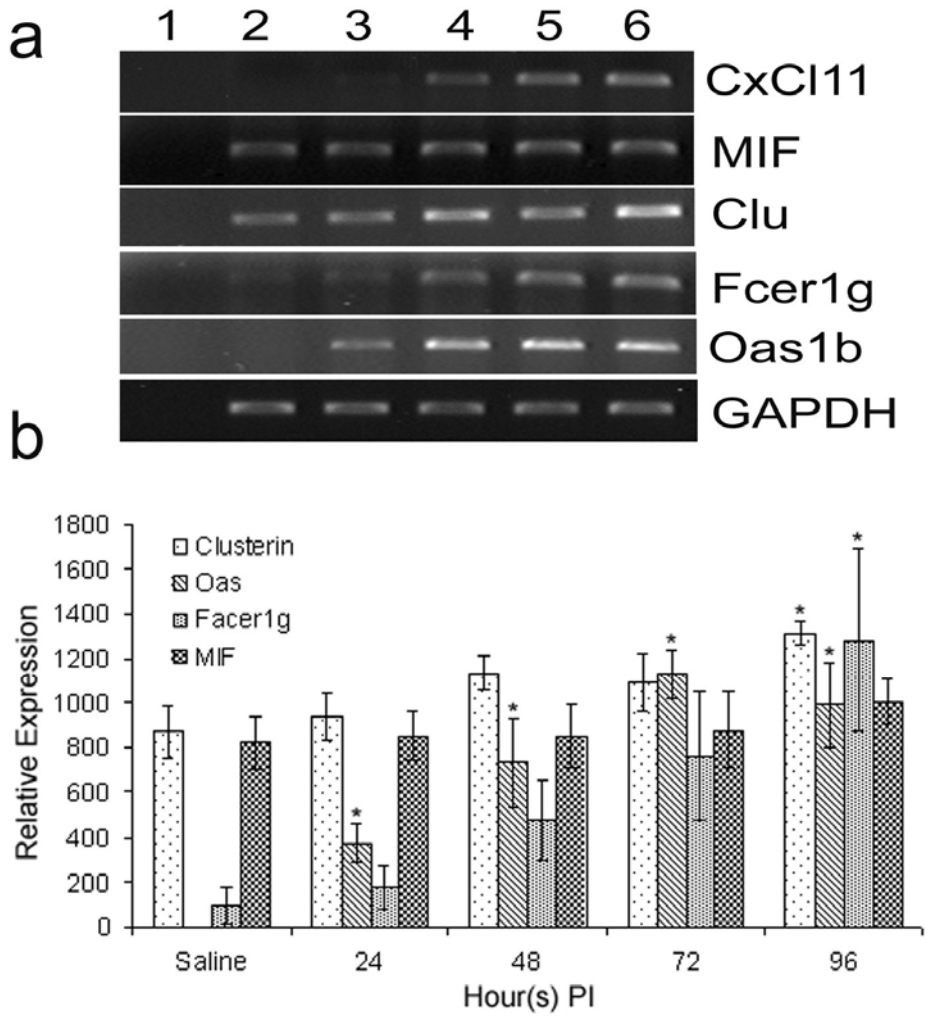

Figure 25: ***Confirmation of selected gene expression by RT-PCR***. (a) Semi quantitative RT-PCR was performed for *Oas1b*, *Fcre1g*, *Clu* and *Mif genes*. Expression was normalized with housekeeping gene *GAPDH*. Lane 1: Negative control, Lane 2: uninfected saline control, Lane 3: 24hr, Lane 4: 48hr, Lane 5: 72hr, Lane 6: 96hr post infection. (b) Quantitative estimation was done by densitometry analysis of PCR product using Scion Image Analysis Software (Scion Corporation, Frederick, Maryland 21701). Values were normalized to the corresponding values of the house keeping genes for individual samples. Values are expressed as mean ± SEM. * $p \leq 0.05$ compared to uninfected control.

Discussion

Proximal cause of death with VEEV infection is attributed to the host immune response to virus replication resulting in lethal encephalitis (Charles et al 2001). Therefore, it becomes important to study the broad range kinetics of gene expression modulation in brain to understand the host immune response against VEEV to identify potential therapeutic targets and markers for VEEV infection treatment. In the present study, we demonstrate that VEE virus appears in the brain at 48 hr post infection accompanied with mild inflammation. Virus antigen and inflammation increased with the progression of the disease and extensive inflammation and virus antigen was detected through out the brain at 96hr post infection. These observations are supportive and consistent with the previously published literature (Charles et al 1995 and 2001, Grieder et al 1995).

Consistent with histopathological changes microarray analysis showed over-expression of the genes involved in the various immune responses towards the pathogen. For example *Oas1b, Ifi27, Ifih1 and Irf7* genes were induced at 72 and 96hr post infection. Cells that express elevated levels of *Oas1b* inhibit West Nile virus (WNV) replication by reducing the positive strand viral RNA level in cells (Kajaste-Rudnitski et al 2006). Since VEEV is a positive single strand RNA virus, increased Oas1b may also potentially inhibit VEEV replication. *Interferon (IFN)* is important in innate immune response to virus pathogens. Anti-VEEV activity of *IFN* and *Irf* is well established (Grieder et al 1999, White et al 2001). *IFN α/β* knock out mice show increased and early spread of VEEV into brain (Schoneboom et al 2000). Therefore, host cells in mouse brain induce a defense response as a result of VEEV infection. However, this immune response is not sufficient to protect from VEEV induced morbidity and mortality.

The ability of microglia, the brain's resident macrophage, to present antigen through the class II MHC to T cells allows these normally quiescent cells to play a critical role in shaping the outcome of many neurological diseases (O'Keefe et al 2002, Dorries 2001). Activated glial cells are observed in the brains of VEEV infected mice (Schoneboom et al 1999, 2000). Consistent with these reported observations upregulated *MHCII* loci such as *H2-D1, H2-D4 H2-Q7 and H2-T23* may reflect the activated state of glial cells in the brain of VEEV infected mice. Several molecules that have *MHC-I* receptor activity such as *B2m, Fcerg1 and Cd1d1* were also found to be upregulated in our study. B2m is also upregulated in acquired immunodeficiency syndrome encephalitic and JC virus (JCV) infection of CNS (Achim 1991, Achim and Wiley 1992). Fc-receptors are important in antigen processing/ presentation myelin proteins during the induction of secondary immune responses locally in the CNS (Abdul-Majid et al 2002) and contribute to the inflammatory damages in CNS. *Cd1d1* play a critical role in control over cytokine production after an acute virus infection (Roberts et al 2004). Thus VEEV infection induces similar host immune response as other viruses.

VEEV infection of CNS has been shown to result in neurodegeneration, perivascular cuffing with infiltrating lymphocytes, gliosis, cerebral edema and apoptotic neurons associated with astrogliosis in the regions of the brain which is free of VEEV antigen (Schoneboom et al 2000). Therefore, it is not clear whether VEEV is directly or indirectly involved with these changes. To understand this phenomenon we asked whether chemokines, cytokines and other inflammatory genes are modulated in the brain. Interestingly, chemokines such as *Cxcl9, Cxcl10, Cxcl11, Cxcl13, Ccl3, Ccl5* and *Ccl12*, Fc-receptor such as *Fcer1g,* and *Mif* genes were upregulated. The chemokines may

contribute to the influx of neutrophils and lymphocytes and severity of the inflammation and encephalitis in VEEV infection of brain. *Fcerg1* Fc-receptor may contribute in VEEV antigen presentation to lymphocytes and induction of inflammatory cytokines. Mif, a proinflammatory cytokine, suppresses the anti-inflammatory effect of glucocorticoids at the site of inflammation. The cytokine expression at the site of inflammation is suggested to be the outcome of interaction of glucocorticoids and *Mif* (Bucala 1998, Baugh and Donnelly 2003). It is also suggested that *Mif* can increase the neutrophil chemoattractant macrophage inflammatory protein-2 (*MIP-2*) and thus may contribute to the inflammation (Makita et al 1998). A concomitant over-expression of *Mif* was observed with the increase in inflammation and neutrophil migration. *Clu*, an anti-apoptotic factor, activates microglia to secrete neurotoxic agents (Xie et al 2005). *Clu* activated microglia show increased *MHCII* expression, secrete reactive nitrogen intermediates and *TNF-α* (Xie et al 2005). VEEV infection of the brain also results in the activation of microglia (Schoneboom et al 2000a, b) and thus *Clu* may contribute to the gliosis observed in VEEV pathogenesis.

Several apoptosis related genes were also upregulated. Clu, an anti-apoptotic factor, activates microglia to secrete neurotoxic agents (Xie et al 2005). Clu activated microglia show increased MHCII expression, secrete reactive nitrogen intermediates and TNF-α (Xie et al 2005). VEEV infection of the brain also results in the activation of microglia (Schoneboom et al 2000a, b) and thus Clu may contribute to the gliosis observed in VEEV pathogenesis. The caspase recruitment domain (CARD) is a protein-binding module that mediates the assembly of CARD-containing proteins into apoptosis and NFκB signaling complexes (Bertin et al 2001). CARD14, a membrane-associated

guanylate kinase (MAGUK) family member containing CARD has been implicated in the antigen specific signaling by the TCR complex via BCL10 mediated NFκB activation (Pomerrantz et al 2002). In our study, CARD14 upregulation was concomitant with the increased inflammation and apoptotic neurons. CARD14 may be involved in the VEEV antigen initiated signaling in the lymphocytes or glial cells and or in the apoptotic pathways in the neurons. Faim2 inhibits the Fas mediated apoptosis and helps in protecting foreign antigen-specific B cells during potentially hazardous interactions with FasL-bearing T cells (Rothstein 2002). Faim2 was upregulated following the VEEV infection and may be involved in the activation and survival of immune cells in the brain.

Our results show a complex immune response to VEEV infection. Several pathways seem to interact for the final outcome of the disease. Thus, suppression of the inflammatory response and enhancement of the antiviral pathways may help in positive outcome and rescue of the patients from lethal VEE. We have identified many potential targets *e.g.,* chemokines, Oas1b*, Fcerg1, Mif* and *Clu* which provide potential targets for therapy.

Chapter 4

Complete Inactivation of Venezuelan Equine Encephalitis Virus by the Photoinducible Hydrophobic Alkylating Compound 1, 5 Iodonaphthylazide and its Protective Efficacy in Mice

Abstract

Hydrophobic alkylating compounds like INA partitions into biological membranes and accumulates selectively into the hydrophobic domain of the lipid bilayer. Upon irradiation with far UV light INA binds selectively to transmembrane proteins in the viral envelope and renders them inactive. Such inactivation does not alter the ectodomains of the membrane proteins thus preserving the structural and conformational integrity of immunogens on the surface of the virus. In this study we have used 1,5-iodonaphthyl-azide (INA) to inactivate Venezuelan Equine Encephalitis Virus (VEEV). Treatment of VEEV with INA followed by irradiation with UV light resulted in complete inactivation of the virus. Immunofluorescence for VEEV and virus titration showed no virus replication *in-vitro*. Complete loss of infectivity was also achieved in mice infected with INA treated plus irradiated preparations of VEEV survived the infection with no clinical sign of disease. This data suggest that such inactivation strategies can be used for developing vaccine candidates for VEEV and other enveloped viruses.

Key Words: Venezuelan equine encephalitis; 1,5-iodonaphthyl-azide; Photoinactivation; Vaccine.

Introduction

Current live attenuated TC-83 vaccine for VEEV is under new- investigational drug status and is given to laboratory personal at –risk. Formaldehyde inactivated TC-83, known as C84, is used as a booster following immunization with live attenuated TC-83 vaccine (Pittman et al 1996, Engler et al 1992). These vaccines have limitations such as, adverse reaction, short-lived immunity and several non-responders **(**Alevizatos et al 1967, Henderson et al 1971, Ludwig et al 2001, Pittman et al 1996). Formalin inactivated vaccine preparation does not provide full protection (Franck 1972, Cole et al 1973) and incompletely inactivated VEEV vaccine has been found to be associated in the outbreak of VEEV (Obreste et al 1998, Kinney et al 1992). Therefore, it is important to develop strategies and techniques to develop new vaccine candidates for VEEV.

Hydrophobic photoactive aryl azides like 1,5 iodonaphthylazide (INA) selectively penetrate into the hydrocarbon core of biological membranes. Upon irradiation, with UV light these compounds directly bind to proteins and lipids embedded in the bilayer (Raviv et al 1984, 1987, Kahane and Gitler 1978, Holowka et al 1981, Jorgensen 1982, Pak et al 1994). Irradiation is applied using light at wavelengths that do not by themselves cause damage to biological molecules (320-360 nm). The resulting inactivation of multiple components in the membrane is efficient and selective so that ectodomain of proteins or lipids outside the bilayer are not affected (Bercovici et al 1978, Raviv et al 1984). Recently this approach was used to produce inactivated HIV and SIV virions for vaccine application (Raviv et al 2005). INA has also been used for inactivation of Ebola and Influenza virus (Raviv et al Personal communication). The mechanism of action of INA is described in Figure 26a.

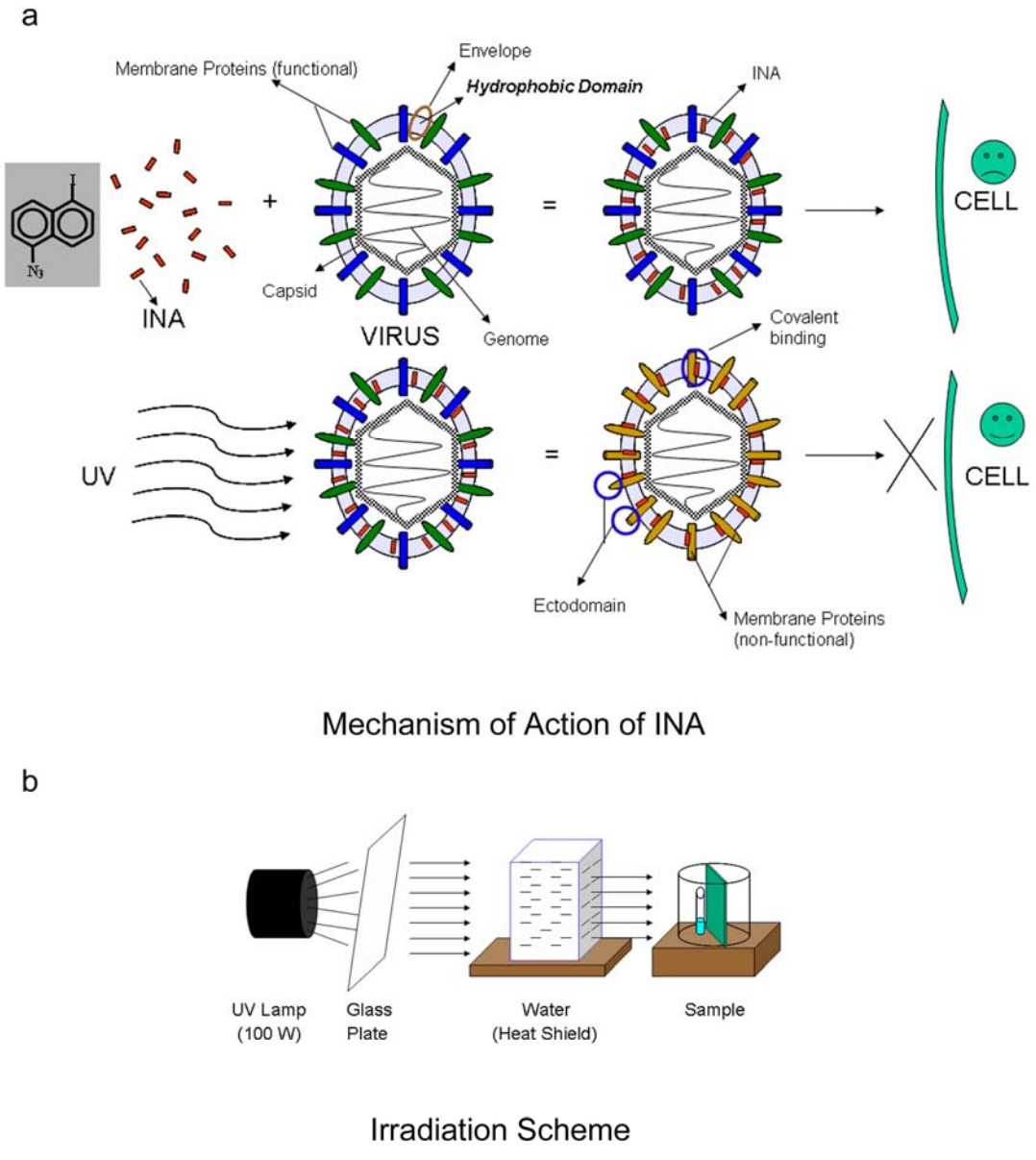

Figure 26: ***Mechanism of action of INA and the sample irradiation scheme.*** a.) INA when added to the virus suspension selectively sequester in the hydrophobic domain of the envelope membrane. But this accumulation of INA does not interfere with the virus envelope proteins function and virus remains infectious. When this virus-INA formulation is irradiated with far UV light INA covalently binds to the transmembrane domain of envelope proteins. This binding of INA to envelope proteins results in functional inactivation of envelope protein which results in blocking of virus fusion to host cell and thus virus inactivation. b.) Sample irradiation scheme as described in materials and methods.

In this study, we demonstrate a complete and efficient inactivation of VEEV upon treatment with INA followed by irradiation with UV light. Inactivation of VEEV by INA was associated specifically with irradiation. There was complete absence of VEEV induced cytopathic effect *in vitro* and clinical sign of disease *in vivo* by INA treated plus irradiated VEEV.

Materials and Methods

Materials

Vero cells were obtained form ATCC, Manassas, VA. Fetal bovine serum (FBS), 1X Minimum Essential Medium (MEM), 0.05%trypsin-EDTA was obtained from Mediatech. Inc., Herendon, VA. 10X Dulbecco's phosphate buffered saline (DPBS) was obtained from Invitrogen Corp. Carlsbad, CA. Crystal violet (CV) and dimethylsulphoxide (DMSO) was obtained from Sigma Aldrich, St. Louis, MO. 10% neutral buffered formalin (NBF) and UV lamp were obtained from VWR International, West Chester, PA. Cell proliferation kit I {MTT (3-[4, 5- dimethylthiazol-2-yl]-2, 5-diphenyl tetrazolium bromide)} and bovine serum albumin (BSA) was obtained from Boehringer Manheim, Indianapolis, IN. Tissue culture flasks, 24 and 96 well plates were obtained from BD Biosciences, Bedford, MA. FITC conjugated goat anti-rabbit IgG was obtained from Molecular probes, Eugene OR. Polyclonal anti-VEEV antibody was provided by Dr Franziska B Grieder, Uniformed Services University of the Health Sciences (USUHS), Bethesda, MD. 1,5 iodonaphthylazide (INA) was kindly provided by Drs Raviv and Blumenthal, NCI, Frederick, MD under a material transfer agreement . INA was solubilized in DMSO at final concentration of 20mM. 1X MEM supplemented with 10% FBS was used through out the study for cell culture.

Animals

Seven to eight week old male Swiss CD-1 mice were obtained from Charles River Laboratories, Wilmington, MA. Mice were housed in micro isolator cages and were provided food and water ad libitum with a 12hr light/dark cycle. All experiments were carried out in bio-safety level 3 (BSL-3) facility and in accordance to Guide for the Care and Use of Laboratory Animals (Committee on Care And Use of Laboratory Animals of The Institute of Laboratory Animal Resources, National Research Council, NIH Publication No. 86-23, revised 1996).

Virus

Molecularly cloned, virulent strain of VEEV, V3000 [Grieder et al 1995], kindly provided by Dr Franziska B Grieder, USUHS, Bethesda, MD was used in the present study.

Inactivation of VEEV with INA

Purified VEEV stocks with known virus titer were suspended in 1X DPBS at a protein concentration of 0.5mg/ml in a clear transparent tube and from this point reduced lighting conditions were used. INA was added to the virus suspension to a final concentration of 10, 50 and 100μM in 3 to 4 installments and samples were incubated for 20 minutes in the dark at room temperature. Samples were then centrifuged at 1000rpm for 1 minute to remove precipitated INA crystals and VEEV containing supernatant was transferred to new tube. Glutathione was added to samples to a final concentration of 20mM. Virus suspension was then irradiated using 100 W mercury UV lamp in the following setup. A clear glass plate was placed immediately in front of the lamp (to filter lower UV wavelengths of light) and water filled 75cm^2 transparent tissue culture flask (used as a heat filter) was placed approximately 6-7 cm apart from the glass plate. Finally

samples were placed 6-7 cm away from the flask in such a way that samples are completely illuminated with the light passing through the flask (Figure 26b). Irradiation was done for 90 seconds, samples were then vortexed and again irradiated for 90 seconds. There after full light conditions were used and samples were stored at -80^{0}C. For infection, *in vitro* and *in vivo*, virus titers were back calculated and dilutions were made accordingly.

Treatment Groups and Controls

To determine the effect of INA treatment procedure and irradiation alone on virulent VEEV, following groups with suitable controls were created. VEEV only, VEEV plus irradiation, VEEV plus DMSO (0.5%), VEEV plus DMSO plus irradiation, VEEV plus INA (100μM) only, VEEV plus INA (10μM) plus irradiation, VEEV plus INA (50μM) plus irradiation, VEEV plus INA (100μM) plus irradiation, PBS only and DMSO only. Since INA is dissolved in DMSO and highest concentration of DMSO (0.5%) was achieved in the 100μM INA treatment, we used 0.5% DMSO in controls.

Infectivity Assay- Cytopathic Effects (CPE)

Vero **c**ells were plated in 24 well tissue culture plates at a density of 10,000 cells per well. Cells were infected with VEEV at a MOI of 0.5 by incubation with the virus for 72 hr. The supernatant medium was removed and plates were washed twice with 1XPBS. Cells were then fixed with 10% NBF for 7 days. Plates were then washed twice with 1XPBS and cells were stained with 0.5% crystal violet for 10 min followed by three washing with distilled water. Experiments were done in replicates of six and repeated twice.

Cell Proliferation (MTT) Assay

Cell proliferation was determined using the Cell Proliferation Kit I according to manufacturer's protocol. Briefly, cells were plated in 96 well tissue culture plates at a density of 3000 cells/well in a final volume of 100µl of MEM and were allowed to attach overnight. The cells were infected with 15µl of VEEV samples at MOI of 0.5 and incubated for 1hr at 37^0C/5%CO_2. Cells were then washed twice and replenished with 200ul of fresh MEM and incubated for 12, 24, 48 and 72hr. At the end of each incubation period culture medium was replaced with 100µl of fresh MEM containing 10µl of MTT dye each well. Plates were incubated for 4 hrs at 37˚C/ 5%CO_2 followed by addition of 100µl solublization buffer. Plates were incubated overnight and color development was quantified using ELISA reader at 570nm. Experiments were done in replicates of ten and repeated twice.

Immunofluorescence for VEEV Antigen

Cells were plated in 8 chamber slides at 10,000cells per chamber and infected with VEEV at MOI of 0.5. After infection and incubation with VEEV, supernatant medium was removed and chambers were detached. Slides were then fixed in chilled acetone: methanol (1:1) solution for 10 min. Excess fixative was blotted off and slides were stored at -20^0C. For immuno-fluorescence staining slides were rinsed thrice with 1X PBS for 5 min each followed by blocking with 1% BSA for 1hr at room temperature (RT). Excess BSA was removed and slides were incubated with polyclonal rabbit anti-VEEV antibody (1:500) diluted in 1%BSA for 1hr/RT. Slides were then rinsed thrice with 1X PBS for 5 min each and incubated with FITC conjugated goat anti-rabbit IgG (1:250) for 1hr at 37^0C. Slides were washed thrice with 1X PBS for 5 min each and mounted with vectasheild mounting medium containing DAPI (Vector laboratories, Inc.

Burlingame, CA). Immuno-fluorescence was observed under fluorescent microscope. Experiments were done in replicates of four and repeated twice.

Virus Titer

Virus titer was determined in the cell supernatant of VEEV infected Vero cell cultures at 72 hr post infection. Four replicates from two different experiments were taken. VEEV titer was determined as a 50% tissue culture infective dose (TCID50) by cytopathic effect (CPE) assay. Serial dilutions of cell supernatant from 10^{-1} to 10^{-10} were made in 1X DPBS supplemented with 0.1%FBS. Vero cells were plated in 96 well plates at a density of 3000 cells per well and cells were infected in 8 replicates with each dilution and incubated at 37^0C/5%CO_2 for 1hr. 200 µl of fresh MEM was added to each well after incubation and plates were incubated for 72hr at 37^0C/5%CO_2. After 72hr incubation infectivity was scored under microscope and TCID50 was calculated.

Electron Microscopy (EM)

Purified VEEV suspension (INA treated and irradiated or no treatment) was spread on the copper EM grids and virus was allowed to adsorb for approximately 5 min. Virus was then fixed with EM grade paraformaldehyde and washed with five serial washes of distilled water. Samples were then stained with negative stain (1% aqueous uranyl acetate) for 2 minutes and were examined in Phillips CM100 transmission electron microscope.

Challenge Procedure and Survival Study In-Vivo

Mice were anesthetized using inhalation anesthesia, isoflurane and 1000 plaque forming units (pfu) of VEEV samples in 25µl volume of 1X DPBS was injected in the

left rear footpad. Animals were observed twice a day for clinical symptoms of disease such as roughening, hunched back, lethargic, hind limb paralysis and mortality.

Vaccine Study

Five – six week old male mice were injected intra-peritoneally with the inactivated VEEV (INA-treated and irradiated V3000) on day zero. There after booster doses were given at day 7 post first vaccination (pfv), day 14 pfv and day 21 pfv (Figure 27). First three vaccines consisted of 10,000 inactivated pfu of V3000 and the fourth vaccine consisted of 50,000 pfu. On the 28^{th} pfv blood was collected by tail vein nick and serum was isolated. On 29^{th} day pfv mice were challenged with virulent V3000 strain of VEEV. There after mice were monitored for the clinical symptoms of disease and mortality for 14 days. Three separate groups were taken as follows 1.) *INA-inactivated VEEV alone* Mice were vaccinated with the INA-inactivated formulation alone at all four vaccinations 2.) *INA-Inactivated VEEV with Alhydrogel* (Brenntag Biosector, Fredeikssund, Denmark) *as adjuvant*. Alhydrogel was used as adjuvant in this group. Alhydrogel was first diluted to a working suspension containing 2mg/ml of aluminum in 1X DPBS. INA-inactivated VEEV formulation was mixed with diluted Alhydrogel in equal volumes. This mixture was ten incubated at room temperature with continuous vortex for 2hr. Mice were then injected with this INA-inactivated VEEV- Alhydrogel preparation. All four vaccinations were done with INA-inactivated- Alhydrogel formulation. ; 3.) *INA-inactivated VEEV with Complete Freund's adjuvant (CFA).* CFA was used as adjuvant in thi group. INA- inactivated VEV was mixed with the equal volume of the CFA just prior to vaccination. This INA-inactivated- CFA preparation as

then injected in the mice. Only first vaccination was done with INA-inactivated- CFA formulation and all other three vaccines contained only INA-inactivated VEEV.

Enzyme-Linked ImmunoSorbent Assay for Detecting Anti-VEEV Antibody in Serum

Blood was allowed to stand on ice for 30 min and was centrifuged at high speed for 30 min. Clear top aqueous layer of serum was then collected and immediately stored at -80^{0}C. For Enzyme-Linked ImmunoSorbent Assay (ELISA) 96 well Immulon 4HBX ultra- high binding polystyrene microtiter plates (Thermo Electron Corp., Milford, MA) were coated with live virulent V3000 strain of VEEV virus at a protein concentration of 5ug/ well in 50µl volume at 4^{0}C / overnight. Virus suspension was then removed and plates were blocked with 50µl/ well of 1% Bovine Serum Albumin (BSA) at 4^{0}C / overnight. Blocking agent was then removed and 50µl serially diluted serum (1:50, 1: 250, 1:625 and 1:1250) was added to each well in triplicates. Plates were then incubated for 4 hrs at 37^{0}C followed by washing twice first with 0.05% Tween 20 in 1X PBS and then with distilled water. 50ul of alkaline phosphatase conjugated goat anti-mouse IgG (secondary antibody) (1:1000) was added to each well and incubated at 37^{0}C for 1hr. Plates were then again washed twice first with 0.05% Tween 20 in 1X PBS and then with distilled water. 50µl of 5mg/ml of phosphatase substrate was then added in each well and color was allowed to develop for 10min at 37^{0}C. Plates were read at 405nm wavelength using ELISA reader (Bio-Rad Laboratories, Inc. Hercules, CA 94547).

Results

INA Plus Irradiation Blocked the Cytopathic Effects (CPE) of VEEV

Healthy live adherent cells when fixed with formalin and washed, sticks to the surface. In contrast, when infected dying cells are fixed with formalin and washed they tend to wash off from the surface. The adherent cells can be visualized by staining with CV, as wells with healthy cells appear blue due to the color taken up by the adherent cells, while the wells with infected dying cells appear colorless, as there are few or no cells on the surface to take the CV color. Cells infected with samples of VEEV treated with various doses of INA (10, 50 and 100μM) combined with irradiation showed inhibition of cell death as was visible by blue staining at the bottom of the wells (Figure 28). Staining was similar to PBS or DMSO treated cells. On the other hand complete cell death was observed in all the other samples i.e. VEEV plus irradiation, VEEV plus DMSO treatment, VEEV plus DMSO plus irradiation and VEEV plus INA (100μM) treatment and was similar control virulent VEEV infection. In replicate experiments VEEV samples treated with 10μM dose of INA combined with irradiation were found to induce cytopathic effect in Vero cells in some of the replicates while 50 and 100μM doses of INA consistently inhibited the CPE when combined with irradiation.

INA Plus Irradiation Inhibited Cell Death Induced by VEEV

Cell proliferation assay was performed as quantitative measurement of inhibition of VEEV infection *in vitro.* Virulent VEEV causes extensive infection and cell death in Vero cells cultures therefore, greater the infectivity lesser is the cell proliferation. Significant inhibition of VEEV infectivity was observed at 72hr post infection (Figure 29) with all three doses of INA (10, 50 and 100μM) combined with irradiation. Cell proliferation was comparable to the positive control for cell proliferation i.e. uninfected

cell cultures. VEEV plus irradiation, VEEV plus DMSO treatment, VEEV plus DMSO plus irradiation, VEEV plus INA (100μM) showed significant infectivity similar to the virulent VEEV infected cells. In replicate experiment VEEV samples treated with 10μM dose of INA combined with irradiation showed partial infectivity where as 50 and 100μM treatment doses of INA consistently inhibited the infection when combined with irradiation.

Infection of VEEV was Inhibited Upon Treatment with INA Plus Irradiation

VEEV specific immuno-fluorescence staining was done to localize the VEEV antigen in the infected Vero cell cultures. VEEV specific staining was positive in the following samples: VEEV plus irradiation; VEEV plus DMSO treatment; VEEV plus DMSO plus irradiation and VEEV plus INA (100μM) and was similar to virulent VEEV infected cells at all time points (12, 24 and 48hr pi). VEEV staining was diffused in the membrane, cytoplasm and also in the nucleus (Figure 30). There was no detectable VEEV staining in cells infected with VEEV that was treated with any of the three doses of INA (10, 50, 100μM) in combination with UV light. The values in those samples were similar to the controls for no VEEV antigen i.e. PBS and DMSO treated cells. Staining with DAPI, that stains the nucleus blue, indicated that cells were present where there was no VEEV antigen thus eliminating the possibility of false results due to loss of cells (Figure 28). In a replicate experiment few microscopic fields were positive for VEEV antigen in the 10μM INA group. However, the VEEV that was treated with 50 and 100μM INA consistently showed no signs of infectivity by immuno-fluorescence staining.

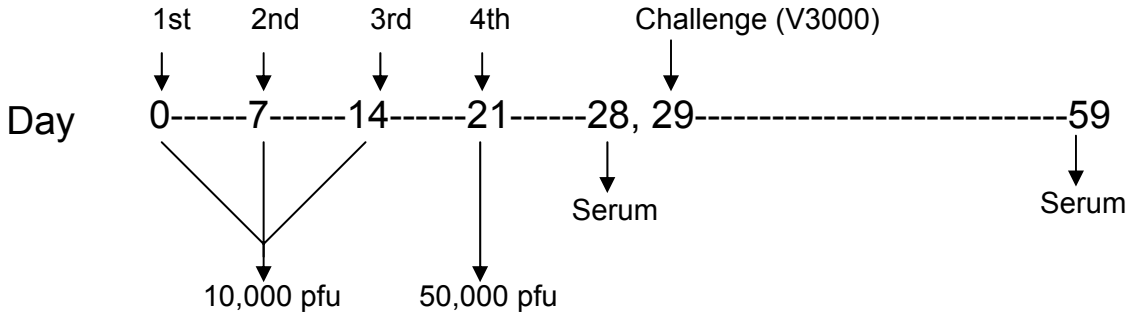

Figure 27*: Schematic representation of the vaccine study with INA-inactivated VEEV.* Five-6 week old mice were given four vaccinations at day 0, 7, 14 and 21. Serum was collected after four weeks of first vaccination and antibody titer was determined in serum. Animals were than challenged with virulent virus and observed for clinical symptoms of disease.

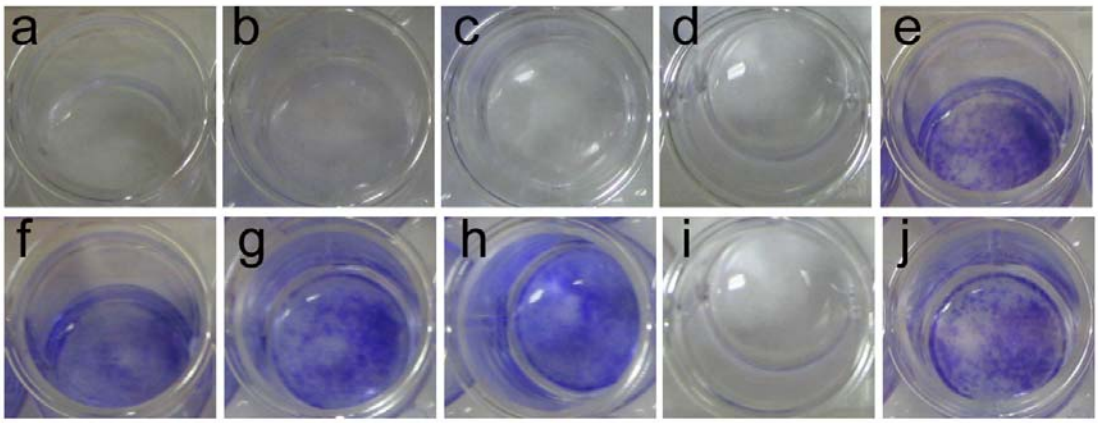

Figure 28: ***Infection of Vero cells with VEEV***: Vero cells were infected with various treatment and control groups of VEEV. Cells were fixed and stained with CV at 72hr post infection and infectivity was observed. Infectivity was inhibited in VEEV samples treated with INA plus irradiation. a) VEEV only; b) VEEV plus irradiation; c)VEEV plus DMSO; d) VEEV plus DMSO plus irradiation; e) PBS only; f)VEEV plus INA(10μM) plus irradiation; g) VEEV plus INA(50μM) plus irradiation; h) VEEV plus INA(100μM) plus irradiation; i)VEEV plus INA (100μM) and j) DMSO only.

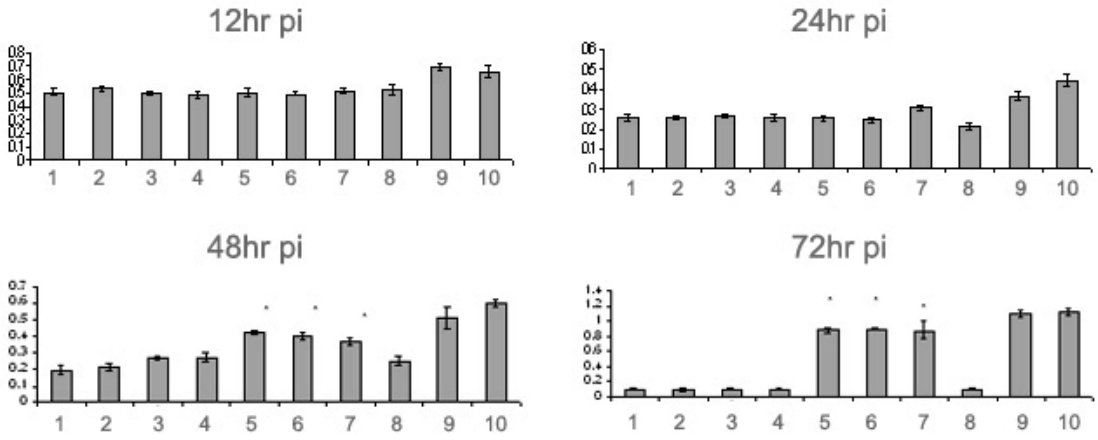

Figure 29: ***Cell proliferation assay***: Vero cells were infected with various treatment and control groups of VEEV. Cell proliferation was assayed at 12, 24, 48 and 72hr post infection using MTT assay. Cell proliferation was significantly higher in the VEEV samples treated with INA plus irradiation at 48 and 72 hr post infection. 1) VEEV only; 2) VEEV plus irradiation; 3) VEEV plus DMSO; 4) VEEV plus DMSO plus irradiation; 5) VEEV plus INA (10μM) plus irradiation; 6) VEEV plus INA (50μM) plus irradiation; 7) VEEV plus INA (100μM) plus irradiation; 8) VEEV Plus INA (100μM); 9) PBS and 10) DMSO.

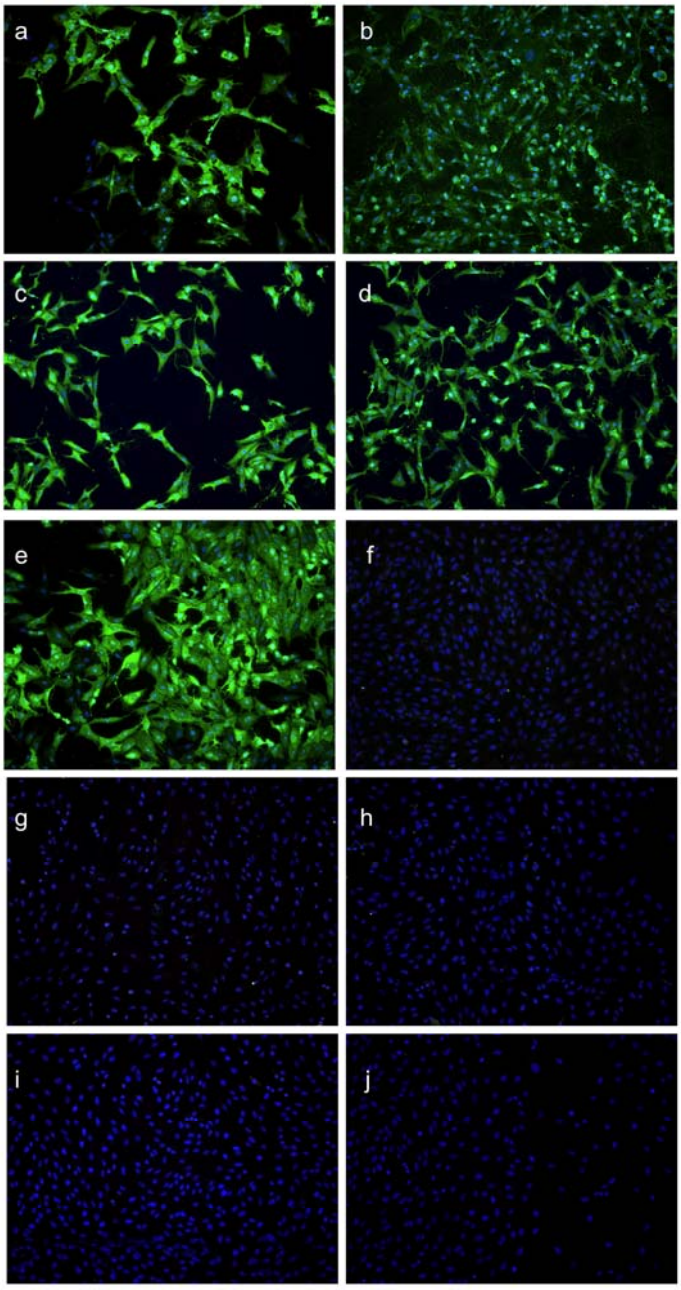

Figure 30: ***Immunofluorescence for VEEV antigen***. Vero cells were infected with various treatment and control groups of VEEV. Cells were fixed and stained for VEEV specific staining at 24hr post infection. There was no detectable VEEV antigen in VEEV samples treated with INA plus irradiated. a) VEEV only; b) VEEV plus irradiation; c) VEEV plus DMSO; d) VEEV plus DMSO plus irradiation; e) VEEV Plus INA (100µM); f) VEEV plus INA (100µM) plus irradiation; g) VEEV plus INA (10µM) plus irradiation; h) VEEV plus INA (50µM) plus irradiation; i) PBS and j) DMSO.

VEEV Replication was inhibited upon treatment with INA plus Irradiation

Virus titer in the cell supernatants was determined as $TCID_{50}$ in four replicates (Table 11). VEEV replication was inhibited in all the four replicates at 50 and 100 μM doses of INA. Two out of four replicates at 10μM dose showed virus titer comparable to that of controls.

INA Treatment plus Irradiation did not affect the Structural Integrity of VEEV

EM revealed that VEEV virions were structurally intact upon treatment with INA followed by irradiation (Figure 31).

VEEV Treated With INA Plus UV Did Not Induce Morbidity and Mortality in Mice

Six group of nine mice each were infected with a single dose of 1000 pfu of VEEV only, VEEV plus irradiation, VEEV plus DMSO (0.5%), VEEV plus DMSO plus Irradiation, VEEV plus INA (100μM) and VEEV plus INA (100μM) plus irradiation. Based on results of *in vitro* experiments, 100μM dose of INA was selected. All the groups except VEEV plus INA (100μM) plus irradiation started showing signs of disease by day 5 post infection. By 13^{th} day post infection all the animals in various groups died except the group infected with VEEV sample treated with 100μM INA combined with irradiation. There was no sign of disease such as roughening, hunched back, excitability, seizures and paralysis in any of the nine mice in INA treated plus irradiated VEEV infected group. The disease progression and mortality is summarized in table 12. One group of two mice was injected with 100μM INA with similar dilutions as made for above mentioned groups in order to observe the toxicity of INA alone in mice. There were no sign of toxicity in these mice consistent as previously reported (Steele et al 2006)

Table 11. ***Virus titer in the cell supernatants.***

Sample Group	Sample 1	Sample 2	Sample 3	Sample 4
VEEV only	1.69×10^6	5.49×10^5	7.5×10^5	6.3×10^5
VEEV + DMSO	6.3×10^5	1.54×10^6	3.71×10^5	2.57×10^5
VEEV + Irrad	6.3×10^5	5.62×10^5	4.57×10^5	6.3×10^5
VEEV + DMSO + Irrad	1.44×10^6	2.13×10^6	6.3×10^5	4.57×10^5
VEEV + INA (100µM) only	6.3×10^5	4.57×10^5	1.69×10^6	4.57×10^5
VEEV + INA (10µM) + Irrad	0	0	3.71×10^6	4.36×10^6
VEEV + INA (50µM) + Irrad	0	0	0	0
VEEV + INA (100µM) + Irrad	0	0	0	0

Vero cells were infected with various sample groups and supernatant was collected at 72hr post infection. Virus titer in the supernatant was determined as $TCID_{50}$ in Vero cell cultures. No virus was detected in supernatants of Vero cultures infected with INA-treated plus irradiated VEEV samples at 50µM and 100µM doses of INA.

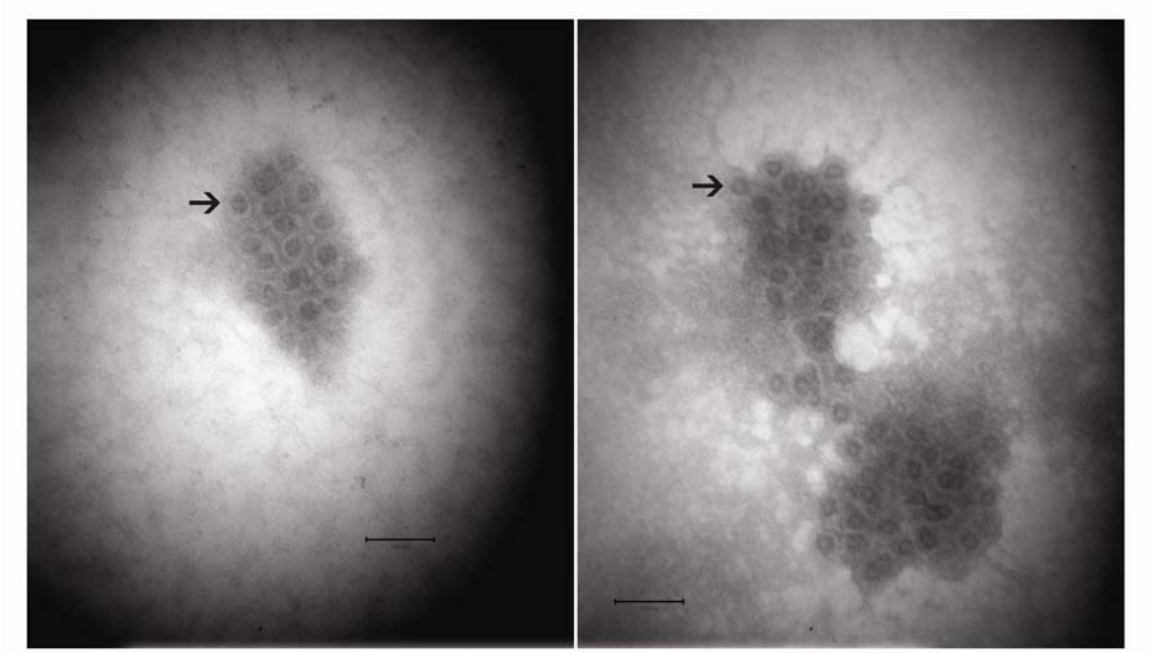

Figure 31: ***Electron Microscopic image of INA treated plus irradiated VEEV***. Structural integrity of VEEV virion was maintained after treatment of VEEV with INA followed by irradiation. This gives a direct proof that treatment with INA does not have detrimental affects on the integrity of VEEV virion.

Table 12: ***Complete Inactivation of VEEV by INA plus Irradiation in vivo.***

Groups: → / Day pi[a] ↓	VEEV	VEEV + DMSO	VEEV + DMSO + I[b]	VEEV + I[b]	VEEV + INA[c]	VEEV + INA[c] + I[b]
1	0	0	0	0	0	0
2	0	0	0	0	0	0
3	0	0	0	0	0	0
4	0	0	0	0	0	0
5	0	3	0	0	0	0
6	0	1 (4)[d]	2	0	0	0
7	1	1 (5)[d]	1 (3)[d]	0	1	0
8	1 (2)[d]	0	1 (4)[d]	4	0	0
9	1 (3)[d]	1 (6)[d]	2 (6)[d]	4 (8)[d]	1 (2)[d]	0
10	0	1 (7)[d]	0	0	3 (5)[d]	0
11	4 (7)[d]	0	2 (8)[d]	0	3 (8)[d]	0
12	1 (8)[d]	2 (9)[d]	1 (9)[d]	1 (9)[d]	1 (9)[d]	0
13	1 (9)[d]	0	0	0	0	0
Percent Mortality	100 (9/9)[e]	100 (9/9)[e]	100 (9/9)[e]	100 (9/9)[e]	100 (9/9)[e]	0 (0/9)[e]

[a] Post infection
[b] Irradiation
[c] 100μM dose
[d] Cumulative mortality
[e] Total dead / total number

Mice were injected with $1x10^3$ pfu of V3000 (various treatments) in the left rear foot pad. Mice in various groups started becoming sick after day 4 post infection and except the group which received INA-treated plus irradiated VEEV. There was 100% mortality in all groups except INA-treated plus irradiated VEEV. Two mice were injected with only INA (similarly diluted as virus suspension) and no toxicity was observed.

Inactivated VEEV Protected Mice from Virulent VEEV Challenge

Ten mice were vaccinated in each group i.e. 1.) INA-inactivated VEEV alone; 2.) INA-inactivated VEEV - Alhydrogel and; 3.) INA- inactivated VEEV- CFA. Fourth Vaccine was followed by challenge with the virulent VEEV i.e. V3000 and animals were thereafter observed for clinical symptoms of disease. One group of ten age matched mice was included in the challenge procedure as non-vaccinated controls. As expected all the mice in the non-vaccinated group succumbed to the challenge with the virulent VEEV (100% mortality). Four out of ten mice succumbed to the virulent VEEV challenge in the group that was vaccinated with INA-inactivated VEEV alone (40% mortality). Two out of ten mice succumbed to the challenge with the virulent VEEV in the group that received vaccine with CFA (20% mortality). One out of ten mice succumbed to the challenge with the virulent VEEV in the group that received vaccine with Alhydrogel as adjuvant (10% mortality). These results are summarized in table 13.

Inactivated VEEV Induced A Neutralizing Anti-VEEV Antibody Response In Mice.

Antibody titer as determined by ELISA in the serum of the vaccinated mice also corroborated the protection data. Vaccination with INA-inactivated VEEV alone resulted in a variable antibody response where some mice showed antibody titer of $>Log_{10}$ 2.1 and some mice showed titer $< Log_{10}$ 2.1. Where as use of CFA as adjuvant resulted in a more consistent antibody response among the animals in the group and was approximately Log_{10} 2.1. Use of Alhydrogel as adjuvant resulted in a consistent higher antibody response among the animals in the group. The antibody titer in this group was above Log_{10} 2.15. These results are summarized in Figure 32

Table 13: ***Vaccination with INA-inactivated VEEV protected mice from virulent VEEV challenge.***

Group(s)	Protection (%) (Total Died/ Total Mice)
Non-vaccinated	0 [a] (10/10) [b]
Inactivated VEEV [c]	60 (4/10)
Inactivated VEEV + CFA [d]	80 (2/10)
Inactivated VEEV + Alum [e]	90 (1/10)

Mice were vaccinated as described in Figure 26. Upon challenge with virulent VEEV (V3000) non vaccinated mice developed the clinical symptom of disease such as ruffled fur, hunched posture, excitability and hind limb paralysis. All the non-vaccinated mice succumbed to the virulent VEEV challenge. Sixty-percent of mice that were vaccinated with INA-inactivated VEEV alone survived the challenge with virulent virus. Protection with INA-Inactivated VEEV vaccine increased with the use of CFA and Alum as adjuvants to 80 and 90 percent respectively. [a] Percent protection; [b] total died / total number; [c] VEEV inactivated with 100μM dose of INA in combination with irradiation; [d] Complete Freund's Adjuvant; [e] Aluminum hydroxide containing 2mg/ml of aluminum.

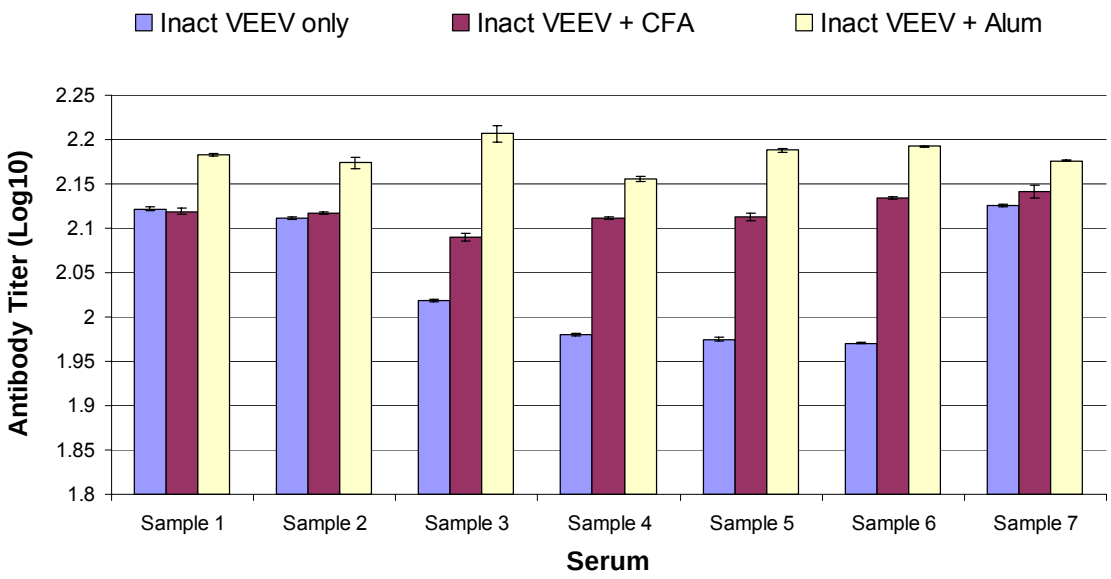

Figure 32: ***Serum antibody titer in mice vaccinated with INA-inactivated VEEV.*** Serum anti-VEEV antibody titer was evaluated using ELISA as described in materials and methods. Vaccination wit INA-inactivated VEEV alone resulted in variable anti-VEEV antibody response. Incorporation of CFA adjuvant in the vaccine resulted in a consistent anti-VEEV antibody response where the titers were similar to the highest titer as observed in INA-inactivated VEEV alone vaccine. Use of Alum adjuvant in the vaccine resulted in consistently higher antibody response across the group.

Discussion

The primary objective of this study was to test the efficacy of targeting the hydrophobic domain of the viral envelope in inactivating the virulent strain V3000 of VEEV. For that purpose we used the hydrophobic photoactive membrane probe INA. This probe selectively concentrates into the lipid bilayer of biomembranes and binds to transmembrane proteins in this domain upon photo activation with UV light. This compound has been previously shown to be effective for inactivating retroviruses while preserving their structure. (Raviv et al 2005).

Treatment of VEEV with INA combined with irradiation completely inactivated the infectivity of VEEV. The ability of VEEV to infect and replicate in cell culture was completely inhibited at a 50μM dose of INA as detected by VEEV specific immuno-fluorescence and virus titer. These results were similar to those reported for retroviruses by Raviv et al (2005). Moreover, in the mice model for VEEV infection that is sensitive to infection with as low as 10 pfu of virus resulting in the host death, INA treatment of VEEV plus irradiation completely inhibited the morbidity and mortality in the animals.

The inactivation of VEEV was dependent on irradiation with UV light in the presence of INA as the infectivity of non-irradiated INA treated VEEV was not inhibited and was similar to the virulent VEEV. This indicates that light induced binding of INA to VEEV envelope proteins is essential for viral inactivation. In this study we did not examine directly the affect of INA on VEEV envelope glycoprotein but it will be safe to assume that the inactivation is occurring due to the light induced binding of INA with VEEV envelope glycoprotein as described for retroviruses. INA alone most probably has no effect on the structural integrity of VEEV as treatment with as high as 100μM of this

compound in the absence of irradiation did not alter the infectivity of the virus. Further EM showed intact virion particles in INA treated plus irradiated VEEV samples. At the same time irradiation alone also did not have any detrimental effect on VEEV infectivity.

Vaccine study using INA-inactivated VEEV further suggests that INA-inactivated VEEV may efficiently induce protective antibody response. Though use of INA-inactivated VEEV alone provided only 60% protection in mice against virulent VEEV challenge this protection was improved by incorporating adjuvant in the vaccine formulation. Alum which is approved for its use as adjuvant in human vaccine effectively increased the antibody titer and conferred 90% protection. Standardization of the doses of INA-inactivated VEEV may provide the desired 100% protection in mice.

There remains an urgent need for an efficient vaccine for immunization against VEEV due to its ability to spread and infect through aerosol route (Steele et al 1998) and its potential to be used as a biowarfare agent (Hawley et al 1997). Currently live attenuated TC83 (Berg et al 1961) which is under investigational new drug status, has limited use due to non-responders and residual virulence (Walton et al 1973, Pittman et al 1996, Alevizatos et al 1967, Ludwig et al 2001) and may not protect against the broad range of VEEV strains (Reed et al 2005). Several other passive and active immunization strategies have been tested (Phillpotts RJ 2006, Rao et al 2006). Genetically engineered live attenuated strains such as V3526 have been shown to be protective in non human primate models of VEEV infection (Rao et al 2004, 2006, Reed et al 2005, Pratt et al 2003, Hart et al 2000). Chimeric SIN/VEE (Paessler et al 2003, 2006), recombinant baculoviruses, adenoviruses and vaccinia virus expressing VEEV structure glycoprotein have also been tested (Hodgson et al 1999, Phillpotts et al 2005, Bennett et al 1998).

Monoclonal antibodies (Phillpotts RJ 2002, 2006), microencapsulated VEE virus vaccine (Greenway et al 1995, 1998) has also been tested and found to be protective against virulent VEEV challenge. Compounds such as melatonin have also been evaluated for their efficacy in increasing the efficiency of TC-83 vaccine (Negrette et al 2000, 2001). These efforts have been plagued by residual virulence, incomplete inactivation, short lived immunity, non- responders and or protection against only few stains of VEEV.

The novel approach described in this study for using hydrophobic alkylating compounds like INA to selectively target the viral envelope may prove useful in generating inactivated VEEV preparations that are fully immunogenic and free from residual virulence. We have shown that such a preparation is non-reactogenic in mice and is able to protect and induce neutralizing antibody response against virulent VEV challenge. Furthermore this approach shall be explored for developing multivalent vaccines against different VEEV subtypes and other alphaviruses. Studies are being planned to test the structural integrity of VEEV envelope protein after treatment with INA and to improve the protective efficacy of INA-inactivated VEEV in mice.

Conclusions

Based on the results in the preceding chapters' following model of VEEV pathogenesis may be defined (Figure 33). As reported earlier, VEEV gains entry into the CNS via olfactory tract. Parallel to this event adhesion molecules are up-regulated on the brain endothelium probably as part of systemic innate immune response towards VEEV. By analogy with other alphaviruses *e.g.,* SFV, receptors of ICAM1 i.e. LFA1 are up-regulated on the activated encephalitic leucocytes. Through binding of LFA to its ligand, ICAM1, leucocytes attach to the brain endothelium. It is now described that binding of ICAM1 on brain endothelium to its receptor induces cellular pathways that results in the opening of the otherwise tight junction of BBB. Various enzymes such as extra-cellular proteases, and chemokines and cytokines also participate in this phenomenon. In our study we have shown that ICAM-1 and associated proteases (cathepsins) are up-regulated in VEEV infected mice brain and ICAM-1 expression is specific to the endothelial lining of brain microvessels. Simultaneous to this, presence of virus in brain activates the brain residential glial cells resulting in the release of inflammatory cytokines, chemokines and interferon. Interferons are well described to have a protective action in VEEV (Grieder et al 1999, Schoneboom et al 2000b). While inflammation constitute to the antiviral response against VEEV it also become detrimental to host in VEEV infection of brain (Schoneboom 2000).

Inside brain initially virus presence may be recognized by multiple TLRs such as Tlr 3, 7 and 9 resulting in the activation of TLR signaling cascade. This results in release of ckemokines, inflammatory cytokines and interferon. Under the influence of chemokines activated lymphocytes and neutrophils enter the brain through BBB. These

leucocytes may be also be infected with VEEV resulting in the increase of viral load in the brain. By analogy in other viruses, microglia, the APCs of brain, may present the VEEV antigen to T-lymphocytes resulting in their activation and further release of cytokines and chemokines. Free virus can further activate the astroglia adding to the inflammatory response. Neutrophils may further add to the inflammatory response in the brain. This results in a cycle where more and more inflammatory cells enter the brain via BBB resulting in the burst of inflammatory response against VEEV. This inflammation then becomes detrimental to the neurons resulting in neuronal degeneration due to prolonged excitation, demylination and virus infection.

Therefore, reduction in the host inflammatory response may be helpful in reducing the inflammatory damage in the brain. As seen in the ICAM-1 KO mice the reduced inflammation in the brain and is concomitant with the delayed onset of the disease and reduced mortality. ICAM-1 KO mice also exhibit reduced inflammatory gene expression with out reduction in the virus antigen in brain.

Our studies also show that several chemokines and cytokines are upregulated in VEEV infected brain. Therefore, it will be safe to assume that activated leucocytes can enter into the brain as a result of modulation of ICAM-1 on the brain microvessel endothelium and under the influence chemotaxis exerted by the several chemokines expressed in the brain following infection and activation of brain residential glial cells with VEEV. Once inside the brain these leucocytes maybe presented with the virus antigens by the microglia cells resulting in the release of inflammatory cytokine, chemokines and interferon. The activated astroglia may further amplify the immune

response. This results in a cycle where more and more leucocytes may enter into the brain resulting in a burst of inflammatory reaction in brain.

Treatment of VEEV by INA in combination with UV irradiation successfully inhibits the infectivity of the virulent VEEV. This formulation also induces protective antibody response against virulent VEEV challenge which is improved with the use of adjuvants. Since current available vaccine (under experimental new drug status) for VEEV does not provide immunity in approximately 20% of immunized population and also has residual virulence the strategy of VEEV inactivation using INA can be further explored and studied to develop a potential VEEV vaccine. This candidate is free from any residual virulence as shown in mice and when used in conjunction with adjuvant may provide sufficient immunity in the population non-respondent to current VEEV vaccine. Third shortcoming of current VEEV vaccine is that it does not provide protection against broad range of VEEV strains. INA inactivated preparations of different strains of VEEV can be combined in a single formulation and may provide a single vaccine solution for broad range of VEEV strains.

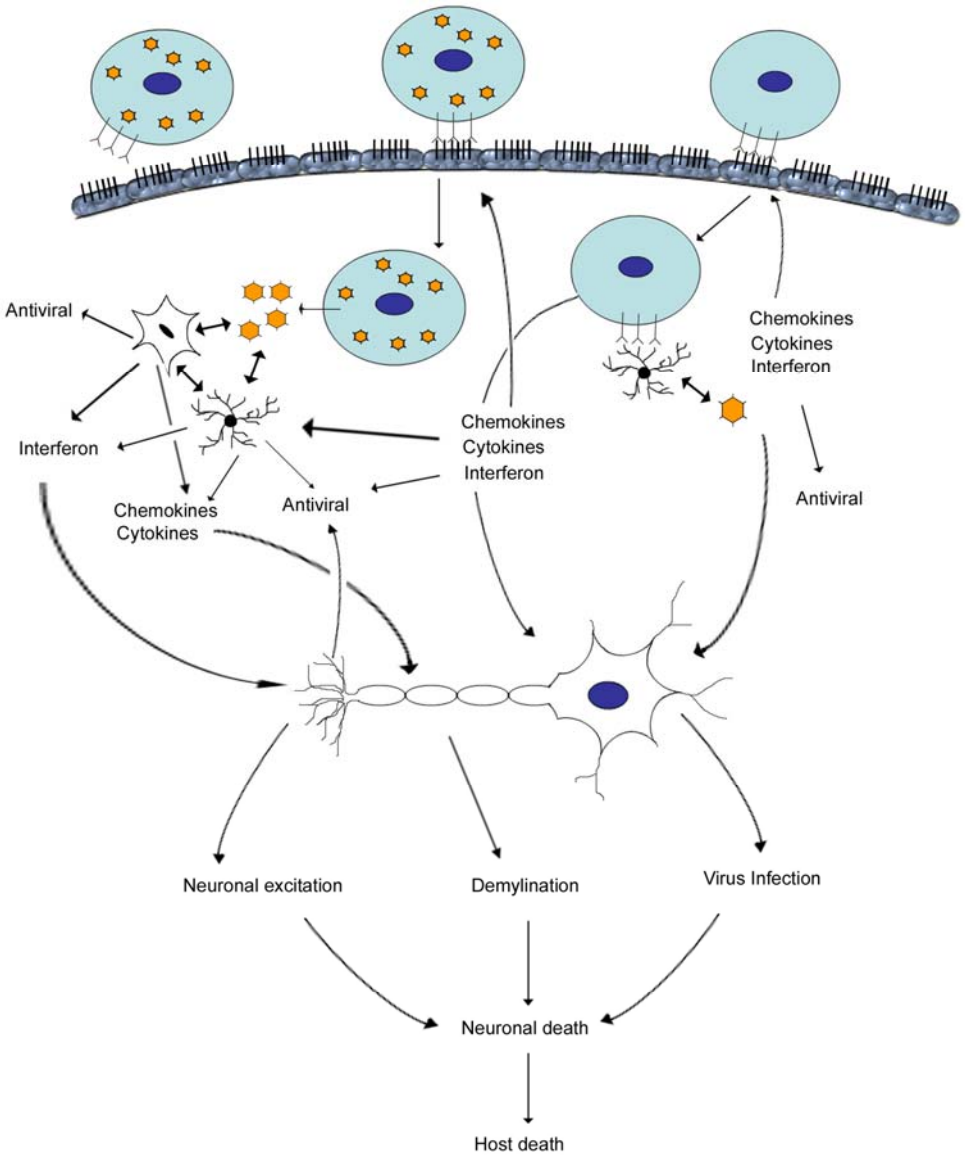

Figure 33: ***Schematic representation of suggested VEEV pathogenesis model***. Upregulation of ICAM-1 on the brain microvessel endothelial linings results in the attachment and transmigration of leucocytes into the brain. These immune cells may either themselves be infected with virus or in activated state. Once inside the brain these cells interact with the brain residential glial cells. Glial cells are the antigen presenting cells of the brain and may present VEEV antigen to the peripheral immune cells thus further activating the immune cells. Activated leukocytes, astrocytes and microglia cells together produce inflammatory cytokines and chemokines and excessive inflammation then results in the neuronal damage such as excitatory death and or demylination of neurons. Toll Like receptor signaling is activated inside the brain and may participate in the production of inflammatory cytokines and chemokines. Some chemokines such as MCP1 may also alter the BBB and further compound the pathology. Thus multiple simultaneous processes results in the detrimental effect on the host in terms of brain tissue damage.

References

Abdul-Majid KB, Stefferl A, Bourquin C, Lassmann H, Linington C, Olsson T, Kleinau S, Harris RA (2002). Fc receptors are critical for autoimmune inflammatory damage to the central nervous system in experimental autoimmune encephalomyelitis. *Scand J Immunol* **55:** 70-81.

Ahmed M, Brzoza KL, Hiltbold EM (2006). Matrix protein mutant of vesicular stomatitis virus stimulates maturation of myeloid dendritic cells. *J Virol* **80:** 2194-2205.

Ahmed Z, Baker D, Cuzner ML (2003). Interleukin-12 induces mild experimental allergic encephalomyelitis following local central nervous system injury in the Lewis rat. *J Neuroimmunol* **140:** 109-17.

Ahmed Z, Gveric D, Pryce G, Baker D, Leonard JP, Cuzner ML, Diemel LT (2001). Myelin/axonal pathology in interleukin-12 induced serial relapses of experimental allergic encephalomyelitis in the Lewis rat. *Am J Pathol* **158:** 2127-38.

Alevizatos AC, McKinney RW, Feigin RD (1967). Live, attenuated Venezuelan equine encephalomyelitis virus vaccine. I. Clinical effects in man. *Am J Trop Med Hyg* **16:** 762-8.

Alexopoulou L, Holt AC, Medzhitov R, Flavell RA (2001). Recognition of double-stranded RNA and activation of NF-kappaB by Toll-like receptor 3. *Nature* **413:** 732-738.

Amy XY, Mejido J, Petersen D, Han J, Kawasaki ES, Puri RK (2006). Quality Analysis of Contact-Pin Fabricated Oligonucleotide Microarrays. *Molecular Biotechnology* **(In press)**.

Anishchenko M, Bowen RA, Paessler S, Austgen L, Greene IP, Weaver SC (2006). Venezuelan encephalitis emergence mediated by a phylogenetically predicted viral mutation. *Proc Natl Acad Sci U S A* **103:** 4994-9.

Arya SC (2001). Comparative neurovirulence of attenuated and non-attenuated strains of Venezuelan equine encephalitis virus in mice. *Am J Trop Med Hyg* **65:** v-vi.

Banks WA, Kastin AJ, Broadwell RD (1995a). Passage of cytokines across the blood-brain barrier. *Neuroimmunomodulation* **2:** 241-248.

Banks WA, Kastin AJ, Broadwell RD (1995b). Permeability of the blood-brain barrier to melanocortins. *Peptides* **16:** 1157-1161.

Bennett AM, Lescott T, Phillpotts RJ (1998). Improved protection against Venezuelan equine encephalitis by genetic engineering of a recombinant vaccinia virus. *Viral Immunol* **11:** 109-17.

Bercovici T, Gitler C (1978). 5-[125I]Iodonaphthyl azide, a reagent to determine the penetration of proteins into the lipid bilayer of biological membranes. *Biochemistry* **17:** 1484-9.

Berge TO, Banks IS, Tigertt WD (1961). Attenuation of Venezuelan equine encephalomyelitis vaccine by in vitro cultivation in guinea-pig heart cells. *Am J Hyg* **73:** 209-218.

Bertin J, Wang L, Guo Y, Jacobson MD, Poyet JL, Srinivasula SM, Merriam S, DiStefano PS, Alnemri ES (2001). CARD11 and CARD14 are novel caspase recruitment domain (CARD)/membrane-associated guanylate kinase (MAGUK) family members that interact with BCL10 and activate NF-kappa B. *J Biol Chem* **276:** 11877-82.

Bhattacharya B, Miura T, Brandenberger R, Mejido J, Luo Y, Yang AX, Joshi BH, Ginis I, Thies RS, Amit M, Lyons I, Condie BG, Itskovitz-Eldor J, Rao MS, Puri RK (2004). Gene expression in human embryonic stem cell lines: unique molecular signature. *Blood* **103:** 2956-64.

Bigler WJ, Ventura AK, Lewis AL, Wellings FM, Ehrenkranz NJ (1974). Venezuelan equine encephalomyelitis in Florida: endemic virus circulation in native rodent populations of Everglades hammocks. *Am J Trop Med Hyg* **23:** 513-21.

Bondarenko EI, Protopopova EV, Konovalova SN, Sorokin AV, Kachko AV, Surovtsev IV, Loktev VB (2003). [Laminin-binding protein (LBP) as a cellular receptor for the virus of Venezuelan equine encephalomyelitis (VEE): Part 1. A study of the interaction between VEE virus virions and the human recombinant LBP]. *Mol Gen Mikrobiol Virusol***:** 36-9.

Bondarenko EI, Protopopova EV, Konovalova SN, Surovtsev IV, Mal'tsev VP, Loktev VB (2004). [Laminin-binding protein as a cellular receptor for the equine Venezuelan encephalomyelitis virus: Report 2. Inhibition of replication of equine Venezuelan encephalomyelitis virus by blocking laminin-binding protein on the surface of Vero cells]. *Mol Gen Mikrobiol Virusol***:** 36-40.

Bonilla E, Valero N, Chacin-Bonilla L, Pons H, Larreal Y, Medina-Leendertz S, Espina LM (2003). Melatonin increases interleukin-1beta and decreases tumor necrosis factor alpha in the brain of mice infected with the Venezuelan equine encephalomyelitis virus. *Neurochem Res* **28:** 681-6.

Bottcher T, von Mering M, Ebert S, Meyding-Lamade U, Kuhnt U, Gerber J, Nau R (2003). Differential regulation of Toll-like receptor mRNAs in experimental murine central nervous system infections. *Neurosci Lett* **344:** 17-20.

Bowen GS (1976). Experimental infection of North American mammals with epidemic Venezuelan encephalitis virus. *Am J Trop Med Hyg* **25:** 891-9.

Bowen GS, Calisher CH (1976). Virological and serological studies of Venezuelan equine encephalomyelitis in humans. *J Clin Microbiol* **4:** 22-7.

Brault AC, Powers AM, Holmes EC, Woelk CH, Weaver SC (2002). Positively charged amino acid substitutions in the e2 envelope glycoprotein are associated with the emergence of venezuelan equine encephalitis virus. *J Virol* **76:** 1718-30.

Brault AC, Powers AM, Ortiz D, Estrada-Franco JG, Navarro-Lopez R, Weaver SC (2004). Venezuelan equine encephalitis emergence: enhanced vector infection from a single amino acid substitution in the envelope glycoprotein. *Proc Natl Acad Sci U S A* **101:** 11344-9.

Calisher CH, Maness KS (1975). Laboratory studies of Venezuelan equine encephalitis virus in equines, Texas, 1971. *J Clin Microbiol* **2:** 198-205.

Callahan MK, Ransohoff RM (2004). Analysis of leukocyte extravasation across the blood-brain barrier: conceptual and technical aspects. *Curr Allergy Asthma Rep* **4:** 65-73.

Carrara AS, Gonzales G, Ferro C, Tamayo M, Aronson J, Paessler S, Anishchenko M, Boshell J, Weaver SC (2005). Venezuelan equine encephalitis virus infection of spiny rats. *Emerg Infect Dis* **11:** 663-9.

Charles PC, Trgovcich J, Davis NL, Johnston RE (2001). Immunopathogenesis and immune modulation of Venezuelan equine encephalitis virus-induced disease in the mouse. *Virology* **284:** 190-202.

Charles PC, Walters E, Margolis F, Johnston RE (1995). Mechanism of neuroinvasion of Venezuelan equine encephalitis virus in the mouse. *Virology* **208:** 662-71.

Choi HK, Lu G, Lee S, Wengler G, Rossmann MG (1997). Structure of Semliki Forest virus core protein. *Proteins* **27:** 345-59.

Choi HK, Tong L, Minor W, Dumas P, Boege U, Rossmann MG, Wengler G (1991). Structure of Sindbis virus core protein reveals a chymotrypsin-like serine proteinase and the organization of the virion. *Nature* **354:** 37-43.

Clarke CJ, Trapani JA, Johnstone RW (2001). Mechanisms of interferon mediated anti-viral resistance. *Curr Drug Targets Immune Endocr Metabol Disord* **1:** 117-30.

Coates DM, Makh SR, Jones N, Lloyd G (1992). Assessment of assays for the serodiagnosis of Venezuelan equine encephalitis. *J Infect* **25:** 279-89.

Cole FE, Jr., May SW, Robinson DM (1973). Formalin-inactivated Venezuelan equine encephalomyelitis (Trinidad strain) vaccine produced in rolling-bottle cultures of chicken embryo cells. *Appl Microbiol* **25:** 262-5.

Cupp EW, Scherer WF, Ordonez JV (1979). Transmission of Venezuelan encephalitis virus by naturally infected Culex (Melanoconion) opisthopus. *Am J Trop Med Hyg* **28:** 1060-3.

Dallasta LM, Pisarov LA, Esplen JE, Werley JV, Moses AV, Nelson JA, Achim CL (1999). Blood-brain barrier tight junction disruption in human immunodeficiency virus-1 encephalitis. *Am J Pathol* **155:** 1915-27.

Davis NL, Grieder FB, Smith JF, Greenwald GF, Valenski ML, Sellon DC, Charles PC, Johnston RE (1994). A molecular genetic approach to the study of Venezuelan equine encephalitis virus pathogenesis. *Arch Virol Suppl* **9:** 99-109.

DeLange EC (2004). Potential role of ABC transporters as a detoxification system at the blood-CSF barrier. *Adv Drug Deliv Rev* **56:** 1793-1809.

Dhawan S, R.K. Puri, Kumar A, Duplan H, Masson JM, Aggarwal BB (1997). Human immunodeficiency virus-1-tat protein induces the cell surface expression of endothelial leukocyte adhesion molecule-1, vascular cell adhesion molecule-1, and intercellular adhesion molecule- 1 in human endothelial cells. *Blood* **90**.

Dickstein JB, Moldofsky H, Hay JB (2000). Brain-blood permeability: TNF-alpha promotes escape of protein tracer from CSF to blood. *Am J Physiol Regul Integr Comp Physiol* **279:** R148-151.

Dietrich JB (2002). The adhesion molecule ICAM-1 and its regulation in relation with the blood-brain barrier. *Journal of Neuroimmunology* **128:** 58-68.

Dorries R (2001). The role of T-cell-mediated mechanisms in virus infections of the nervous system. *Curr Top Microbiol Immunol* **253:** 219-45.

Elvin SJ, Bennett AM, Phillpotts RJ (2002). Role for mucosal immune responses and cell-mediated immune functions in protection from airborne challenge with Venezuelan equine encephalitis virus. *J Med Virol* **67:** 384-93.

Engler RJ, Mangiafico JA, Jahrling P, Ksiazek TG, Pedrotti-Krueger M, Peters CJ (1992). Venezuelan equine encephalitis-specific immunoglobulin responses: live attenuated TC-83 versus inactivated C-84 vaccine. *J Med Virol* **38:** 305-10.

Eralinna JP, Soilu-Hanninen M, Roytta M, Hukkanen V, Salmi AA, Salonen R (1996). Blood-brain barrier breakdown and increased intercellular adhesion molecule (ICAM-1/CD54) expression after Semliki Forest (A7) virus infection facilitates the development of experimental allergic encephalomyelitis. *J Neuroimmunol* **66:** 103-114.

Esparza J, Sanchez A (1975). Multiplication of Venezuelan equine encephalitis (Mucambo) virus in cultured mosquito cells. *Arch Virol* **49:** 273-80.

Estrada-Franco JG, Navarro-Lopez R, Freier JE, Cordova D, Clements T, Moncayo A, Kang W, Gomez-Hernandez C, Rodriguez-Dominguez G, Ludwig GV, Weaver SC (2004). Venezuelan equine encephalitis virus, southern Mexico. *Emerg Infect Dis* **10:** 2113-21.

Eugenin EA, Berman JW (2003). Chemokine-dependent mechanisms of leukocyte trafficking across a model of the blood-brain barrier. *Methods* **29:** 351-361.

Eugenin EA, Osiecki K, Lopez L, Goldstein H, Calderon TM, Berman JW (2006). CCL2/monocyte chemoattractant protein-1 mediates enhanced transmigration of human immunodeficiency virus (HIV)-infected leukocytes across the blood-brain barrier: a potential mechanism of HIV-CNS invasion and NeuroAIDS. *J Neurosci* **26:** 1098-106.

Ferro C, Boshell J, Moncayo AC, Gonzalez M, Ahumada ML, Kang W, Weaver SC (2003). Natural enzootic vectors of Venezuelan equine encephalitis virus, Magdalena Valley, Colombia. *Emerg Infect Dis* **9:** 49-54.

Festjens N, Cornelis S, Lamkanfi M, Vandenabeele P (2006). Caspase-containing complexes in the regulation of cell death and inflammation. *Biol Chem* **387:** 1005-16.

Fine DL, Roberts BA, Teehee ML, Terpening SJ, Kelly CL, Raetz JL, Baker DC, Powers AM, Bowen RA (2006). Venezuelan equine encephalitis virus vaccine candidate (V3526) safety, immunogenicity and efficacy in horses. *Vaccine*.

Franck P (1972). Venezuelan encephalitis. In: *Round table on epidemic control*. Washington, Pan American Health Organisation, pp 400-401.

Franck PT, Johnson KM (1971). An outbreak of Venezuelan equine encephalomeylitis in Central America. Evidence for exogenous source of a virulent virus subtype. *Am J Epidemiol* **94:** 487-95.

Frolova E, Frolov I, Schlesinger S (1997). Packaging signals in alphaviruses. *J Virol* **71:** 248-58.

Garmashova N, Gorchakov R, Volkova E, Paessler S, Frolova E, Frolov I (2006). The Old World and New World alphaviruses use different virus-specific proteins for induction of the transcriptional shutoff. *J Virol*.

Gray C, McCormick C, Turner G, Craig A (2003). ICAM-1 can play a major role in mediating P. falciparum adhesion to endothelium under flow. *Mol Biochem Parasitol* **128:** 187-193.

Gray P, Dunne A, Brikos C, Jefferies CA, Doyle SL, O'Neill LA (2006). MyD88 adapter-like (Mal) is phosphorylated by Bruton's tyrosine kinase during TLR2 and TLR4 signal transduction. *J Biol Chem* **281:** 10489-95.

Greene IP, Paessler S, Anishchenko M, Smith DR, Brault AC, Frolov I, Weaver SC (2005a). Venezuelan equine encephalitis virus in the guinea pig model: evidence for epizootic virulence determinants outside the E2 envelope glycoprotein gene. *Am J Trop Med Hyg* **72:** 330-8.

Greene IP, Paessler S, Austgen L, Anishchenko M, Brault AC, Bowen RA, Weaver SC (2005b). Envelope glycoprotein mutations mediate equine amplification and virulence of epizootic venezuelan equine encephalitis virus. *J Virol* **79:** 9128-33.

Greenway TE, Eldridge JH, Ludwig G, Staas JK, Smith JF, Gilley RM, Michalek SM (1995). Enhancement of protective immune responses to Venezuelan equine encephalitis (VEE) virus with microencapsulated vaccine. *Vaccine* **13:** 1411-20.

Greenway TE, Eldridge JH, Ludwig G, Staas JK, Smith JF, Gilley RM, Michalek SM (1998). Induction of protective immune responses against Venezuelan equine encephalitis (VEE) virus aerosol challenge with microencapsulated VEE virus vaccine. *Vaccine* **16:** 1314-23.

Grieder FB, Davis BK, Zhou XD, Chen SJ, Finkelman FD, Gause WC (1997a). Kinetics of cytokine expression and regulation of host protection following infection with molecularly cloned Venezuelan equine encephalitis virus. *Virology* **233:** 302-12.

Grieder FB, Davis NL, Aronson JF, Charles PC, Sellon DC, Suzuki K, Johnston RE (1995). Specific restrictions in the progression of Venezuelan equine encephalitis virus-induced disease resulting from single amino acid changes in the glycoproteins. *Virology* **206:** 994-1006.

Grieder FB, Davisa BK, Zhoua XD, Chena SJ, Finkelmanb FD, Gause WC (1997b). Kinetics of Cytokine Expression and Regulation of Host Protection Following Infection with Molecularly Cloned Venezuelan Equine Encephalitis Virus. *Virology* **233:** 302-312.

Grieder FB, Nguyen HT (1996). Virulent and attenuated mutant Venezuelan equine encephalitis virus show marked differences in replication in infection in murine macrophages. *Microb Pathog* **21:** 85-95.

Grieder FB, Vogel SN (1999). Role of interferon and interferon regulatory factors in early protection against Venezuelan equine encephalitis virus infection. *Virology* **257:** 106-18.

Griffin DE (1999). *Equine Encephalitis Viruses (Togaviridae)*, 2 edn. Academic Press.

Guo LH, Mittelbronn M, Brabeck C, Mueller CA, Schluesener HJ (2004). Expression of interleukin-16 by microglial cells in inflammatory, autoimmune, and degenerative lesions of the rat brain. *J Neuroimmunol* **146:** 39-45.

Guzman H, Ding X, Xiao SY, Tesh RB (2005). Duration of infectivity and RNA of Venezuelan equine encephalitis, West Nile, and yellow fever viruses dried on filter paper and maintained at room temperature. *Am J Trop Med Hyg* **72:** 474-7.

Hahn CS, Strauss EG, Strauss JH (1985). Sequence analysis of three Sindbis virus mutants temperature-sensitive in the capsid protein autoprotease. *Proc Natl Acad Sci U S A* **82:** 4648-52.

Han J, Lee H, Nguyen NY, Beaucage SL, Puri RK (2005). Novel multiple 5'-amino-modified primer for DNA microarrays. *Genomics* **86:** 252-8.

Hart MK, Caswell-Stephan K, Bakken R, Tammariello R, Pratt W, Davis N, Johnston RE, Smith J, Steele K (2000). Improved mucosal protection against Venezuelan equine encephalitis virus is induced by the molecularly defined, live-attenuated V3526 vaccine candidate. *Vaccine* **18:** 3067-75.

Hart MK, Lind C, Bakken R, Robertson M, Tammariello R, Ludwig GV (2001). Onset and duration of protective immunity to IA/IB and IE strains of Venezuelan equine encephalitis virus in vaccinated mice. *Vaccine* **20:** 616-22.

Hart MK, Pratt W, Panelo F, Tammariello R, Dertzbaugh M (1997). Venezuelan equine encephalitis virus vaccines induce mucosal IgA responses and protection from airborne infection in BALB/c, but not C3H/HeN mice. *Vaccine* **15:** 363-9.

Hartung HP, Archelos JJ, Zielasek J, Gold R, Koltzenburg M, Reiners KH, Toyka KV (1995). Circulating adhesion molecules and inflammatory mediators in demyelination: a review. *Neurology* **45:** S22-32.

Hartung HP, Michels M, Reiners K, Seeldrayers P, Archelos JJ, Toyka KV (1993). Soluble ICAM-1 serum levels in multiple sclerosis and viral encephalitis. *Neurology* **43:** 2331-2335.

Hawley RJ, Eitzen Jr EM (2001). Biological weapons--a primer for microbiologists. *Annu Rev Microbiol* **55:** 235-253.

Hearn HJ, Jr., Soper WT (1967). Properties of Venezuelan equine encephalomyelitis virus accompanying attenuation in vitro. *J Virol* **1:** 453-9.

Heise MT, Simpson DA, Johnston RE (2000). A single amino acid change in nsP1 attenuates neurovirulence of the Sindbis-group alphavirus S.A.AR86. *J Virol* **74:** 4207-13.

Henderson BE, Chappell WA, Johnston JG, Jr., Sudia WD (1971). Experimental infection of horses with three strains of Venezuelan equine encephalomyelitis virus. I. Clinical and virological studies. *Am J Epidemiol* **93:** 194-205.

Hodgson LA, Ludwig GV, Smith JF (1999). Expression, processing, and immunogenicity of the structural proteins of Venezuelan equine encephalitis virus from recombinant baculovirus vectors. *Vaccine* **17:** 1151-60.

Holowka D, Gitler C, Bercovici T, Metzger H (1981). Reaction of 5-iodonaphthyl-1-nitrene with the IgE receptor on normal and tumour mast cells. *Nature* **289:** 806-8.

Honda K, Yanai H, Mizutani T, Negishi H, Shimada N, Suzuki N, Ohba Y, Takaoka A, Yeh WC, Taniguchi T (2004). Role of a transductional-transcriptional processor complex

involving MyD88 and IRF-7 in Toll-like receptor signaling. *Proc Natl Acad Sci U S A* **101:** 15416-21.

Horner AA (2006). Toll-like receptor ligands and atopy: a coin with at least two sides. *J Allergy Clin Immunol* **117:** 1133-40.

Houston WE, Kremer RJ, Crabbs CL, Spertzel RO (1977). Inactivated Venezuelan equine encephalomyelitis virus vaccine complexed with specific antibody: enhanced primary immune response and altered pattern of antibody class elicited. *J Infect Dis* **135:** 600-10.

Jackson AC, Rossiter JP (1997). Apoptotic cell death is an important cause of neuronal injury in experimental Venezuelan equine encephalitis virus infection of mice. *Acta Neuropathol (Berl)* **93:** 349-53.

Jackson AC, SenGupta SK, Smith JF (1991). Pathogenesis of Venezuelan equine encephalitis virus infection in mice and hamsters. *Vet Pathol* **28:** 410-8.

Johnson KM, Martin DH (1974). Venezuelan equine encephalitis. *Adv Vet Sci Comp Med* **18:** 79-116.

Johnson MD, Anderson BD (1996). Localization of purine metabolizing enzymes in bovine brain microvessel endothelial cells: an enzymatic blood-brain barrier for dideoxynucleosides? *Pharm Res* **13:** 1881-1886.

Johnston RE, Peters CJ (1996). Alphaviruses. In: *Fields virology*. Fields N, Knipe DM, Howley PM, (eds). Lippincott raven: Philadelphia, pp 843-898.

Jones LD, Bennett AM, Moss SR, Gould EA, Phillpotts RJ (2003). Cytotoxic T-cell activity is not detectable in Venezuelan equine encephalitis virus-infected mice. *Virus Res* **91:** 255-9.

Jorgensen PL, Karlish SJ, Gitler C (1982). Evidence for the organization of the transmembrane segments of (Na,K)-ATPase based on labeling lipid-embedded and surface domains of the alpha-subunit. *J Biol Chem* **257:** 7435-42.

Kahane I, Gitler C (1978). Red cell membrane glycophorin labeling from within the lipid bilayer. *Science* **201:** 351-2.

Kaisho T, Akira S (2006). Toll-like receptor function and signaling. *J Allergy Clin Immunol* **117:** 979-87; quiz 988.

Kastin AJ, Akerstrom V, Pan W (2002). Interactions of glucagon-like peptide-1 (GLP-1) with the blood-brain barrier. *J Mol Neurosci* **18:** 7-14.

Kim HJ, Biernacki K, Prat A, Antel JP, Bar-Or A (2004). Inflammatory potential and migratory capacities across human brain endothelial cells of distinct glatiramer acetate-reactive T cells generated in treated multiple sclerosis patients. *Clin Immunol* **111:** 38-46.

Kinney RM, Chang GJ, Tsuchiya KR, Sneider JM, Roehrig JT, Woodward TM, Trent DW (1993). Attenuation of Venezuelan equine encephalitis virus strain TC-83 is encoded by the 5'-noncoding region and the E2 envelope glycoprotein. *J Virol* **67:** 1269-77.

Kinney RM, Esposito JJ, Mathews JH, Johnson BJ, Roehrig JT, Barrett AD, Trent DW (1988). Recombinant vaccinia virus/Venezuelan equine encephalitis (VEE) virus protects mice from peripheral VEE virus challenge. *J Virol* **62:** 4697-702.

Kinney RM, Johnson BJ, Welch JB, Tsuchiya KR, Trent DW (1989). The full-length nucleotide sequences of the virulent Trinidad donkey strain of Venezuelan equine encephalitis virus and its attenuated vaccine derivative, strain TC-83. *Virology* **170:** 19-30.

Kinney RM, Tsuchiya KR, Sneider JM, Trent DW (1992). Molecular evidence for the origin of the widespread Venezuelan equine encephalitis epizootic of 1969 to 1972. *J Gen Virol* **73 (Pt 12):** 3301-5.

Kissling RE, Chamberlain RW (1967). Venezuelan equine encephalitis. *Adv Vet Sci* **11:** 65-84.

Kjerrulf M, Grdic D, Ekman L, Schon K, Vajdy M, Lycke NY (1997). Interferon-gamma receptor-deficient mice exhibit impaired gut mucosal immune responses but intact oral tolerance. *Immunology* **92:** 60-8.

Kolokoltsov AA, Fleming EH, Davey RA (2006). Venezuelan equine encephalitis virus entry mechanism requires late endosome formation and resists cell membrane cholesterol depletion. *Virology* **347:** 333-42.

Kolykhalov AA, Frolov IV, Agapov EV, Netesov SV, Sandakhchiev LS (1992). [Obtaining infectious Venezuelan equine encephalomyelitis virus based on a full length DNA copy of its genome]. *Dokl Akad Nauk* **327:** 160-4.

Kubes V, Rios FA (1939). The causative agent of infectious equine encephalitis in Venezuela. *Science* **90:** 20-21.

Leppert D, Leib SL, Grygar C, Miller KM, Schaad UB, Hollander GA (2000). Matrix metalloproteinase (MMP)-8 and MMP-9 in cerebrospinal fluid during bacterial meningitis: association with blood-brain barrier damage and neurological sequelae. *Clin Infect Dis* **31:** 80-4.

Linssen B, Kinney RM, Aguilar P, Russell KL, Watts DM, Kaaden OR, Pfeffer M (2000). Development of reverse transcription-PCR assays specific for detection of equine encephalitis viruses. *J Clin Microbiol* **38:** 1527-35.

Linthicum KJ, Logan TM, Bailey CL, Gordon SW, Peters CJ, Monath TP, Osorio J, Francy DB, McLean RG, Leduc JW, et al. (1991). Venezuelan equine encephalomyelitis virus infection in and transmission by the tick Amblyomma cajennense (Arachnida: Ixodidae). *J Med Entomol* **28:** 405-9.

Lord RD (1974). History and geographic distribution of Venezuelan equine encephalitis. *Bull Pan Am Health Organ* **8:** 100-10.

Lucas M, Mashimo T, Frenkiel MP, Simon-Chazottes D, Montagutelli X, Ceccaldi PE, Guenet JL, Despres P (2003). Infection of mouse neurones by West Nile virus is modulated by the interferon-inducible 2'-5' oligoadenylate synthetase 1b protein. *Immunol Cell Biol* **81:** 230-6.

Ludwig GV, Kondig JP, Smith JF (1996). A putative receptor for Venezuelan equine encephalitis virus from mosquito cells. *J Virol* **70:** 5592-9.

Ludwig GV, Turell MJ, Vogel P, Kondig JP, Kell WK, Smith JF, Pratt WD (2001). Comparative neurovirulence of attenuated and non-attenuated strains of Venezuelan equine encephalitis virus in mice. *Am J Trop Med Hyg* **64:** 49-55.

Luedke AJ, Barber TL, Foster NM, Batalla D, Mercado S (1972). Effect of back passage of Venezuelan equine encephalomyelitis TC-83 vaccine virus on clinical, virologic, and immune responses in horses. *J Am Vet Med Assoc* **161:** 824-31.

MacDonald GH, Johnston RE (2000). Role of dendritic cell targeting in Venezuelan equine encephalitis virus pathogenesis. *J Virol* **74:** 914-22.

Mangiafico JA, Rossi CA, Ludwig GV (2002). Short report: Isolation and identification of Venezuelan equine encephalitis virus from a human in Panama. *Am J Trop Med Hyg* **67:** 112-3.

Mansur DS, Kroon EG, Nogueira ML, Arantes RM, Rodrigues SC, Akira S, Gazzinelli RT, Campos MA (2005). Lethal encephalitis in myeloid differentiation factor 88-deficient mice infected with herpes simplex virus 1. *Am J Pathol* **166:** 1419-26.

Mark KS, Burroughs AR, Brown RC, Huber JD, Davis TP (2004). Nitric oxide mediates hypoxia-induced changes in paracellular permeability of cerebral microvasculature. *Am J Physiol Heart Circ Physiol* **286:** H174-80.

Marlin SD, Springer TA (1987). Purified intercellular adhesion molecule-1 (ICAM-1) is a ligand for lymphocyte function associated antigen (LFA-1). *Cell* **51:** 813-819.

McKimmie CS, Johnson N, Fooks AR, Fazakerley JK (2005). Viruses selectively upregulate Toll-like receptors in the central nervous system. *Biochem Biophys Res Commun* **336:** 925-33.

Mehlhorn G, Hollborn M, Schliebs R (2000). Induction of cytokines in glial cells surrounding cortical beta-amyloid plaques in transgenic Tg2576 mice with Alzheimer pathology. *Int J Dev Neurosci* **18:** 423-31.

Montgomery SA, Berglund P, Beard CW, Johnston RE (2006). Ribosomal protein S6 associates with alphavirus nonstructural protein 2 and mediates expression from alphavirus messages. *J Virol* **80:** 7729-39.

Moynagh PN (2005). TLR signalling and activation of IRFs: revisiting old friends from the NF-kappaB pathway. *Trends Immunol* **26:** 469-76.

Muller DM, Pender MP, Greer JM (2004). Chemokines and chemokine receptors: potential therapeutic targets in multiple sclerosis. *Curr Drug Targets Inflamm Allergy* **3:** 279-90.

Negi SS, Kolokoltsov AA, Schein CH, Davey RA, Braun W (2006). Determining functionally important amino acid residues of the E1 protein of Venezuelan equine encephalitis virus. *J Mol Model* **12:** 921-9.

Negrette B, Bonilla E, Valero N, Giraldoth D, Medina-Leendertz S, Anez F (2001a). In mice the efficiency of immunization with Venezuelan Equine Encephalomyelitis virus TC-83 is transiently increased by dehydroepiandrosterone. *Invest Clin* **42:** 235-40.

Negrette B, Bonilla E, Valero N, Pons H, Garcia Tamayo J, Chacin-Bonilla L, Medina-Leendertz S, Anez F (2001b). Melatonin treatment enhances the efficiency of mice immunization with Venezuelan equine encephalomyelitis virus TC-83. *Neurochem Res* **26:** 767-70.

Nygardas PT, Hinkkanen AE (2002). Up-regulation of MMP-8 and MMP-9 activity in the BALB/c mouse spinal cord correlates with the severity of experimental autoimmune encephalomyelitis. *Clin Exp Immunol* **128:** 245-54.

O'Brien L (2006). Inhibition of multiple strains of Venezuelan equine encephalitis virus by a pool of four short interfering RNAs. *Antiviral Res*.

O'Keefe GM, Nguyen VT, Benveniste EN (2002). Regulation and function of class II major histocompatibility complex, CD40, and B7 expression in macrophages and microglia: Implications in neurological diseases. *J Neurovirol* **8:** 496-512.

O'Neill LA (2006). How Toll-like receptors signal: what we know and what we don't know. *Curr Opin Immunol* **18:** 3-9.

Oberste MS, Fraire M, Navarro R, Zepeda C, Zarate ML, Ludwig GV, Kondig JF, Weaver SC, Smith JF, Rico-Hesse R (1998). Association of Venezuelan equine encephalitis virus subtype IE with two equine epizootics in Mexico. *Am J Trop Med Hyg* **59:** 100-7.

Olson JK, Miller SD (2004). Microglia initiate central nervous system innate and adaptive immune responses through multiple TLRs. *J Immunol* **173:** 3916-3924.

Omari KM, Chui R, Dorovini-Zis K (2004). Induction of beta-chemokine secretion by human brain microvessel endothelial cells via CD40/CD40L interactions. *J Neuroimmunol* **146:** 203-8.

Oshiumi H, Matsumoto M, Funami K, Akazawa T, Seya T (2003). TICAM-1, an adaptor molecule that participates in Toll-like receptor 3-mediated interferon-beta induction. *Nat Immunol* **4:** 161-7.

Paessler S, Fayzulin RZ, Anishchenko M, Greene IP, Weaver SC, Frolov I (2003). Recombinant sindbis/Venezuelan equine encephalitis virus is highly attenuated and immunogenic. *J Virol* **77:** 9278-86.

Paessler S, Ni H, Petrakova O, Fayzulin RZ, Yun N, Anishchenko M, Weaver SC, Frolov I (2006). Replication and clearance of Venezuelan equine encephalitis virus from the brains of animals vaccinated with chimeric SIN/VEE viruses. *J Virol* **80:** 2784-96.

Pak CC, Krumbiegel M, Blumenthal R, Raviv Y (1994). Detection of influenza hemagglutinin interaction with biological membranes by photosensitized activation of [125I]iodonaphthylazide. *J Biol Chem* **269:** 14614-9.

Paredes A, Alwell-Warda K, Weaver SC, Chiu W, Watowich SJ (2001). Venezuelan equine encephalomyelitis virus structure and its divergence from old world alphaviruses. *J Virol* **75:** 9532-7.

Paredes A, Alwell-Warda K, Weaver SC, Chiu W, Watowich SJ (2003). Structure of isolated nucleocapsids from venezuelan equine encephalitis virus and implications for assembly and disassembly of enveloped virus. *J Virol* **77:** 659-64.

Park H, Li Z, Yang XO, Chang SH, Nurieva R, Wang YH, Wang Y, Hood L, Zhu Z, Tian Q, Dong C (2005). A distinct lineage of CD4 T cells regulates tissue inflammation by producing interleukin 17. *Nat Immunol* **6:** 1133-41.

Perry VH (1998). A revised view of the central nervous system microenvironment and major histocompatibility complex class II antigen presentation. *J Neuroimmunol* **90:** 113-21.

Peters A, Schweiger U, Pellerin L, Hubold C, Oltmanns KM, Conrad M, Schultes B, Born J, Fehm HL (2004). The selfish brain: competition for energy resources. *Neurosci Biobehav Rev* **28:** 143-180.

Petrakova O, Volkova E, Gorchakov R, Paessler S, Kinney RM, Frolov I (2005). Noncytopathic replication of Venezuelan equine encephalitis virus and eastern equine encephalitis virus replicons in Mammalian cells. *J Virol* **79:** 7597-608.

Phillpotts RJ (1999). Immunity to airborne challenge with Venezuelan equine encephalitis virus develops rapidly after immunization with the attenuated vaccine strain TC-83. *Vaccine* **17:** 2429-35.

Phillpotts RJ (2006). Venezuelan equine encephalitis virus complex-specific monoclonal antibody provides broad protection, in murine models, against airborne challenge with viruses from serogroups I, II and III. *Virus Res* **120:** 107-12.

Phillpotts RJ, Jones LD, Howard SC (2002). Monoclonal antibody protects mice against infection and disease when given either before or up to 24 h after airborne challenge with virulent Venezuelan equine encephalitis virus. *Vaccine* **20:** 1497-504.

Phillpotts RJ, Jones LD, Lukaszewski RA, Lawrie C, Brooks TJ (2003). Antibody and interleukin-12 treatment in murine models of encephalitogenic flavivirus (St. Louis encephalitis, tick-borne encephalitis) and alphavirus (Venezuelan equine encephalitis) infection. *J Interferon Cytokine Res* **23:** 47-50.

Phillpotts RJ, Lescott TL, Jacobs SC (2000). Vaccinia virus recombinants encoding the truncated structural gene region of Venezuelan equine encephalitis virus (VEEV) give solid protection against peripheral challenge but only partial protection against airborne challenge with virulent VEEV. *Acta Virol* **44:** 233-9.

Phillpotts RJ, O'Brien L, Appleton RE, Carr S, Bennett A (2005). Intranasal immunisation with defective adenovirus serotype 5 expressing the Venezuelan equine encephalitis virus E2 glycoprotein protects against airborne challenge with virulent virus. *Vaccine* **23:** 1615-23.

Phillpotts RJ, Wright AJ (1999). TC-83 vaccine protects against airborne or subcutaneous challenge with heterologous mouse-virulent strains of Venezuelan equine encephalitis virus. *Vaccine* **17:** 982-8.

Pittman PR, Makuch RS, Mangiafico JA, Cannon TL, Gibbs PH, Peters CJ (1996). Long-term duration of detectable neutralizing antibodies after administration of live-attenuated VEE vaccine and following booster vaccination with inactivated VEE vaccine. *Vaccine* **14:** 337-43.

Pomerantz JL, Denny EM, Baltimore D (2002). CARD11 mediates factor-specific activation of NF-kappaB by the T cell receptor complex. *Embo J* **21:** 5184-94.

Pratt WD, Davis NL, Johnston RE, Smith JF (2003). Genetically engineered, live attenuated vaccines for Venezuelan equine encephalitis: testing in animal models. *Vaccine* **21:** 3854-62.

Prehaud C, Megret F, Lafage M, Lafon M (2005). Virus infection switches TLR-3-positive human neurons to become strong producers of beta interferon. *J Virol* **79:** 12893-904.

Preston R (1998). The Bioweaponeers. In the last few years, Russian scientists have invented the world'd deadliest plagues. Have we learned this too late to stop it? In: *New Yorker*, pp 53-65.

Pu H, Tian J, Flora G, Lee YW, Nath A, Hennig B, Toborek M (2003). HIV-1 Tat protein upregulates inflammatory mediators and induces monocyte invasion into the brain. *Mol Cell Neurosci* **24:** 224-237.

Rao V, Hinz ME, Roberts BA, Fine D (2004). Environmental hazard assessment of Venezuelan equine encephalitis virus vaccine candidate strain V3526. *Vaccine* **22:** 2667-73.

Rao V, Hinz ME, Roberts BA, Fine D (2006). Toxicity assessment of Venezuelan Equine Encephalitis virus vaccine candidate strain V3526. *Vaccine* **24:** 1710-5.

Raviv Y, Bercovici T, Gitler C, Salomon Y (1984). Selective photoinduced uncoupling of the response of adenylate cyclase to gonadotropins by 5-iodonaphthyl 1-azide. *Biochemistry* **23:** 503-8.

Raviv Y, Bercovici T, Gitler C, Salomon Y (1989). Detection of nearest neighbors to specific fluorescently tagged ligands in rod outer segment and lymphocyte plasma membranes by photosensitization of 5-iodonaphthyl 1-azide. *Biochemistry* **28:** 1313-9.

Raviv Y, Pollard HB, Bruggemann EP, Pastan I, Gottesman MM (1990). Photosensitized labeling of a functional multidrug transporter in living drug-resistant tumor cells. *J Biol Chem* **265:** 3975-80.

Raviv Y, Salomon Y, Gitler C, Bercovici T (1987). Selective labeling of proteins in biological systems by photosensitization of 5-iodonaphthalene-1-azide. *Proc Natl Acad Sci U S A* **84:** 6103-7.

Raviv Y, Viard M, Bess JW, Jr., Chertova E, Blumenthal R (2005). Inactivation of retroviruses with preservation of structural integrity by targeting the hydrophobic domain of the viral envelope. *J Virol* **79:** 12394-400.

Razumov IA, Agapov EV, Pereboev AV, Protopopova EV, Lebedeva SD, Loktev VB (1991). Investigation of antigenic structure of attenuated and virulent Venezuelan equine encephalomyelitis virus by means of monoclonal antibodies. *Biomed Sci* **2:** 615-22.

Redzic ZB, Segal MB, Gasic JM, Markovic ID, Vojvodic VP, Isakovic A, Thomas SA, Rakic LM (2001). The characteristics of nucleobase transport and metabolism by the perfused sheep choroid plexus. *Brain Res* **888:** 66-74.

Reed DS, Lind CM, Lackemeyer MG, Sullivan LJ, Pratt WD, Parker MD (2005). Genetically engineered, live, attenuated vaccines protect nonhuman primates against aerosol challenge with a virulent IE strain of Venezuelan equine encephalitis virus. *Vaccine* **23:** 3139-47.

Reiss Y, Engelhardt B (1999). T cell interaction with ICAM-1-deficient endothelium in vitro: transendothelial migration of different T cell populations is mediated by endothelial ICAM-1 and ICAM-2. *Int Immunol* **11:** 1527-39.

Reynolds JA, Harrington DG, Crabbs CL, Peters CJ, Di Luzio NR (1980). Adjuvant activity of a novel metabolizable lipid emulsion with inactivated viral vaccines. *Infect Immun* **28:** 937-43.

Rico-Hesse R, Weaver SC, de Siger J, Medina G, Salas RA (1995). Emergence of a new epidemic/epizootic Venezuelan equine encephalitis virus in South America. *Proc Natl Acad Sci U S A* **92:** 5278-81.

Risinger JI, Maxwell GL, Chandramouli GV, Jazaeri A, Aprelikova O, Patterson T, Berchuck A, Barrett JC (2003). Microarray analysis reveals distinct gene expression profiles among different histologic types of endometrial cancer. *Cancer Res* **63:** 6-11.

Roehrig JT (1993). Immunogens of encephalitis viruses. *Vet Microbiol* **37:** 273-84.

Rolland A, Jouvin-Marche E, Viret C, Faure M, Perron H, Marche PN (2006). The Envelope Protein of a Human Endogenous Retrovirus-W Family Activates Innate Immunity through CD14/TLR4 and Promotes Th1-Like Responses. *J Immunol* **176:** 7636-7644.

Romero JR, Kimberlin DW (2003). Molecular diagnosis of viral infections of the central nervous system. *Clin Lab Med* **23:** 843-65, vi.

Rothstein TL (2000). Inducible resistance to Fas-mediated apoptosis in B cells. *Cell Res* **10:** 245-66.

Russo AT, Watowich SJ (2006). Purification, crystallization and X-ray diffraction analysis of the C-terminal protease domain of Venezuelan equine encephalitis virus nsP2. *Acta Crystallograph Sect F Struct Biol Cryst Commun* **62:** 514-7.

Russo AT, White MA, Watowich SJ (2006). The crystal structure of the Venezuelan equine encephalitis alphavirus nsP2 protease. *Structure* **14:** 1449-58.

Ryzhikov AB, Ryabchikova EI, Sergeev AN, Tkacheva NV (1995). Spread of Venezuelan equine encephalitis virus in mice olfactory tract. *Arch Virol* **140:** 2243-54.

Sahu SP, Pedersen DD, Jenny AL, Schmitt BJ, Alstad AD (2003). Pathogenicity of a Venezuelan equine encephalomyelitis serotype IE virus isolate for ponies. *Am J Trop Med Hyg* **68:** 485-94.

Saikh KU, Lee JS, Kissner TL, Dyas B, Ulrich RG (2003). Toll-like receptor and cytokine expression patterns of CD56+ T cells are similar to natural killer cells in response to infection with Venezuelan equine encephalitis virus replicons. *J Infect Dis* **188:** 1562-70.

Sanmartin-Barberi C, Groot H, Osorno-Mesa E (1954). Human epidemic in Colombia caused by the Venezuelan equine encephalomyelitis virus. *Am J Trop Med Hyg* **3:** 283-93.

Sanmartin C, Mackenzie RB, Trapido H, Barreto P, Mullenax CH, Gutierrez E, Lesmes C (1973). [Venezuelan equine encephalitis in Colombia, 1967]. *Bol Oficina Sanit Panam* **74:** 108-37.

Sanmartin C, Trapido H, Barreto P, Lesmes CI (1971). Isolations of Venezuelan and Eastern equine encephalomyelitis viruses from sentinel hamsters exposed in the Pacific lowlands of Colombia. *Am J Trop Med Hyg* **20:** 469-73.

Sawicki DL, Perri S, Polo JM, Sawicki SG (2006). Role for nsP2 proteins in the cessation of alphavirus minus-strand synthesis by host cells. *J Virol* **80:** 360-71.

Schaller MD (2001). Paxillin: a focal adhesion-associated adaptor protein. *Oncogene* **20:** 6459-72.

Scherbik SV, Paranjape JM, Stockman BM, Silverman RH, Brinton MA (2006). RNase L plays a role in the antiviral response to West Nile virus. *J Virol* **80:** 2987-99.

Scherer WF, Dickerman RW, Ordonez JV, Seymour C, 3rd, Kramer LD, Jahrling PB, Powers CD (1976). Ecologic studies of Venezuelan encephalitis virus and isolations of Nepuyo and Patois viruses during 1968-1973 at a marsh habitat near the epicenter of the 1969 outbreak in Guatemala. *Am J Trop Med Hyg* **25:** 151-62.

Schlesinger MJ, Kaariainen L (1980). *Translation and processing of alphavirus proteins*. Academic Press: New York.

Schoneboom BA, Catlin KM, Marty AM, Grieder FB (2000a). Inflammation is a component of neurodegeneration in response to Venezuelan equine encephalitis virus infection in mice. *J Neuroimmunol* **109:** 132-146.

Schoneboom BA, Fultz MJ, Miller TH, McKinney LC, Grieder FB (1999). Astrocytes as targets for Venezuelan equine encephalitis virus infection. *J Neurovirol* **5:** 342-54.

Schoneboom BA, Lee JS, Grieder FB (2000b). Early expression of IFN-alpha/beta and iNOS in the brains of Venezuelan equine encephalitis virus-infected mice. *J Interferon Cytokine Res* **20:** 205-215.

Seth P, Husain MM, Gupta P, Schoneboom A, Grieder BF, Mani H, Maheshwari RK (2003). Early onset of virus infection and up-regulation of cytokines in mice treated with cadmium and manganese. *Biometals* **16:** 359-68.

Shabman RS, Morrison TE, Moore C, White L, Suthar MS, Hueston L, Rulli N, Lidbury B, Ting JP, Mahalingam S, Heise MT (2007). Differential induction of type I interferon responses in myeloid dendritic cells by mosquito and mammalian-cell-derived alphaviruses. *J Virol* **81:** 237-47.

Sharp CD, Fowler M, Jackson TH, Houghton J, Warren A, Nanda A, Chandler I, Cappell B, Long A, Minagar A, Alexander JS (2003). Human neuroepithelial cells express NMDA receptors. *BMC Neurosci* **4:** 28.

Shope (1976). *Alphaviruses*, 2 edn. Raven Press: New York.

Simons K, Garoff H, Helenius A (1980). *Alphavirus Proteins*. Academic Press: New York.

Smith DR, Aguilar PV, Coffey LL, Gromowski GD, Wang E, Weaver SC (2006). Venezuelan equine encephalitis virus transmission and effect on pathogenesis. *Emerg Infect Dis* **12:** 1190-6.

Smith Jf, Davis K, Hart Mk, Ludwig Gv, Mcclain Dj, Michael Dp, William Dp (1997a). *Viral encephalitides*. Office of the Surgeon General: Washington, DC.

Smith JF, Davis K, Hart MK, Ludwig GV, McClain DJ, Parker MD (1997b). *Viral encephalitides*. office of the Surgeon General: Washington DC.

Soilu-Hanninen M, Eralinna JP, Hukkanen V, Roytta M, Salmi AA, Salonen R (1994). Semliki Forest virus infects mouse brain endothelial cells and causes blood-brain barrier damage. *J Virol* **68:** 6291-6298.

Song L, Pachter JS (2004). Monocyte chemoattractant protein-1 alters expression of tight junction-associated proteins in brain microvascular endothelial cells. *Microvasc Res* **67:** 78-89.

Spertzel RO, Hilmas DE, Brown JR, Mason DW (1975). Response of irradiated mice to live-virus (TC-83) immunization. *Infect Immun* **11:** 481-7.

Stamatovic SM, Shakui P, Keep RF, Moore BB, Kunkel SL, Van Rooijen N, Andjelkovic AV (2005). Monocyte chemoattractant protein-1 regulation of blood-brain barrier permeability. *J Cereb Blood Flow Metab* **25:** 593-606.

Stanley J, Cooper SJ, Griffin DE (1985). Alphavirus neurovirulence: monoclonal antibodies discriminating wild-type from neuroadapted Sindbis virus. *J Virol* **56:** 110-9.

Steele KE, Davis KJ, Stephan K, Kell W, Vogel P, Hart MK (1998a). Comaparative neurovirulence and tissue trophism of wild type and attenuated strains of Venezuelan Equine Encephalitis virus administered by aerosol in C3H/HeN and BALB/c mice. *Vet Pathol* **35:** 386-397.

Steele KE, Davis KJ, Stephan K, Kell W, Vogel P, Hart MK (1998b). Comparative neurovirulence and tissue tropism of wild-type and attenuated strains of Venezuelan equine encephalitis virus administered by aerosol in C3H/HeN and BALB/c mice. *Vet Pathol* **35:** 386-97.

Steele KE, Seth P, Catlin-Lebaron KM, Schoneboom BA, Husain MM, Grieder F, Maheshwari RK (2006). Tunicamycin enhances neuroinvasion and encephalitis in mice infected with Venezuelan equine encephalitis virus. *Vet Pathol* **43:** 904-13.

Stover JF, Pleines UE, Morganti-Kossmann MC, Kossmann T, Lowitzsch K, Kempski OS (1997). Neurotransmitters in cerebrospinal fluid reflect pathological activity. *Eur J Clin Invest* **27:** 1038-1043.

Strauss EG, Strauss JH (1986). *Structure and Replication of Alphavirus Genome*. Plenum Press: New York.

Strauss JH, Jr., Burge BW, Pfefferkorn ER, Darnell JE, Jr. (1968). Identification of the membrane protein and "core" protein of Sindbis virus. *Proc Natl Acad Sci U S A* **59:** 533-7.

Sudia WD, Newhouse VF, Beadle ID, Miller DL, Johnston JG, Jr., Young R, Calisher CH, Maness K (1975). Epidemic Venezuelan equine encephalitis in North America in 1971: vector studies. *Am J Epidemiol* **101:** 17-35.

Sun H, Fang H, Chen T, Perkins R, Tong W (2006). GOFFA: Gene Ontology For Functional Analysis - A FDA Gene Ontology Tool for Analysis of Genomic and Proteomic Data. *BMC Bioinformatics* **7 Suppl 2:** S23.

Tabeta K, Georgel P, Janssen E, Du X, Hoebe K, Crozat K, Mudd S, Shamel L, Sovath S, Goode J, Alexopoulou L, Flavell RA, Beutler B (2004). Toll-like receptors 9 and 3 as essential components of innate immune defense against mouse cytomegalovirus infection. *Proc Natl Acad Sci U S A* **101:** 3516-21.

Takeda K, Akira S (2004). TLR signaling pathways. *Semin Immunol* **16:** 3-9.

Takeda K, Akira S (2005). Toll-like receptors in innate immunity. *Int Immunol* **17:** 1-14.

Timms JF, Carlberg K, Gu H, Chen H, Kamatkar S, Nadler MJ, Rohrschneider LR, Neel BG (1998). Identification of major binding proteins and substrates for the SH2-containing protein tyrosine phosphatase SHP-1 in macrophages. *Mol Cell Biol* **18:** 3838-50.

Turell MJ, Ludwig GV, Beaman JR (1992). Transmission of Venezuelan equine encephalomyelitis virus by Aedes sollicitans and Aedes taeniorhynchus (Diptera: Culicidae). *J Med Entomol* **29:** 62-5.

Turell MJ, Ludwig GV, Kondig J, Smith JF (1999). Limited potential for mosquito transmission of genetically engineered, live-attenuated Venezuelan equine encephalitis virus vaccine candidates. *Am J Trop Med Hyg* **60:** 1041-4.

Turner GD, Morrison H, Jones M, Davis TM, Looareesuwan S, Buley ID, Gatter KC, Newbold CI, Pukritayakamee S, Nagachinta B (1994). An immunohistochemical study of the pathology of fatal malaria. Evidence for widespread endothelial activation and a potential role for intercellular adhesion molecule-1 in cerebral sequestration. *Am J Pathol* **145:** 1057-1069.

Valero N, Espina LM, Mosquera J (2006). Melatonin decreases nitric oxide production, inducible nitric oxide synthase expression and lipid peroxidation induced by Venezuelan encephalitis equine virus in neuroblastoma cell cultures. *Neurochem Res* **31:** 925-32.

Valero N, Melean E, Bonilla E, Arias J, Espina LM, Chacin-Bonilla L, Larreal Y, Maldonado M, Anez F (2005). In vitro, melatonin treatment decreases nitric oxide levels

in murine splenocytes cultured with the venezuelan equine encephalomyelitis virus. *Neurochem Res* **30:** 1439-42.

Vogel P, Abplanalp D, Kell W, Ibrahim MS, Downs MB, Pratt WD, Davis KJ (1996). Venezuelan equine encephalitis in BALB/c mice: kinetic analysis of central nervous system infection following aerosol or subcutaneous inoculation. *Arch Pathol Lab Med* **120:** 164-172.

Walton TE, Alvarez O, Jr., Buckwalter RM, Johnson KM (1972). Experimental infection of horses with an attenuated Venezuelan equine encephalomyelitis vaccine (strain TC-83). *Infect Immun* **5:** 750-6.

Wang T, Town T, Alexopoulou L, Anderson JF, Fikrig E, Flavell RA (2004). Toll-like receptor 3 mediates West Nile virus entry into the brain causing lethal encephalitis. *Nat Med* **10:** 1366-73.

Weaver SC (2005). Host range, amplification and arboviral disease emergence. *Arch Virol Suppl***:** 33-44.

Weaver SC, Ferro C, Barrera R, Boshell J, Navarro JC (2004). Venezuelan equine encephalitis. *Annu Rev Entomol* **49:** 141-74.

Weaver SC, Rico-Hesse R, Scott TW (1992). Genetic diversity and slow rates of evolution in New World alphaviruses. *Curr Top Microbiol Immunol* **176:** 99-117.

Weaver SC, Salas R, Rico-Hesse R, Ludwig GV, Oberste MS, Boshell J, Tesh RB (1996). Re-emergence of epidemic Venezuelan equine encephalomyelitis in South America. VEE Study Group. *Lancet* **348:** 436-40.

Webb AA, Muir GD (2000). The blood-brain barrier and its role in inflammation. *J Vet Intern Med* **14:** 399-411.

White DO, Fenner FJ (1994). *Togaviridae*, 4 edn. Academic Press: San Diego.

White LJ, Wang JG, Davis NL, Johnston RE (2001). Role of alpha/beta interferon in Venezuelan equine encephalitis virus pathogenesis: effect of an attenuating mutation in the 5' untranslated region. *J Virol* **75:** 3706-18.

Wilkinson TA, Tellinghuisen TL, Kuhn RJ, Post CB (2005). Association of sindbis virus capsid protein with phospholipid membranes and the E2 glycoprotein: implications for alphavirus assembly. *Biochemistry* **44:** 2800-10.

Woodman SE, Benveniste EN, Nath A, Berman JW (1999). Human immunodeficiency virus type 1 TAT protein induces adhesion molecule expression in astrocytes. *J Neurovirol* **5:** 678-684.

Wu DT, Woodman SE, Weiss JM, McManus CM, D'Aversa TG, Hesselgesser J, Major EO, Nath A, Berman JW (2000). Mechanisms of leukocyte trafficking into the CNS. *J Neurovirol* **6:** S82-85.

Xiang J, Ennis SR, Abdelkarim GE, Fujisawa M, Kawai N, Keep RF (2003). Glutamine transport at the blood-brain and blood-cerebrospinal fluid barriers. *Neurochem Int* **43:** 279-288.

Xie Z, Harris-White ME, Wals PA, Frautschy SA, Finch CE, Morgan TE (2005). Apolipoprotein J (clusterin) activates rodent microglia in vivo and in vitro. *J Neurochem* **93:** 1038-46.

Zehmer RB, Dean PB, Sudia WD, Calisher CH, Sather GE, Parker RL (1974). Venezuelan equine encephalitis epidemic in Texas, 1971. *Health Serv Rep* **89:** 278-82.

List of Publications

Manuscript Accepted for Publication

1. **Sharma A**, Raviv Y, Puri A, Viard M, Blumenthal R, Maheshwari RK. Complete inactivation of Venezuelan equine encephalitis virus by 1,5-iodonaphthylazide. Biochem Biophys Res Commun. 2007 Jun 29;358(2):392-8. Epub 2007 Apr 26.

2. Singh, A. K., **Sharma, A.**, Warren, J., Madhavan, S., Steele, K., Rajeshkumar, N. V., Thangapazham, R. L., Sharma, S. C., Kulshreshtha, D. K., Gaddipati, J., and Maheshwari, R. K. (2007). Picroliv Accelerates Epithelialization and Angiogenesis in Rat Wounds. *Planta Med* **22,** 22.

3. **Sharma, A**., Singh, A. K., Warren, J., Thangapazham, R. L., and Maheshwari, R. K. (2006). Differential regulation of angiogenic genes in diabetic wound healing. *J Invest Dermatol* **126**(10)**,** 2323-31.

4. Thangapazham, R. L., **Sharma, A.**, Gaddipati, J. P., Singh, A. K., and Maheshwari, R. K. (2006). Inhibition of tumor angiogenesis by Brahma Rasayana (BR). *J Exp Ther Oncol* **6**(1)**,** 13-21.

5. Thangapazham, R. L., **Sharma, A.**, and Maheshwari, R. K. (2006). Multiple molecular targets in cancer chemoprevention by curcumin. *Aaps J* **8**(3)**,** E443-9.

6. Gaddipati, J. P., Rajeshkumar, N. V., Thangapazham, R. L., **Sharma, A.**, Warren, J., Mog, S. R., Singh, A. K., and Maheshwari, R. K. (2004). Protective effect of a polyherbal preparation, Brahma rasayana against tumor growth and lung metastasis in rat prostrate model system. *J Exp Ther Oncol* **4**(3)**,** 203-12.

7. Thangapazham, R. L., Singh, A. K., **Sharma, A.**, Warren, J., Gaddipati, J. P., and Maheshwari, R. K. (2007). Green tea polyphenols and its constituent epigallocatechin gallate inhibits proliferation of human breast cancer cells in vitro and in vivo. *Cancer Lett* **245**(1-2)**,** 232-41.

8. A.K. Singh, **A. Sharma**, J. Warren, K. Steele and R.K. Maheshwari. *Joint Meeting of ICS and ISICR San Juan, Puerto Rico, October 21-25, 2004* Phytochemical Picroliv Enhances Impaired Wound Healing

List of Communicated Manuscript

1. **Anuj Sharma**, Radha K Maheshwari Venezuelan Equine Encephalitis Virus Infection Modulates Toll Like Receptors and Associated Signaling Genes in Mice Brain. (Manuscript Communicated to Archives of virology)

2. **Anuj Sharma**, Bhaskar Bhattacharya, Raj K Puri, Radha K Maheshwari. Venezuelan Equine Encephalitis Virus Infection Causes Modulation of Inflammatory and Immune Response Genes in Mouse Brain. (Manuscript Communicated to BMC Genomics)

List of Manuscript in Preparation

1. **Anuj Sharma**, Radha K Maheshwari. Role of Adhesion molecules in Venezuelan Equine Encephaliitis Virus Pathogenesis in Mice Brain.

2. **Anuj Sharma,** Yossi Raviv, Blumenthal R, Maheshwari RK. Photoinactivated Venezuelan Equine Encephalitis Virus Confers Protection Against Virulent Virus Challenge in Mice.

List of Papers Presented in Conferences

1. *Complete Inactivation of Venezuelan Equine Encephalitis Virus by the Photoinducible Hydrophobic Alkylating Compound 1,15 Iododnapthylazide.* **Sharma A.**, Raviv, Y., Puri, A., Viard, M., Blumenthal, R and Maheshwari, R.K. Oral and Poster presentation at **26th Annual Meeting of the American Society of Virology**, July 14-18, 2007 at Oregon State University, Corvallis, Oregon, USA, MD,

2. *Toll Like Receptor 3 and associated signaling pathway genes are modulated in Venezuelan equine encephalitis virus infected brain.* **International Society of neurovirology, Philadelphia, 2006.** Anuj Sharma, Haresh Mani, Radha K Maheshwari. Department of Pathology, USUHS, Bethesda, MD, USA.

3. *Mechanism(s) of Neuroinvasion of Venezuelan Equine Encephalitis Virus: Role of Cytokines and Adhesion Molecules.* **International society for Interferon and cytokine research, Puerto Rico, 2004. Anuj Sharma**, Anoop K Singh, James Warren, Rajesh L Thangapazham and Radha K Maheshwari. Department of Pathology, USUHS, Bethesda, MD, USA.

4. *Modulation of Adhesion Molecules and Extracellular Matrix Proteins in Venezuelan Equine Encephalitis Virus Pathogenesis.* **American Society of Virology, Penn State, 2005. Anuj Sharma**, Anoop K Singh, James Warren, Keith Steele and Radha K Maheshwari. Department of Pathology, USUHS, Bethesda, MD, USA.

5. *Toll Like Receptors And Adhesion Molecules Are Modulated In Brain of Venezuelan Equine Encephalitis Virus Infected Mice.* **ATAAC, Florida 2005**. **Anuj Sharma**, Anoop K Singh, James Warren, Rajesh L Thangapazham and Radha K Maheshwari. Department Of Pathology, USUHS, Bethesda, MD, USA.

6. *Induction of Toll-Like Receptor 3 and Chemokines in Venezuelan Equine Encephalitis Virus Pathogenesis.* **USUHS Research day, 2005**. **Anuj Sharma**, Anoop K Singh, James Warren and Radha K Maheshwari. Department of Pathology, USUHS, Bethesda, MD, USA.

7. *Enhancement of Wound Healing and Angiogenesis by Novel Botanicals***. University of Mississippi, Oxford, 2005.** Radha K Maheshwari[1], **Anuj Sharma[1,2]**, Rajesh Thangapazham[1,2] and Anoop K Singh[1]. [1] Department of Pathology**,** Uniformed Services University of the Health Sciences, Bethesda, Maryland, USA [2] Birla Institute of Technology and Sciences, Pilani, India.

8. *Enhancement of woundhealing by novel phytochemicals in normal and diabetic impaired animals: A successful Indo-US collaboration. International conference on ethnopharmacology and alternate medicine.* Maheshwari RK, **Sharma A**, Thangapazham RL**,** Singh AK, Kulreshtha D, Sharma S. Amala Cancer Institute, Kerala, India, January 20-22, 2006

9. *Green tea induces cell cycle arrest estrogen independent human breast cancer cell line.* Thangapazham R.L, Singh AK, Gaddipati JP, **Sharma A**, Warren J, Maheshwari RK. Research Week. Uniformed Services University of the Health Sciences Research Day, Bethesda, MD, May 16-17, 2006

10. *Evaluation of anti-angiogenic activity of Brahma Rasayana in a rat prostate tumor model system in-vivo and in HUVEC in-vitro.* Thangapazham R.L, Gaddipati JP, **Sharma A**, Singh AK, Maheshwari RK. Research Week. Uniformed Services University of the Health Sciences Research Day, Bethesda, MD, May 17-19, 2005

11. *Toll Like Receptor 3 and associated signaling pathway genes are modulated in Venezuelan equine encephalitis virus infected brain.* **International Society of neurovirology, Philadelphia, 2006. Anuj Sharma**, Haresh Mani, Radha K Maheshwari. Department of Pathology, USUHS, Bethesda, MD, USA.

12. *Green tea induces cell cycle arrest estrogen independent human breast cancer cell line.* Thangapazham R.L, Singh AK, Gaddipati JP, **Sharma A**, Warren J, Maheshwari RK. Research Week. Uniformed Services University of the Health Sciences Research Day, Bethesda, MD, May 16-17, 2006

13. *Evaluation of anti-angiogenic activity of Brahma Rasayana in a rat prostate tumor model system in-vivo and in HUVEC in-vitro.* Thangapazham R.L, Gaddipati JP, **Sharma A**, Singh AK, Maheshwari RK. Research Week. Uniformed Services University of the Health Sciences Research Day, Bethesda, MD, May 17-19, 2005

14. *Green tea polyphenols and its constituent epigallocatechin gallate influences the proliferation of highly invasive estrogen independent breast cancer cell line.* Thangapazham R.L, Singh AK, Gaddipati JP, **Sharma A**, Warren J, Maheshwari RKUniformed Services University of the Health Sciences Research Day, Bethesda, MD, May 17-19, 2005

15. *Anti-proliferative, apoptotic and anti-invasive effect of green tea in estrogen independent human breast cancer cell line.* Thangapazham R.L, Singh AK, Gaddipati JP, **Sharma A**, Warren J, Maheshwari RK. Combined Faculty Retreat, CCR, National Cancer Institute, NIH, Rocky Gap, MD, July 20-22, 2005.

16. Green tea induces cell cycle arrest and apoptosis in estrogen independent human breast cancer cell line. Thangapazham RL**,** Singh AK, **Sharma A**, Gaddipati JP, Warren J, Maheshwari RK. Frontiers in cancer prevention research. Baltimore, MD, October 30 – November 2, 2005

17. *Molecular targets involved in the anti-angiogenic activity of a polyherbal chemopreventive agent Brahma Rasayana.*Thangapazham R.L, Gaddipati JP, **Sharma A**, Singh AK, Maheshwari RK. 96th American Association for Cancer Research Annual Meeting, Anaheim, CA, April 16-20, 2005

18. *Anti-proliferative effect of green tea polyphenols and its constituent epigallocatechin gallate against human breast cell line.* Thangapazham RL**,** Singh AK, Gaddipati JP, **Sharma A**, Warren J, Maheshwari RK. 96th American Association for Cancer Research Annual Meeting, Anaheim, CA, April 16-20, 2005

19. *Regulation of angiogenesis by Brahma Rasayana a polyherbal preparation in vitro and in vivo models.* Gaddipati JP, Thangapazham R.L, **Sharma A**, Singh AK, Maheshwari RK. The American Society for Cell Biology 44th Annual Meeting Washington, DC, December 4-8, 2004

20. *In-vitro and in-vivo assessment of homeopathic treatment for prostate cancer.* Jonas WB, Gaddipati JP, Rajeshkumar NV, **Sharma A**, Thangapazham R.L**,** Warren J, Singh AK, Ives J, Olsen C, Mog SR, Maheshwari RK. Society of Integrative Oncology 1st International Conference, New York, November 18, 2004

21. *Brahma Rasayana: A polyherbal preparation as a chemopreventive agent against prostate cancer.* Thangapazham R.L**,** Gaddipati JP, Rajeshkumar NV, **Sharma A**, Warren J, Mog SR, Singh AK, Maheshwari RK. American Institute for Cancer Research-International Research Conference on Food, Nutrition and Cancer, Washington, DC, July 15-16, 2004

Co-Investigator in grants:

1. Funded: Post-transcriptional silencing of Venezuelan Equine Encephalitis Virus (VEEV) RNA for developing an antiviral therapy against exposure with VEEV, a bio-warfare agent. Defense Treat Reduction Agency, DOD, USA (2006-2009). PI: Radha K Maheshwari.

2. Under review: A new approach for the Inactivation of Venezuelan Equine Encephalitis virus (VEEV), a bio-warfare virus for vaccine application. Defense Treat Reduction Agency, DOD, USA (2007-2010). PI: Radha K Maheshwari.

List of Chapters

1. Beneficial Role of Curcumin in Skin Diseases. Molecular targets and therapeutic uses of curcumin in health and disease. Edited by Bharat B.Aggarwal, Young Jun-Surh and Shishir Shishodia.343-358. Thangapazham R. L**, Sharma A**, Maheshwari R. K.